University of São Paulo
"Luiz de Queiroz" College of Agriculture

Soil-plant-atmosphere water transfer mechanisms and their relation to crop water stress

Angelica Durigon

Thesis presented to obtain the degree of Doctor of Science. Area: Agro-Environmental Physics

Piracicaba
2011

Angelica Durigon
Bachelor in Meteorology

Soil-plant-atmosphere water transfer mechanisms and their relation to crop water stress

Advisor:
Prof. Dr. QUIRIJN DE JONG VAN LIER

Thesis presented to obtain the degree of Doctor of Science. Area: Agro-Environmental Physics

Piracicaba
2011

Dados Internacionais de Catalogação na Publicação
DIVISÃO DE BIBLIOTECA - ESALQ/USP

Durigon, Angelica
Soil-plant-atmosphere water transfer mechanisms and their relation to crop water stress / Angelica Durigon. - - Piracicaba, 2011.
143 p. : il.

Tese (Doutorado) - - Escola Superior de Agricultura "Luiz de Queiroz", 2011.

1.Água no solo - Disponibilidade 2. Estresse hídrico - Modelagem 3. Feijão 4. Relação solo-água-planta-atmosfera I. Título

CDD 635.652
D962s

Aos meus pais, Mariangela e José Eugênio, dedico.

AGRADECIMENTOS

A Deus, pelo sagrado dom da vida.

À minha querida família: meus pais, Mariangela e José Eugênio Durigon, meus irmãos Leandro Durigon e Luciana de Almeida da Silva, e Leonardo Durigon e Priscila de Paula Bueno, e meus nonos Maria e Antero Durigon, e Anilva e Itacir Lizot.

Ao meu orientador Quirijn de Jong van Lier, pelo bom humor e pela paciência que sempre teve comigo, por ser o maior exemplo profissional que tenho e por tratar com tanta retidão a profissão a qual eu também escolhi. Agradeço também por me receber, juntamente com sua esposa Iara Silva Fino e seus filhos Maíra e Matias de Jong van Lier, em sua casa, onde passei momentos muito agradáveis.

Ao Programa de Pós-Graduação em Física do Ambiente Agrícola, atualmente Engenharia de Sistemas Agrícolas, e à Escola Superior de Agricultura “Luiz de Queiroz”, pela oportunidade de concluir mais essa etapa em minha formação.

À Coordenação de Aperfeiçoamento de Pessoal de Nível Superior - CAPES - pelas bolsas de doutoramento e de estágio *sandwich*.

À Fundação de Amparo à Pesquisa do Estado de São Paulo - FAPESP - pelo financiamento do projeto para realização do experimento de campo.

Ao professor Luiz Roberto Angelocci, pelo exemplo profissional e pessoal. O carinho e receptividade com que sempre me tratou, e a ajuda incondicional no experimento de campo fazem com que eu o admire ainda mais.

Aos sempre gentis e prestativos funcionários de Departamento de Engenharia de Biossistemas da ESALQ, em especial a Angela Derigi Silva, Luiz Fernando Novello, Francisco Bernardo Dias, Edivaldo Modesto de Abreu, Beatriz Regina Duarte Novaes, Hélio de Toledo Gomes, Osvaldo Rettore Neto, Antônio Agostinho Gozzo, Áureo Santana de Oliveira, Juarez Renó do Amaral, Davilmar Aparecida Colevatti, Luiz Custódio Camargo, Lúcia Monteiro de Campos Nogueira Ribeiro e Luiz Afonso da Costa.

Ao professor Durval Dourado Neto, pelo apoio operacional ao projeto.

Aos funcionários de campo do Departamento de Produção Vegetal, em especial aos funcionários Erreinaldo Donizeti Bortolazzo, Edson Ademir de Moraes e Ananias Ferreira de Souza pelo apoio no experimento de campo.

Ao professor Tarlei Botrel, pelo auxílio na esquematização do sistema de irrigação do experimento de campo.

Ao professor Carlos Alberto Vettorazzi, pelo empréstimo do ceptômetro.

Aos membros da banca de qualificação Juan Sinforiano e Evandro Zanini, pelo comprometimento com que avaliaram e aprimoraram o projeto.

Ao professor Paulo César Sentelhas, pela supervisão no estágio em docência.

A Lucas Vellame, pelo auxílio na instalação dos sensores no armazenador de dados.

A Lucas Fernandes de Souza, pelas instruções sobre o porômetro.

Aos professores Sérgio de Oliveira Moraes, Paulo Leonel Libardi e Jarbas Honório de Miranda, pelo agradável convívio diário.

Aos amigos de longa data Lucía Iracema Chipponelli Pinto, Michel Nobre Muza e Juliana Schontag Muza, Edmílson Dias de Freitas, Marcelo Belantani de Bianchi, Cátia Rodriguez e Luciene Natali.

Aos meus queridos amigos e companheiros do “ramal 207” Roque Emanuel da Costa de Pinho e Valéria Cristina Rodrigues Sarnighausen.

Aos queridos colegas do corredor mais inspirador de toda a ESALQ: Jaedson Claudio Anunciato Mota, Alexsandro Brito, Pablo Ghiberto, Helon Ébano de Freitas, Luciano Roberto da Silveira, Neilo Bergamini, João Batista Reis, Marcos Alex dos Santos, Cristhiane Neiverth, Marcelo Dias Oliveira, Dirceu Arraes e Monica Salvador.

Às pessoas queridas que Piracicaba me trouxe Rochane de Oliveira Caram, Ana Carolina Nascimento dos Santos, Lia Silvia Nogueira Amuy, Paula Preeg, Adriana Ferreira da Silva e Flávio Cardoso da Silva, e Luzimario Lima Pereira.

À equipe do curso de Licenciatura em Ciências da USP - Pólo Piracicaba, pelo carinho e incentivo nesses últimos meses: Profa. Maria Angélica Penatti Pipitone, Profa. Vânia Galindo Massabni, Cindy Silva Moreira, Fábio de Souza Fidelis, Giovana Cabianchi, Thomas Barcelos, Ricardo Bull, Robson Arthur, Rodrigo Dantas Amancio,

Rodrigo Lorenzi e Irene Valdriguis Facciolli. Agradeço ainda as palavras carinhosas vindas de muitos de nossos alunos.

From The Netherlands, I would like to thank…

To my Dutch supervisor Klaas Metselaar who kindly received me at Wageningen University and at his place together with his wife Jet Drenth and their sweet daughter Hannah Metselaar.

To Professor Sjoerd van der Zee, the chair group head of Soil Physics, Ecohydrology and Groundwater Management Group of Wageningen University and Research Centre, and in his name, the entire group, especially Harm Gooren.

To my friends Marijke Wijman, Josien Tonijk, Jasper Tonijk, Frans Tromp, Alba Santos and Rik van Rijzingen, and Oksana Bolkina.

“If I saw further than other men, it was because I stood on the shoulders of giants.”

Isaac Newton

CONTENT

RESUMO

Mecanismos de transferência de água entre solo, planta e atmosfera e sua relação com o estresse hídrico vegetal

Parametrizações mecanísticas descrevem fisicamente a interação das plantas com o ambiente baseando-se em processos fundamentais, como assimilação de líquida de CO_2 e extração da água do solo pelas raízes, influenciados pelas condições do ambiente. O objetivo principal dessas rotinas é aumentar o entendimento do sistema estudado pela integração quantitativa e qualitativa do conhecimento em um modelo de simulação dinâmica do sistema real. Definindo estresse hídrico como a condição em que uma planta aumenta a resistência estomática em conseqüência do aumento da demanda atmosférica e/ou da redução da disponibilidade hídrica no solo, tem-se como hipótese que o déficit hídrico em plantas é causado por fatores ambientais relacionados com as interfaces solo-raiz e folha-atmosfera. O objetivo geral desse estudo é identificar quais são as variáveis do solo e da atmosfera determinantes e que devem ser consideradas na modelagem da deficiência hídrica em plantas. Os teores de água no solo e na atmosfera foram monitorados em condições de campo durante o desenvolvimento da cultura de feijão (*Phaseolus vulgaris* L.) entre Junho e Setembro de 2010, e correlacionados ao estresse hídrico caracterizado por medições de temperatura do dossel. As variáveis de interesse, especificamente o potencial matricial da água do solo, a temperatura e a umidade do ar e a temperatura do dossel foram medidas regularmente em intervalos de 30 minutos. A taxa de transpiração e a condutância estomática foram medidas ocasionalmente. Uma parcela foi irrigada durante todo o ciclo da cultura (tratamento totalmente irrigada), enquanto a outra foi submetida ao estresse hídrico na fase reprodutiva (tratamento com déficit de irrigação). A metodologia utilizada neste estudo deu suporte à hipótese inicial. Os principais fatores relacionados à interface solo-raiz são as propriedades hidráulicas do solo, especialmente a condutividade hidráulica e da densidade de comprimento radicular; na interface atmosfera de folhas, os fatores mais importantes são o déficit de pressão de vapor do ar atmosférico *VPD*. Estes fatores devem ser considerados de alguma forma na modelagem estresse hídrico em plantas. A detecção da ocorrência de estresse hídrico nas plantas no tratamento com déficit de irrigação foi feito por comparações entre o *VPD* e diferença de temperatura entre o dossel e o ar $\Delta t_{dossel\text{-}ar}$ e entre t_{dossel} e a temperatura do bulbo úmido t_{wb} dos dois tratamentos hídricos. O início do estresse hídrico nas plantas com déficit de irrigação ocorreu em 05 de Agosto. As simulações com os modelos mecanísticos de extração da água do solo pelas raízes proposto por Jong van Lier et al. (2008) e de assimilação de CO_2 proposto por Jacobs (1994) foram feitos com os dados de ambos os tratamentos. O modelo de extração foi sensível aos parâmetros hidráulicos do solo, especialmente a condutividade hidráulica e o comprimento radicular. A taxa de transpiração estimada pelo modelo de Jacobs (1994) mostrou-se dependente da temperatura do dossel utilizada para calcular o déficit de umidade específica folha-ar D_s e a condutância do mesofilo, do próprio D_s (dependente também da temperatura do ar), e do índice de área foliar.

Palavras-chave: Estresse hídrico em plantas; Modelagem mecanística; Feijão (*Phaseolus vulgaris* L.)

ABSTRACT

Soil-plant-atmosphere water transfer mechanisms and their relation to crop water stress

Mechanistic parameterizations describe physically the interactions between crop and environment based on primary processes such as CO_2 net assimilation and root water uptake from soil and how they are influenced by environmental conditions. An important purpose of developing mechanistic routines is to improve the understanding of a system by qualitative and quantitative integration of knowledge in a dynamic simulation model of a real system. Defining water stress as the condition in which stomatal resistance of plant leaves increases as a consequence of enhanced atmospheric demand and/or reduced soil water availability, the investigated hypothesis was that plant water stress is caused by environmental factors related to both the soil-root and leave-atmosphere interfaces. The main objective of the research was to identify which atmosphere and soil parameters are determinant and must be considered in crop water stress modeling. Soil and atmosphere water content were monitored under field conditions during the growing season of a Common Bean (*Phaseolus vulgaris* L.) crop between June and September, 2010, and correlated to plant water stress characterized by measurements of canopy temperature. The variables of interest, specifically the soil water pressure head, air temperature and humidity and canopy temperature were measured regularly at short intervals. Transpiration rate and stomatal conductance were measured occasionally. One plot was irrigated during the whole crop cycle (fully irrigated treatment), while the other one was subject to water stress in the reproductive phase (deficit irrigated treatment). The methodology used in this study supported the initial hypothesis. The main soil-root interface related factors that determine water stress are the soil hydraulic properties, especially the hydraulic conductivity, and the root length density; at the leaf atmosphere interface, the most important factor is the vapor pressure deficit of atmospheric air *VPD*. These factors must be somehow considered in crop water stress modeling. The detection of water stress occurrence in the deficit irrigated plants was made by comparisons between *VPD* and temperature difference between canopy and air $\Delta t_{canopy\text{-}air}$ and between t_{canopy} and wet bulb temperature t_{wb} of the two irrigation treatments. The onset of water stress in deficit irrigated plants occurred on August 5. The simulations with the mechanistic models of soil water root uptake proposed by Jong van Lier et al. (2008) and of CO_2 assimilation by Jacobs (1994) were made with data from the two treatments. The soil water uptake model was sensitive to soil hydraulic parameters, especially hydraulic conductivity and root length density. The transpiration rate estimated by the Jacobs (1994) model showed to be dependent on the canopy temperature used to calculate the specific humidity deficit between leaves and air D_s and the mesophyll conductance, on D_s (on its turn also dependent on air temperature), and on the leaf area index.

Keywords: Crop water stress; Mechanistic modeling; Common Bean (*Phaseolus vulgaris* L.)

LIST OF FIGURES

LIST OF TABLES

LIST OF ABBREVIATIONS

ARPEGE	Action de Recherche Petite Echelle – Grande Echelle
CO_2	Carbon dioxide
CSI	Canopy Stress Index
CWSI	Crop Water Stress Index
ESALQ	"Luiz de Queiroz" College of Agriculture
FAO	Food and Agricultural Organization of the United Nations
ISBA	Interactions between Soil, Biosphere, and Atmosphere
PoT	Polymer Tensiometer
SVAT	Soil-Vegetation-Atmosphere Transfer
TDR	Time-Domain Reflectometry
USP	University of São Paulo
WUR	Wageningen University and Research Centre

LIST OF SYMBOLS

A	Net CO_2 assimilation rate (mg m^{-2} s^{-1})
A_g	Gross CO_2 assimilation rate (mg m^{-2} s^{-1})
A_m	Photosynthetic rate at saturating light intensity (mg m^{-2} s^{-1})
$A_{m,max}$	Leaf photosynthetic capacity (mg m^{-2} s^{-1})
A_{min}	Minimum A_m (mg m^{-2} s^{-1})
a_z	Ratio between root distance of mean soil water content and r_m (m m^{-1} = -)
$Coef_t$	PoT coefficient (bar °C^{-1})
C_i	Intercellular CO_2 concentration (mg m^{-3})
C_{min}	Minimum intercellular CO_2 concentration (mg m^{-3})
C_s	CO_2 concentration at surface (leaf or canopy) (mg m^{-3})
c_p	Heat capacity of air at constant pressure (MJ kg^{-1} °C^{-1})
D	Soil hydraulic diffusivity (m^2 d^{-1})
D_s	Specific humidity deficit between leaf and air (g kg^{-1})
D_{max}	Value of D_s at complete stomata closure (g kg^{-1})
E	Water evaporation rate (kg m^{-2} s^{-1})
E_n	Water evaporation rate of bare soil (mm d^{-1})
E_s	Water evaporation rate of soil surface (mm d^{-1})
e_a	Actual water vapor pressure (kPa)
e_s	Saturation pressure of water vapor (kPa)
f	Ratio C_i/C_s (-)
$f_{\min}$	Ratio C_i/C_s at $D_s = D_{max}$ (-)
f_z	Empirical parameter of the Jong van Lier et al. (2008) model
f_0	Ratio C_i/C_s at $D_s = 0$ (-)
G	Soil heat flux (W m^{-2})
g_{bl}	Boundary layer conductance (mm s^{-1})
g_m	Mesophyll conductance (mm s^{-1})
g_s	Stomatal conductance for water vapor (mm s^{-1})
g_{sc}	Stomatal conductance for CO_2 (mm s^{-1})
g^*_{sc}	First approximation of stomatal conductance for CO_2 (mm s^{-1})

H	Sensible heat flux (W m^{-2})
h	Pressure head (m)
h_{crit}	Critical value of pressure head (m)
h_w	Pressure head at permanent wilting point (m)
h_r	Pressure head at root surface (m)
K	Soil hydraulic conductivity (m d^{-1})
K_s	Saturated hydraulic conductivity (m d^{-1})
$\overline{K}(h)$	Mean soil hydraulic conductivity between two layers (m d^{-1})
k	Empirical constant to estimate the boundary layer conductance (mm $s^{-0.5}$)
k_e	Coefficient of visible light extinction
L	Root length (m)
LAI	Leaf Area Index (m^2 m^{-2})
M	Matric flux potential (m^2 d^{-1})
M_{wa}	Molar mass of water (g mol^{-1})
M_{air}	Molar mass of dry air (g mol^{-1})
M_{crit}	Critical value of matric flux potential (m^2 d^{-1})
M_w	Matric flux potential at permanent wilting point (m^2 d^{-1})
M_r	Relative matric flux potential (m^2 d^{-1})
M_0	Matric flux potential at root surface (m^2 d^{-1})
$\overline{M}$	Mean matric flux potential in the rhizosphere (m^2 d^{-1})
m	Empirical parameter of Van Genuchten (1980) equation (-)
n	Empirical parameter of Van Genuchten (1980) equation (-)
PAR	Photosynthetically active radiation (W m^{-2})
P_{cor}	PoT pressure corrected by temperature (bar)
q	Flux density of soil water (m^3 m^{-2} d^{-1})
q_a	Air specific humidity (g kg^{-1})
q_{sat}	Air specific humidity at saturation (g kg^{-1})
R	Root length density (m m^{-3})
R_d	Dark respiration (mg m^{-2} s^{-1})
RH	Relative air humidity (Pa Pa^{-1} = -)
RH_s	Relative soil air humidity (Pa Pa^{-1} = -)

R_n Net radiation (W m^{-2})

r Radial distance from the root surface (m)

r_m Rhizosphere radius (m)

r_t Total resistance to water vapor flux (s mm^{-1})

r_0 Root radius (m)

$\bar{r}$ Mean radial distance from the root surface (m)

S_{mod} Actual root water uptake rate estimated by Jong Van Lier et al. (2008) model (m^3 m^{-3} d^{-1})

S_{exp} Actual root water uptake rate estimated by experimental data (m^3 m^{-3} d^{-1})

T Leaf transpiration rate (mg m^{-2} s^{-1})

T_a Actual leaf transpiration rate (mg m^{-2} s^{-1})

T_{Ags} Leaf transpiration rate estimated by Ag_s model (mg m^{-2} s^{-1})

T_p Potential leaf transpiration rate (mg m^{-2} s^{-1})

T_w Transpiration rate at permanent wilting point (m d^{-1})

T_r Relative transpiration rate (mg m^{-2} s^{-1})

t_{air} Air temperature (°C)

t_{canopy} Canopy temperature (°C)

t_s Surface temperature (°C)

t_{wb} Wet bulb temperature (°C)

t_1 Lower reference temperature in inhibition function (°C)

t_2 Upper reference temperature in inhibition function (°C)

u Wind speed (m s^{-1})

V_E Volume of evaporated soil water (m^3)

VPD Vapor pressure deficit (hPa)

W_l Leaf width (mm)

α Empirical parameter of Van Genuchten (1980) equation (m^{-1})

β Empirical parameter of Black, Gardner e Thurtell (1969) evaporation parameterization (m $d^{-0.5}$)

γ Psychrometric constant (kPa $°C^{-1}$)

ε Initial quantum use efficiency (mg J^{-1})

ε_o Maximum initial quantum use efficiency (mg J^{-1})

Γ CO_2 compensation concentration (mg m^{-3})

λ Empirical parameter of Van Genuchten (1980) equation (-)

λ_v Latent heat of water vaporization (J kg^{-1})

∇ Mean hydraulic gradient as a function of time (-)

ρ_{air} Density of air at constant pressure (kg m^{-3})

ρ_w Density of water (kg m^{-3})

ρ_z Root water uptake weighing parameter (m^{-2})

Θ Effective saturation (-)

θ Soil water content (m^3 m^{-3})

θ_{crit} Critical value of soil water content (m^3 m^{-3})

θ_w Soil water content at permanent wilting point (m^3 m^{-3})

θ_r Residual soil water content (m^3 m^{-3})

θ_s Saturated soil water content (m^3 m^{-3})

$\bar{\theta}$ Mean soil water content in the rhizosphere (m^3 m^{-3})

1 INTRODUCTION

Agricultural production in Brazil is prone to variations in rainfall regimes related to phenomena on macro and meso meteorological scales. Macro scale systems, such as ENSO (El Niño – Southern Oscillation), and meso scale systems, such as the South Atlantic Convergence Zone (SACZ) and Mesoscale Convective Complexes (MCC), act sometimes increasing and sometimes reducing Brazilian grain production. Observed global changes in rainfall regimes show an increase in extreme weather events related to systems at different meteorological scales. The economical and social burden of more extreme weather events may be high and the impacts will be substantial for agricultural food production, hydroelectric energy production and biodiversity. For example, the effect of an increase in “veranico” events in South and Central of Brazil related to ENSO would be minimized by intensive irrigation. However, irrigation is less and less stimulated as the competition for water for human consumption and grain production increases.

Simulation of the reaction of crops to changes in rainfall regime needs reliable numerical codes for diverse soil and climate conditions in order to minimize possible errors of extrapolation to future environmental conditions. Meteorological weather and climate models as well as crop models have numerical routines designated just to represent the interaction between vegetation and environment. They treat the relationship between the root system and soil and between the above ground part of the crop with the atmosphere under different environmental conditions regarding water and energy supply. As the numerical routines are connected to robust models, they must be at the same time simple enough to allow temporal performance and detailed enough to represent in a mechanistic way the hydrological and gas exchange processes that occur in the soil-plant-atmosphere continuum in a certain environment.

The interactions between vegetation and environment are sometimes described by empirical parameterizations with regression equations including environmental variables like radiation and rainfall. For example, crop yield can be related to the total rainfall during the growing season. This kind of parameterization can show a good performance provided that the regression parameters are estimated by large

experimental data sets. On the other hand, the forecasts are restricted to the same environmental condition crops used to perform the regression. Moreover, these kind of empirical parameterizations do not explain the causes of observed variations in productivity.

On the other hand, mechanistic parameterizations describe physically the interactions between crop and environment based on primary processes such as CO_2 net assimilation and root water uptake from soil and how they are influenced by the environmental conditions. Nevertheless, the capacity of prediction of such parameterizations is not always high because of errors in parameter estimation and flaws in the representation of the physical processes. However, an important goal of mechanistic routines is to improve the understanding of a system by qualitative and quantitative integration of knowledge in a dynamic simulation model of a real system.

Water exchange between plant leaves and atmosphere occurs as vapor flow mainly in the stomata. In experimental and numerical studies, stomatal conductance has been related to the net CO_2 assimilation rate A, the atmospheric vapor pressure deficit VPD, the specific humidity deficit between leaves and air D_s and the intercellular CO_2 concentration C_i. A mechanistic way to parameterize the transpiration rate of plants is to relate it to the stomatal conductance by determining these parameters.

Soil water uptake by plant roots is a function of the hydraulic gradient between soil water in the rhizosphere and the water at the root surface. Numerical parameterization of water flux between soil and roots can be performed, and a convenient soil hydraulic property in this matter is the matric flux potential M, a composite property defined by the soil hydraulic conductivity and pressure head h. It is closely related to water movement and together with root length density and atmospheric demand allows estimating the water flux between the rhizosphere and root system.

1.1 Objectives

The main objective of the research described in this thesis is to identify which atmospheric and soil parameters are determinant and must be considered in crop water stress modeling. Defining water stress as the condition in which stomatal resistance of

plant leaves increases as a consequence of the atmospheric demand increase and/or the reduction of soil water availability, the hypothesis is that plant water stress is caused by environmental factors related to the soil-root and leave-atmosphere interfaces.

The specific objectives are:

1. To identify plant water stress occurrence in an agricultural crop by infrared thermometry data.
2. To experimentally determine which parameters of soil and atmosphere are related to the plant water stress occurrence.
3. To estimate the root soil water uptake (S_{mod}) using the mechanistic model of Jong Van Lier et al. (2008) and to discuss the correlation between model parameters that determine S_{mod} in plant water stress conditions.
4. To estimate the plant transpiration rate (T_{Ags}) using the mechanistic model of CO_2 assimilation (Ag_s model) proposed by Jacobs (1994) and discuss the correlation between model parameter that determine T_{Ags} in plant water stress conditions.

2 DEVELOPMENT

2.1 Literature review

2.1.1 Water movement between soil, plant and atmosphere

The development of plants depends on water for maintenance of turgor and for cooling of the leaves. When the water supply is insufficient, stomata close. Water shortage reduces the elongation of plant cells, whereas stomatal closure reduces the CO_2 availability and thus the production of assimilates and growth (KUIPER, 1961; JARVIS; DAVIES, 1998).

The water moves through the soil-plant-atmosphere system by mass flow, mainly in the liquid phase (in very dry conditions, vapor flux in the soil may play an important role) and the flux occurs by water vapor diffusion from the intercellular air spaces of leaves (TARDIEU; DAVIES, 1992; TARDIEU; SIMONNEAU, 1998). The water flows through a pathway composed by a system of hydraulic resistances from the soil, passing through the plant and finally reaching the atmosphere (ZIMMERMANN; MEINZER; BENTRUP, 1995). Several studies describe details about the resistances of each part of soil-plant-atmosphere continuum, for example Angelocci (2002), Tuzet, Perrier and Leuning, (2003), Raats (2007) and Jong Van Lier et al. (2008). In summary, hydraulic resistances occur as described below.

For the water to flow towards the root surface, first it is necessary to overcome the hydraulic resistance of the soil itself. This resistance is dependent on soil hydraulic properties, on water content and on the distance. After reaching the root surface, water needs to pass through the radial resistance inside the root until getting to the xylem vases. Unlike the relatively high radial root resistance, the xylem vases have a low hydraulic resistance. From here, ascends inside the plants through xylem vases until getting to the mesophyll cell walls, still as a liquid. From there it evaporates and is diffused, as water vapor, though the intercellular air spaces of leaves getting to the atmosphere via the epidermis and cuticle, and/or via stomata. The cuticular pathway has a high hydraulic resistance, therefore the stomata are the main route of water vapor diffusion from leaves to atmosphere. The air resistance to water vapor diffusion in the

close vicinity of leaves is represented by the boundary layer resistance or aerodynamic resistance. It depends on the wind speed, leave size and shape and surface properties and temperature, and can be of great importance to water vapor flux.

There is no consensus about the part of the system responsible for the occurrence of water stress. Frequently the reduction in soil water content and the resulting increase of soil hydraulic resistance are indicated as the main mechanisms leading to plant water stress (CARBON, 1973; HULUGALLE; WILLATT, 1983; SCHRÖDER et al., 2008). Other researchers, however, pointed out plant resistances our resistance between plant and atmosphere as the main cause (TAYLOR; KLEPPER, 1975; BLIZZARD; BOYER, 1980; VERHOEF et al., 1996; AGELE; COHEN, 2007). The water absorption by roots depends on water movement in the soil toward root surfaces but also can be influenced by transpiration. However, the transpiration rate depends on the stomatal conductance and environmental conditions that affect evaporation (CAMPBELL; NORMAN, 1998).

The stomatal conductance of leaves is a direct indicator of plant water stress and is frequently used in SVAT models (*Soil-Vegetation-Atmosphere Transfer*). It is simultaneously affected by different environmental conditions (COLLATZ et al., 1991; JACOBS et al., 1996). The efforts to correlate it with environmental parameters are not always successful. Stomatal conductance of sunlit leaves depends on air temperature and air CO_2 concentration, but the air vapor pressure deficit and the soil water status also play an important role (JARVIS, 1976; PASSOS et al., 2009). The following two parts of the soil-water-atmosphere system need special attention in mechanistic modeling of plant water stress:

a. *the rhizosphere* (soil-root interface) where the dynamics of root soil water uptake, influenced by root length density and root distribution, soil hydraulic properties and soil hydraulic conditions, determine the water uptake rate; and
b. *the plant-atmosphere interface*, where the stomatal conductance and environmental or meteorological parameters (air temperature and humidity, wind and radiation) determine the rate of water loss by transpiration.

a. *the rhizosphere*

The rhizosphere (soil-root system) has been pointed as crucial for the occurrence of plant water stress, especially in the view of soil physicists and hydrologists (MOLDRUP et al., 1992; ROOSE; FOWLER, 2004; RAATS, 2007). According to their point of view, the reduction of hydraulic conductivity in the dry zones that form around a water extracting root, as well as the reduction of the contact area between soil and roots when the soil dries and soil and roots shrink are the limiting factors to water flux in the system.

b. *the plant-atmosphere interface*

A reduction of stomatal conductance and plant water stress occurrence can be caused also by conditions that are not related to the rhizosphere. Especially in meteorological models it is common to find the interpretation that a plant reduces its stomatal conductance as a mere reaction to a water vapor pressure deficit between intercellular air spaces of leaves and atmosphere. The mechanism of stomatal reactions to air humidity is not exactly known (JACOBS et al., 1996; COHEN, 2007). Some authors proposed mechanisms to describe transpiration as a function of stomatal conductance and saturation deficit. Bunce (1985) refers to the direct effect of cuticular evaporation in stomata while Monteith (1995) uses the interaction between water vapor flux and stomatal conductance.

2.1.2 Detection of plant water stress by infrared thermometry

The energy balance of a canopy is given by (ALLEN; PEREIRA; RAES, 1998):

$$R_n = H + \lambda_v E + G \qquad [1]$$

where R_n is the net radiation (W m^{-2}), H is the sensible heat flux of canopy to air (W m^{-2}), $\lambda_v E$ is the latent heat flux to air (W m^{-2}) with E being the evaporation rate (kg m^{-2} s^{-1}) and λ_v being latent heat of water vaporization (J kg^{-1}), and G is the soil heat flux (W m^{-2}). The canopy temperature is directly related to water and energy balance at plant leaves. If a decrease in water availability to leaves decreases the latent heat flux at their surfaces, an incremental sensible heat flux may occur and a temperature difference between canopy and air is created. A direct effect of stomatal closure is the increase of canopy

temperature as transpiration rate and energy dissipation are reduced (GROSSNICKLE; RUSSEL, 1991).

Monitoring the direct responses of crops to water shortage by observing the leave temperature allows the early detection of water stress conditions. Infrared thermometry is an accurate technique for measuring the leaf temperature. Infrared temperature measurements of leaves are robust, noninvasive, nondestructive and automated, thus promising for measuring the crop water status (JACKSON; REGINATO; IDSO, 1977).

The use of infrared thermometers to monitor canopy temperature has been described by many authors (JACKSON et al., 1981; HATFIELD et al., 1990; WANJURA; MAHAN, 1994; PINTER et al., 2003; PETERS; EVETT, 2004; MAHAN; YEATER, 2008). Leaf temperature or canopy temperature is used as a quantitative indicator of plant water stress (BROWN; ESCOMBE, 1905 apud JONES, 2004; GUILIONI et al., 2008). Efforts have been made to correlate leaf or canopy temperature and plant water stress conditions in order to provide, for example, irrigation guidelines. Stress indices have been proposed (JACKSON; REGINATO; IDSO, 1977; CLAWSON; BLAD, 1982; IDSO et al., 1981; JACKSON et al., 1981; MORAN et al., 1994), directly or empirically related to stomatal conductance which is the key physiological parameter linked to plant water status. More recently, several studies have been reported on the use of infrared thermometry and thermal images to directly estimate stomatal resistance to water vapor flux (JONES, 1999; JONES et al., 2002; LEINONEN et al., 2006).

Idso, Jackson and Reginato (1977) and Jackson, Reginato and Idso (1977) included the temperature difference between canopy (measured with infrared thermometers) and air in an index of plant water status, the Stress-Degree-Index. Their objective was to develop a technique to remotely evaluate plant water status using a small number of measurements. They supposed that environmental parameters such as vapor pressure deficit, net radiation and wind speed would be largely manifested in the temperature difference.

Idso et al. (1981) used the temperature difference between canopy and atmospheric air $\Delta t_{canopy\text{-}air}$ (°C) and water vapor pressure deficit at atmospheric air (*VPD*, hPa) and showed that the relationship between $\Delta t_{canopy\text{-}air}$ and *VPD* for well-watered crops was linear, as also observed by Erhler (1973) and later by Shimoda and Oikawa

(2006). From these observations Idso et al. (1981) together with Jackson et al. (1981) defined the *Crop Water Stress Index* (CWSI). Rodriguez et al. (2005) defined the *Canopy Stress Index* (CSI) which is given by the temperature difference between canopy and atmospheric air and normalized by vapor pressure deficit. The CSI is expected to be positive and high if the canopy capacity to dissipate heat is reduced, as when stomata close. Many environmental parameters, such as droughts and pests and diseases that affect vascular tissues, roots and leaves can cause stomatal closure (BOCCARA et al., 2001; CHAERLE et al., 1999; BOWDEN; ROUSE; SHARKEY, 1990; SADRAS; WILSON, 1997). Stomatal closure can also be induced by shortage of nutrients (RADIN, 1994; BROADLEY et al., 2001) or by hormonal signals (BRINGHAM, 2001).

There are other ways to use canopy temperatures obtained by infrared thermometry to detect the occurrence of plant water stress. One way is the comparison to the wet bulb temperature t_{wb} (°C). The wet bulb temperature is the temperature of a surface adiabatically cooled by evaporation, saturating the air with water vapor. The geometry of the leaves is different from the geometry of a wet bulb thermometer and the leaves are exposed to radiation. Therefore, the cooling of leaves is not exactly an adiabatic process and the leaf temperature will be higher than t_{wb}. The approximation of leaf temperature to wet bulb temperature is controlled by the wind and radiation, the structure of plants and the soil water content (WANJURA; UPCHURCH, 1997; MAHAN et al. 2005). Wanjura, Upchurch and Mahan (1995) estimated that a peanut canopy is able to cool down to a maximum of 2°C above the wet bulb temperature of ambient air.

Another common phenomenon observed in different crops, especially when plants are under water stress, is called the afternoon dip of photosynthesis (WANG; LEUNING, 1998; WANG et al., 2006). Even when soil water conditions are favorable, the photosynthetic rate is sometimes reduced at midday or early afternoon. This occurs by stomatal closure due to high atmospheric demand (i.e., high *VPD*). Leuning (1995) and Tuzet, Perrier and Leuning (2003) explained in details the afternoon dip of photosynthesis. Following these authors, stomatal conductance depends not only on net radiation, temperature and intercellular CO_2 concentration via photosynthesis, but also on leaf water potential, which is in turn a function of soil water potential and water flux

rate between soil and plant. As the soil dries out, a midday depression of photosynthesis can develop by stomatal closure due to a lower leaf water potential than earlier on the day, as a result of increased atmospheric demand and reduced ability of the soil to provide water to the roots. As a result, the canopy temperature at midday has a maximum value (WANG et al., 2006). Using canopy temperature data measured by infrared thermometry as input in a CO_2 assimilation model that uses the vapor pressure deficit between intercellular air spaces of leaves and atmospheric air as the driving force for the diffusion of vapor, the afternoon dip of photosynthesis can be identified (JACOBS, 2004).

2.1.3 Root water uptake models

Questions about plant water stress caused by water shortage in the rhizosphere can be elucidated by modeling soil water uptake at the single root scale (GARDNER, 1960; COWAN, 1965; MOLDRUP et al., 1992; ROOSE; FOWLER, 2004; JONG VAN LIER; METSELAAR; VAN DAM, 2006; RAATS, 2007). These models treat a root as a cylindrical sink to which water flows in a radial geometry. The water flux can be described by the Richards equation (1928). However, the nonlinearity of its parameters limits the analytical solutions to restrictive boundary conditions. Such analytical solutions were presented by Gardner (1960) and Cowan (1965).

Currently, the availability of computational resources enables the use of iterative numerical algorithms with less restrictive boundary conditions. An algorithm of this kind was used by Jong Van Lier, Metselaar and Van Dam (2006) and by Metselaar and Jong Van Lier (2007) to simulate soil water uptake by root systems. These authors concluded that the matric flux potential M ($m^2\ d^{-1}$) is the parameter of the soil most closely linked to water stress. M is a soil property defined as a function of pressure head or water content. At a certain pressure head h, M is the integral of the hydraulic conductivity K ($m\ d^{-1}$) in the range of pressure heads between the pressure head corresponding to the permanent wilting point (h_w, m) and the pressure head of interest. Casaroli (2008) tested the root water extraction model presented by Jong Van Lier, Metselaar and Van Dam (2006) and by Metselaar and Jong Van Lier (2007) and concluded that the relative matric flux potential M_r ($m^2\ d^{-1}$), defined as the ratio between M and M_{crit} ($m^2\ d^{-1}$) (M_{crit}

being the value of M in the onset of water stress), is a good indicator of relative transpiration T_r (mm d^{-1}), but differences in magnitude occur between the values of M_{crit} experimentally observed in relation to the values estimated by the model. One reason for this discrepancy is the fact that the model considers a root system homogeneously distributed in the soil, a simplification of reality which overestimates the ability of roots to take up water from the soil.

The hypothesis of a unique M at the root surface of all roots of a root system allows estimating the root water uptake on a macroscopic scale by a multilayer root system and the partition of extraction by layers. Using this approach, a weighing factor ρ_z (m^{-2}) was derived to calculate the root water uptake distribution from different soil layers in terms of root length density or mean root distance. Jong Van Lier et al. (2008) and Casaroli (2009) demonstrated a correlation between extractions measured and estimated by this method. However, the experimental data available did not allow a rigorous test of the model.

The lack of experimental verification of many of the available models for describing the mechanism of root water uptake is due, among other factors, to the complex root architecture and the inability, until recently, to measure the soil water pressure head under field conditions in the relevant range, that is, until the permanent wilting point, corresponding to -15 atm or -150 m. Conventional tensiometers filled with water have a physical restriction to the range of pressure head between 0 and -0.8 atm, corresponding to (very) wet conditions and of minor interest in plant water stress studies.

In hydrological modeling, a transpiration reduction factor is commonly expressed by the relative transpiration $T_r = T_a / T_p$, where T_a is the actual transpiration rate and T_p is the potential transpiration rate. T_r is a function of soil water status (Figure 1) and the shape of this reduction function is sometimes supposed to be linear when expressed as a function of soil water content θ (DOORENBOS; KASSAM, 1979) or pressure head h (FEDDES et al., 1988), but also curvilinear shapes have been proposed (METSELAAR; JONG VAN LIER, 2007; JONG VAN LIER; VAN DAM; METSELAAR, 2009). The range of water contents in which soil water uptake by roots and transpiration by leaves occurs at a potential rate ($T_r = 1$) is called the constant rate phase. This phase corresponds to non-limiting soil water conditions. The range of water contents in which conditions are

not ideal (i.e., soil water content below a limiting value θ_{crit} (m^{-3} m^{-3}) or pressure head h more negative than a limiting pressure h_{crit} (m)) is called the falling rate phase ($T_r < 1$). The transpiration rate is assumed to be zero ($T_r = 0$) for soil water contents lower than the permanent wilting point (pressure head h_w (m) or soil water content θ_w (m^3 m^{-3})).

Studies show that values of θ_{crit} and h_{crit} depend on the root length density of plant (root length per soil volume, m m^{-3}) in addition to soil water conditions and potential transpiration. The root length density and pressure head of soil water determine whether the plant can or cannot extract water from the soil at a sufficient rate to support the potential transpiration (LASCANO; VAN BAVEL, 1984; WILLIGEN; VAN NOORDWIJK, 1987; HEINEN, 1997). Despite their importance, comparatively roots are the least studied, understood and appreciated, because they cannot be seen (HUGHES; JOLLEY; BROWN, 1992) and because one needs, in most cases, destructive methods for determining their properties.

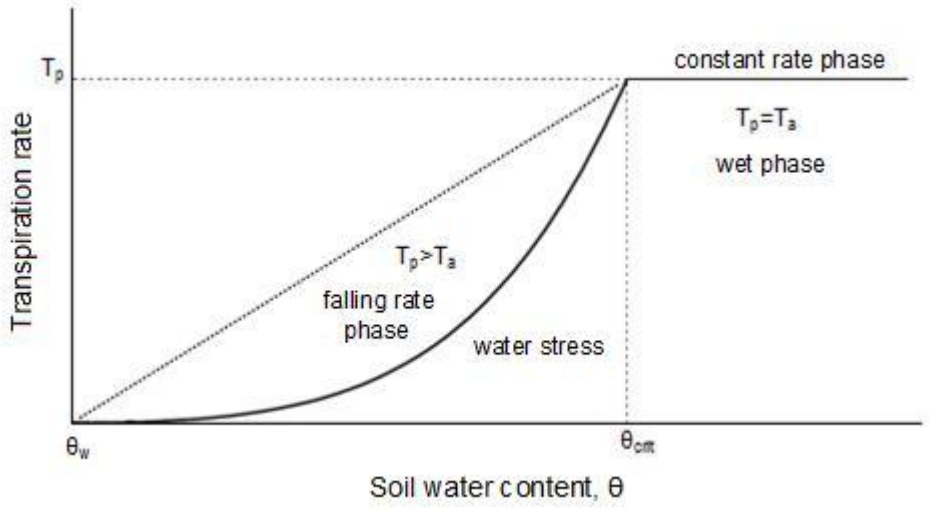

Figure 1 – Transpiration rate as a function of soil water content (θ) showing the constant rate phase ($\theta \geq \theta_{crit}$) and the falling rate phase ($\theta_w \leq \theta < \theta_{crit}$)

Matric flux potential M (m^2 d^{-1}) is defined as the integral of the hydraulic conductivity, $K(h)$ (m d^{-1}), over a pressure head interval, or equivalently as the integral of the diffusivity $D(\theta)$ (m^2 d^{-1}) over a soil water content (θ, m^3 m^{-3}) interval. If the permanent wilting point in terms of pressure head or soil water content is chosen as the lower bound of the integral sensitivity of values of M in the dry range is warranted. Then:

$$M = \int_{h_w}^{h} K(h)dh = \int_{\theta_w}^{\theta} D(\theta)d\theta \,. \qquad [2]$$

Jong Van Lier, Metselaar and Van Dam (2006) with contributions of Schröder et al. (2007) derived an expression to describe *M* as a function of the radial distance from the root surface *r* (m) at the beginning of the falling rate phase, based on the continuity equation for one-dimensional axisymmetric flux density *q*:

$$\frac{\partial \theta}{\partial t} = -\frac{q}{r} - \frac{\partial q}{\partial r} \,. \qquad [3]$$

From mass conservation, and ignoring the root volume, it follows that:

$$\frac{\partial \bar{\theta}}{\partial t} = -\frac{T_p}{z} \qquad [4]$$

where $\bar{\theta}$ is the average water content in the rhizosphere and *z* (m) is the rooting depth. Assuming that *dθ/dt* is not a function of *r*, eq. 4 can be generalized for any *r*:

$$\frac{\partial \theta}{\partial t} = -\frac{T_p}{z} \,. \qquad [5]$$

Eq. 5 can be combined with eq. 3 and with Darcy's equation to yield the following second-order differential equation:

$$-\frac{T_p}{z} = -\frac{q}{r} - \frac{\partial q}{\partial r} = \frac{\partial M}{r \partial r} + \frac{\partial^2 M}{\partial r^2} \qquad [6]$$

for which the following general solution is found:

$$M = -\frac{T_p}{4z} r^2 + C_1 \ln r + C_2 \qquad [7]$$

where C_1 and C_2 are integral constants.

Jong Van Lier, Metselaar and Van Dam (2006) and Schröder et al. (2007) used the following boundary condition to express the conditions at the beginning of falling rate phase:

$$M = 0;\ r = r_0 \qquad [8]$$

in which r_0 (m) is the root radius. The following boundary condition was used to represent the entire constant rate phase:

$$M = M_0;\ r = r_0 \qquad [9]$$

where M_0 (m^2 d^{-1}) is the matric flux potential at root surface. The second boundary condition is:

$$\frac{dM}{dr} = T_p \frac{r_m^2}{2zr_0}; r = r_0 \quad [10]$$

where r_m (m) is the (single root) rhizosphere radius, which is equal to the half mean distance between roots and is related to the root length density R (m m^{-3}) by:

$$R = \frac{1}{\pi r_m^2} \quad \text{or} \quad r_m = \sqrt{\frac{1}{\pi R}}. \quad [11]$$

Applying the boundary conditions (eq. 9 and 10) yields:

$$C_1 = \frac{T_p}{2z}(r_m^2 + r_0^2) \quad [12]$$

$$C_2 = \frac{T_p}{2z}\left[\frac{r_0^2}{2} - (r_m^2 + r_0^2) ln\, r_0\right] + M_0 \quad [13]$$

and

$$M - M_0 = \frac{T_p}{2z}\left[\frac{r_0^2 - r}{2} + (r_m^2 + r_0^2) ln \frac{r}{r_0}\right]. \quad [14]$$

Metselaar and Jong Van Lier (2007) showed by numerical analysis that *M(r)* under hydraulic limiting conditions has the same shape as under non-limiting conditions and may be described with an expression equivalent to eq. 14, with T_p replaced by the actual transpiration rate T_a and M_0 equal to the matric flux potential at permanent wilting point (M_w), which is equal zero by definition (eq. 2). Therefore, in the falling rate phase,

$$M = \frac{T_a}{2z}\left[\frac{r_0^2 - r^2}{2} + (r_m^2 + r_0^2) ln \frac{r}{r_0}\right]. \quad [15]$$

An equation similar to eq. 14 can be deduced to calculate the water uptake per layer, substituting the T_p/z term by the root water uptake per unit of thickness for layer z, S_{mod} (m^3 m^{-3} d^{-1}):

$$M_z - M_{0,z} = \frac{S_{mod}}{2}\left[\frac{r_{0,z}^2 - r^2}{2} + (r_{m,z}^2 + r_{0,z}^2) ln \frac{r}{r_{0,z}}\right] \quad [16]$$

in which the index z refers to the layer-dependent parameters.

At some radial distance from the axial center $\bar{r}$ (m), the water content is equal to the mean soil water content in the rhizosphere, and $\overline{M}$ (m^2 d^{-1}) is the corresponding matric flux potential. The coefficient a_z is defined by:

$$a_z = \frac{\bar{r}_z}{r_{m,z}}. \qquad [17]$$

Jong Van Lier, Metselaar and Dam (2006), using analytical methods, showed that the value of *a* is equal to $e^{-1/2}$ (≈ 0.607) for a soil with constant hydraulic diffusivity. For soils with Van Genuchten hydraulic functions, these authors showed by numerical simulations that the value of *a* is slightly lower (0.56 ± 0.06, with a median value of 0.53).

Substituting $\overline{M}$ and $\bar{r}$ into eq. 16 and incorporating eq. 17, yields:

$$\overline{M}_z - M_{0,z} = \frac{S_{mod}}{2}\left[\frac{r_{0,z}^2 - a_z^2 r_{m,z}^2}{2} + (r_{m,z}^2 + r_{0,z}^2)\ln\frac{a_z r_{n,z}}{r_{0,z}}\right]. \qquad [18]$$

Rewriting eq. 18:

$$S_{mod} = \frac{4(\overline{M}_z - M_{0,z})}{r_{0,z}^2 - a_z^2 r_{m,z}^2 + 2(r_{m,z}^2 + r_{0,z}^2)\ln(a_z r_{m,z} / r_{0,z})} = \rho_z(\overline{M}_z - M_{0,z}). \qquad [19]$$

From the above equation it can be seen that ρ_z is a weighing factor for matric flux potential dependent root water uptake, function of a_z, $r_{0,z}$ and $r_{m,z}$. Values of $r_{m,z}$ are related with root length density of a layer R_z through eq. 11. As can be seen in Figure 2 of Jong Van Lier et al. (2008), the sensitivity of ρ to variation of *a* is small, especially at low root length densities. Given this insensitivity and the small range of variation of *a* encountered in numerical studies, in agreement to the suggestion of Jong Van Lier et al. (2008) *a* may be considered independent of depth and equal to 0.53.

The sensitivity of ρ_z to root radius variations r_0 and root length density *R* is shown in Figure 3 of Jong Van Lier et al. (2008). Values of ρ increase with increasing *R* (reduction of r_m) and also with increasing r_0. However, the sensitivity to root length density is much higher than to root radius. The root length densities vary strongly between soil types and crops. In the surface layers, the range of reported values varies between 0.2 cm cm^{-3} in oat (*Avena* L.) and soybean (*Glycine max* L. Merrill), for example, to 40 cm cm^{-3} in some grass species (WILLIGEN; VAN NOORDWIJK, 1987). Both root length density and root radius vary between soil layers but on the contrary of

root length density, root radii are rarely measured (MATERECHERA et al., 1992). Due to the relative insensitivity of r_0, it can be assumed that for the practical application of eq. 19 estimations of root length density distribution are more important than estimations of root radius.

To derive eq. 19 and parameter ρ_z, Jong Van Lier et al. (2008) assumed that roots were homogeneously distributed in the soil, that is, each root length L explores a volume of soil equal to the volume of a cylinder with radius r_m and length L. Furthermore, the authors did not consider any difference in singular root characteristics and in the pressure head at root surface, and also the radial and internal resistances were considered equal for all roots. The soil-root contact was also considered to be perfect, in other words, no resistance to water flux at the soil-root contact was considered. All of these factors converge to an estimated water extraction greater than for a real root. To count for all these factors of overestimation of soil water uptake, an empirical parameter f_z was added to eq. 19 (FARIA et al., 2010):

$$S_{mod} = f_z \rho_z (\overline{M}_z - M_{0,z}). \qquad [20]$$

Values of f_z vary between 0 and 1, and f_z equal to 1 corresponds to a perfectly distributed root system composed by roots with same radius, without resistance to water flow and with a perfect soil-root contact. The parameter f_z can be interpreted to be an efficiency factor of the root system with respect to its water uptake.

The value of $\overline{M}_z$ is a function of soil water status and hydraulic properties (eq. 2), which makes $M_{0,z}$ the single unknown parameter. Assuming $M_{0,z}$ ($M_{0,z} = M_0$ for any layer z) a value independent of the layer, M_0 can be determined from known values of ρ_z, $\overline{M}_z$ and potential transpiration rate. A constant value of pressure head at the root surface, independent of depth, is often supposed (for example, KLUTE; PETERS, 1969; OZIER-LAFONTAINE et al., 1998), although in other studies (NIMAH; HANKS, 1973) the pressure head at the root surface is considered to vary with depth according to gravity and/or a friction loss term. Jong Van Lier et al. (2008) considered both effects negligible. Additionally, variation in soil hydraulic functions along depth might influence root water uptake during the constant rate phase, as they affect in $M_{0,z}$ (eq. 19). During the falling rate phase, however, $M_{0,z} = M_0 = 0$, independent of depth and soil hydraulic properties.

2.1.4 Plant-atmosphere transfer models

Empirical models of stomatal behavior have been developed based on experimental and observational studies. The models proposed by Ball (1987) and Leuning (1995) received great attention, testing, acceptance and application. These models describe the dependence of stomatal conductance by the net CO_2 assimilation, by the relative humidity or water vapor pressure deficit, and by the CO_2 concentration in the leaf. Applications of these models to CO_2 exchange studies resulted in coupled equations for carbon assimilation and stomatal conductance. The correct parameterization of the models provides a good correlation between simulated and observed stomatal conductance and carbon assimilation. However, the empirical nature of these models makes it difficult to extrapolate them to different environmental conditions. For example, the effect of soil water deficit on stomatal conductance is not explicitly included in these models. Therefore, it is not possible to apply the model to different soil hydraulic conditions. The depression of photosynthesis or transpiration at midday as a strategy for water conservation is observed in some species but not in others. This difference in plant behavior cannot be explained by the model proposed by Ball (1987).

The numerical schemes of soil-vegetation atmosphere transfer (SVAT) models employed in meteorology are designed to describe the basic processes of surface evaporation along with the partition of water between the plant transpiration, drainage, superficial runoff and soil water content. The SVAT model ISBA, for example, is used in simulations for operational weather forecast in France and in the climate model ARPEGE (Action de Recherche Petite Echelle - Grande Echelle) (NOILHAN; PLANTON, 1989; NOILHAN; MAHFOUF, 1996). In this SVAT weather model, as in others (e.g. NIYOGI; RAMAN, 1997), the description of biological control of transpiration is made by a simple empirical parameterization of stomatal conductance g_s, adapting the algorithm proposed by Jarvis (1976). By this method of parameterization it is assumed that environmental parameters act independently on g_s. The description of the temperature dependence on stomatal conductance can be based on leaf temperature when soil water conditions are non-limiting, or alternatively on air temperature, eliminating the requirement of non-limiting soil water conditions.

A SVAT model is able to describe the effect of radiative and atmospheric forcing on g_s. The temperature and humidity at a reference level and the net radiation are used to calculate g_s. In general, the parameterization of Jarvis (1976) used by ISBA model provides good quantitative estimations of transpiration rate. However, the stomatal response to air humidity is poorly simulated and usually requires a flux analysis and in situ measurements of stomatal conductance to calibrate the model. In fact, it is assumed that various environmental factors act independently on g_s, while measurements suggest that interactions may occur (COLLATZ et al., 1991; JACOBS, 1994; JACOBS; VAN DEN HURK; BRUIN, 1996). Another limitation of this kind of parameterization is the lack of feedback to the atmospheric CO_2 concentration, especially in climatic studies. In fact, an increase in CO_2 concentration induces a physiological response of plants by reducing g_s. This effect can influence the energy and water balances of a surface on various time scales of changes in CO_2 concentration: daily, seasonal, and especially secular. This is why CO_2 physiological parameterizations that consider the effect of CO_2 are more appropriate for the parameterization proposed by Jarvis (1976). This is particularly important for simulations of global change (BETTS et al., 1997) in which the response of vegetation-climate-CO_2 interaction needs to be described.

As an alternative to the parameterization of Jarvis (1976) and Stewart (1988), the parameterization of the g_s in SVAT models can also be performed by semi-empirical physiological models of CO_2 assimilation by leaves in which stomatal conductance is deduced from the net CO_2 assimilation rate A (mg m^{-2} s^{-1}) (COLLATZ et al., 1991; JACOBS, 1994; JACOBS; HURK; BRUIN, 1996), the so-called Ag_s models. In this case, the physiological responses to external variables and to the nonlinear interactions between them are treated. Stomatal conductance, for example, can be calculated as a function of CO_2 assimilation, since observations show a strong correlation between water use and CO_2 assimilation (COWAN, 1982; JACOBS, 1994). This observed correlation is associated with a quasi-conservative ratio between intercellular CO_2 concentration (C_i, mg m^{-3}) and the concentration of CO_2 in the air near to the leaf surface (C_s, mg m^{-3}).

Therefore, an appropriate model for describing the stomatal behavior must contain parameterizations of stomatal responses to each of these and other factors such

as air temperature, humidity and radiation. Moreover, one of the variables can influence the sensitivity of stomata to other factors. Therefore, a model of stomatal conductance should also describe synergistic interactions between these different stimuli. The Ag_s physiological model proposed by Jacobs (1994) and Jacobs, Hurk and Bruin (1996) contains parameterizations that describe most of these interactions, and uses the specific humidity deficit between leaf and ambient air D_s as the descriptor for the moisture difference between leaf and air. D_s (g kg^{-1}) is defined as:

$$D_s = q_{sat}(t_s) - q_a \qquad [21]$$

in which $q_{sat}(t_s)$ is the specific humidity at saturation (g kg^{-1}) as a function of surface temperature t_s (in this case equal to canopy temperature t_{canopy}) and q_a is the specific humidity of the atmospheric air near leaves (g kg^{-1}).

In the model proposed by Jacobs (1994) and Jacobs, Hurk and Bruin (1996), the relationship between stomatal conductance to water vapor g_s, expressed in mm s^{-1}, and net CO_2 assimilation A (mg m^{-2} s^{-1}) is given, as a first approximation, by:

$$g_s = 1.6 g_{sc} = 1.6 \frac{A}{C_s - C_i} \qquad [22]$$

where g_{sc} (mm s^{-1}) is the stomatal conductance to CO_2. The difference of CO_2 concentration between the leaf surface and the intercellular air spaces in the leaves (C_s - C_i, mg m^{-3}) is parameterized as a function of specific humidity deficit between leaf and air D_s by taking the ratio f:

$$f = f_o \left(1 - \frac{D_s}{D_{max}} \right) \qquad [23]$$

and

$$C_i = fC_s + \Gamma(1 - f)\,. \qquad [24]$$

Here Γ is the CO_2 compensation concentration (mg m^{-3}), f_o is the value of f at $D_s = 0$, and D_{max} is the value of D_s when stomata are completely closed. Air in the stomata is considered saturated with water vapor, i.e., the water vapor pressure in the stomata is equal to the saturation pressure of water vapor at mean canopy temperature.

Physiological parameters governing the magnitude of g_s and its sensitivity to D_s are, respectively, the mesophyll conductance g_m and the maximum deficit of water vapor

between leaf and air D_{max}. The parameter g_m affects the highest possible stomatal conductance, and D_{max} represents the sensitivity of stomatal aperture to humidity.

The first approximation to the CO_2 stomatal conductance g^*_{sc} is estimated using a relationship of flux gradient modified to consider the effect of water vapor deficit in the stomatal aperture and accurately describe both extremes of high and low light intensities:

$$g^*_{sc} = \frac{A - A_{min}\dfrac{D_s}{D_{max}}\dfrac{A_g}{A_{m,g}} + R_d\left(1 - \dfrac{A_g}{A_{m,g}}\right)}{C_s - C_i}. \quad [25]$$

Here, $A_{m,g} = A_m + R_d$ and A_g is the gross CO_2 assimilation (= $A + R_d$) (both in mg m^{-2} s^{-1}). A_{min} (mg m^{-2} s^{-1}) represents the residual photosynthetic rate (at high light intensity) associated with transfer by cuticle when stomata are closed as a function of high humidity deficit ($D_s = D_{max}$), and R_d (mg m^{-2} s^{-1}) is the dark respiration.

Assuming that the ratio between stomatal conductance to water vapor and CO_2 equals the diffusivity ratio (1.6), g_s is given by:

$$g_s = 1.6 g^*_{sc} \quad [26]$$

and the transpiration rate T_1 (mg m^{-2} s^{-1}) is given by:

$$T_1 = \rho_{air} g_s D_s \quad [27]$$

where ρ_{air} is the density of air at constant pressure (kg m^{-3}). In this case, T_1 is calculated to refine the estimation of CO_2 conductance since the CO_2 diffusion interacts with water vapor diffusion. This effect is included by:

$$g_{sc} = g^*_{sc} + T_1 \frac{M_{air}}{\rho_{iar} M_{wa}} \frac{C_s + C_i}{2(C_s - C_i)} \quad [28]$$

and subsequently eq. 26 is recalculated substituting g^*_{sc} by g_{sc}. M_{air} and M_{wa} are the molar mass of dry air and the molar mass of water (g mol^{-1}), respectively. The transpiration rate of a leaf T_{Ags} is determined by the total leaf resistance to the water vapor flux r_t:

$$T_{Ags} = \frac{\rho_{air} D_s}{r_t} \quad [29]$$

$$r_t = \frac{1}{g_t} = \frac{1}{g_s} + \frac{1}{g_m} + \frac{1}{2g_{bl}} \quad [30]$$

where g_{bl} is the boundary layer conductance around leaf calculated by:

$$g_{bl} = k\left(\frac{u}{W_l}\right)^{0.5} \quad [31]$$

In which k is an empirical constant (5.6 mm $s^{-0.5}$), u is the wind speed (mm s^{-1}) and W_l is the leaf width parallel to wind (assumed to be 100 mm). The cuticular conductance was considered negligible as compared to other conductances and was not included in eq. 30. Also in this equation, g_{bl} is multiplied by 2 to account for both sides of leaves.

Jacobs (1994) deduced the parameterizations assuming plant roots were deep and plants did not suffer from water stress during the observations. Calvet et al. (1998) and Ronda, Bruin and Holtslag (2001) proposed modifications that take into account the relationships between soil water content and mesophyll conductance g_m and the gross assimilation rate of CO_2 A_g, respectively. These relationships, usually linear, were developed based on empirical considerations and, therefore, fail to describe the responses of plants to soil water content in a mechanistic way.

2.1.5 The Common Bean crop (*Phaseolus vulgaris* L.)

Common beans have a growth development that can be divided in two phases: the vegetative phase and the reproductive phase. The vegetative stage is characterized by the number of nodes on the main stem, while the reproductive stage is described according to the appearance of pods and grains. According to Silveira and Stone (1981) and Steinmetz (1984), the highest consumption of water by bean plants occurs during flowering. Beans are cultivated in regions with temperatures between 10°C and 35°C, although most of the commercial production originates from regions with air temperature between 17°C and 25°C, the temperature range considered appropriate for the species (PORTES, 1996). High air temperature with intense radiation increases transpiration rate and can cause water stress, whereas temperatures below 12°C can cause abortion of flowers decreasing the total production. In addition, areas with relative humidity and air temperature above 70°C and 35%, respectively, are more prone to diseases. The water consumption of the bean plants varies per location and it is usually estimated by

measuring a field or lysimeter water balance. In Piracicaba, Encarnação (1980) found an average daily water consumption of 4.37 mm d^{-1}, while Bergamaschi et al. (1989) and Santos and André (1992) observed consumptions of 3.80 mm d^{-1} and 4.01 mm d^{-1}, respectively.

The radiation intensity significantly influences the photosynthetic rate of the plants. The saturation limit of solar radiation varies with plant age and type and regions with solar radiation between 150 W m^{-2} and 250 W m^{-2} are considered ideal for growing beans. Being a C3 plant, beans saturate photosynthetically at relatively low light intensities.

The soil water status directly affects the yield of bean plants depending on the development stage. According to Doorenbos and Pruitt (1976), the periods of flowering and pod appearance are more sensitive to drought than the vegetative growth phase, which is more sensitive than the pod ripening stage. Water deficit also affects the phenology of beans: if it occurs after the appearance of the first pods, the maturation is anticipated; if it occurs during the formation of flower buds and blooming, the cycle is prolonged (BERGAMASCHI et al., 1988). Furthermore, studies have shown that bean plants under water stress increased stomatal resistance and respiration rate, and decreased net photosynthetic rate, plant height and leaf area (COSTA; LOPES; OLIVA, 1991). The reduction of leaf area, i.e. the photosynthetic surface, implies a decrease in dry matter accumulation.

The climate of São Paulo State is favorable to the cultivation of common bean. The climate of Piracicaba region is classified as humid subtropical, with dry winters and hot summers. According to the Köppen classification (KÖPPEN, 1900; GEIGER, 1954) it is a Cwa climate. The mean maximum air temperature in the warmest months reaches 29°C, while the average minimum air temperature is equal to 10.5°C in the winter months. The annual rainfall is approximately 1300 mm, while in the winter months the monthly accumulated values are close to 25 mm. In these months, beans should be grown with irrigation to meet plant water requirements.

2.2 Material and methods

In this section the applied methodology and the materials used in this study are described. The water conditions in soil and atmosphere were monitored under field conditions during the growing season of a Common Bean (*Phaseolus vulgaris* L.) crop and correlated to plant water stress characterized by measurements of canopy temperature. The variables of interest, specifically the soil water pressure head, air temperature and humidity and canopy temperature were measured regularly at short intervals. Other variables were measured occasionally: the transpiration rate and stomatal conductance.

2.2.1 Field experiment

The field experiment was conducted with a Common Bean crop (*Phaseolus vulgaris* L.), cultivar Pérola. The experimental site was located at the “Luiz de Queiroz” College of Agriculture – ESALQ/USP (22° 42’ 30” S, 47° 38’ 00” E, 546 m above sea level) and the soil at the location is classified as a Rhodic Kanhapludalf, according to the USDA Soil Taxonomy. The automatic meteorological observatory of ESALQ/USP is located at a distance of 20 m from the experimental site and provided all meteorological data during the experiment. The agronomic operations like soil preparation, sowing and crop operations were done with the support of Department of Crop Science of ESALQ/USP.

The experiment was conducted between June and September, 2010. The area of approximately 990 m^2 (22 m x 45 m) was divided into two plots (22 m x 22.5 m) (Figure 2). A sprinkler irrigation installation was mounted at the site. One plot was irrigated during the whole crop cycle (fully irrigated treatment - FI), while the other one was subject to water stress in the reproductive phase (deficit irrigated treatment - DI).

During the 92 days of field experiment, rainfall was only registered on July 13, 14 and 15, with an accumulated height of 62.9 mm (Figure 3). There were also rain on September 7, (12.8 mm) and September 21 (38 mm), during the ripening period. In total, the fully irrigated treatment received 426.5 mm of water and the deficit irrigated treatment received 314.5 mm. In the periods between August 2 and 23 and between

August 25 and September 1, only the fully irrigated treatment was irrigated. On August 24, a small irrigation gift was applied to the deficit irrigated treatment to enable the measurement of transpiration by porometry. These measurements require a relative humidity between 20% and 80% in the sensor chamber, while the relative humidity, before irrigation, was about 9%. During a month, between August 2 and September 2, there was no occurrence of rain in the experimental area, in favor of the intended treatments for this study. Irrigation was applied six times in the fully irrigated treatment (~ 127 mm) and once in the deficit irrigated treatment (~ 15 mm). This month was defined as the interval of analysis of field experiment. In the fully irrigated treatment, the average plant height during the study period was 0.6 m, whereas in the deficit irrigated treatment it was 0.55 m. These values were obtained by averaging three measurements made on 10 plants per treatment on August 4 and 19 and on September 2.

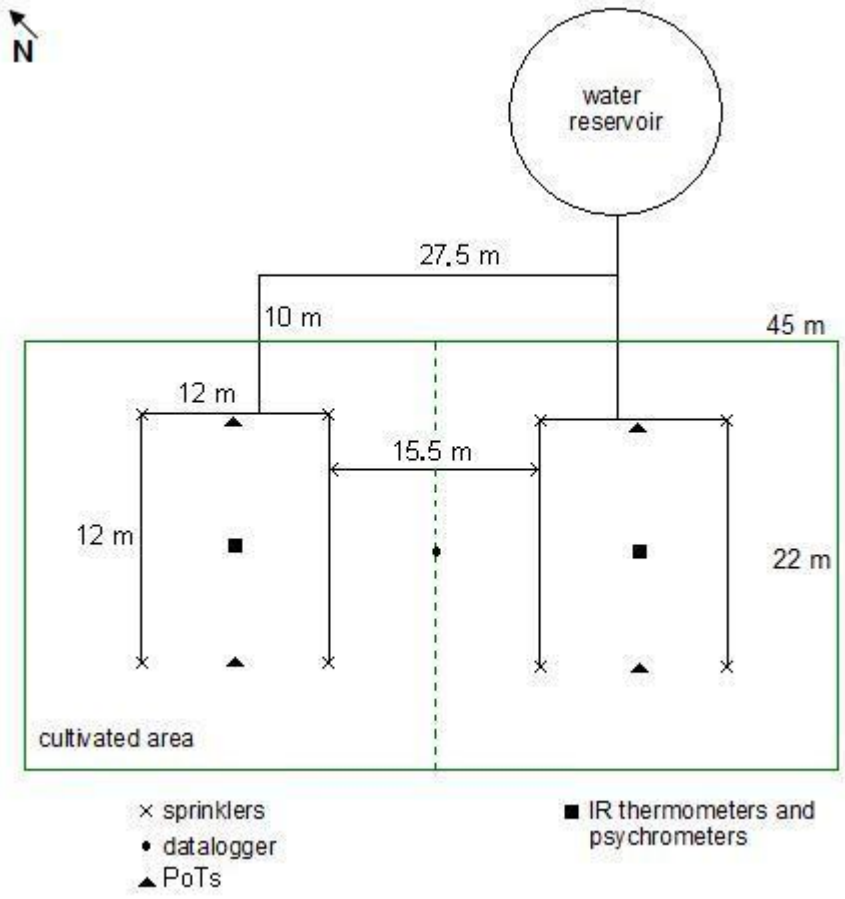

Figure 2 – Spatial distribution of equipments and irrigation system in field area (PoTs: Polymer Tensiometers; IR thermometers: Infrared thermometers)

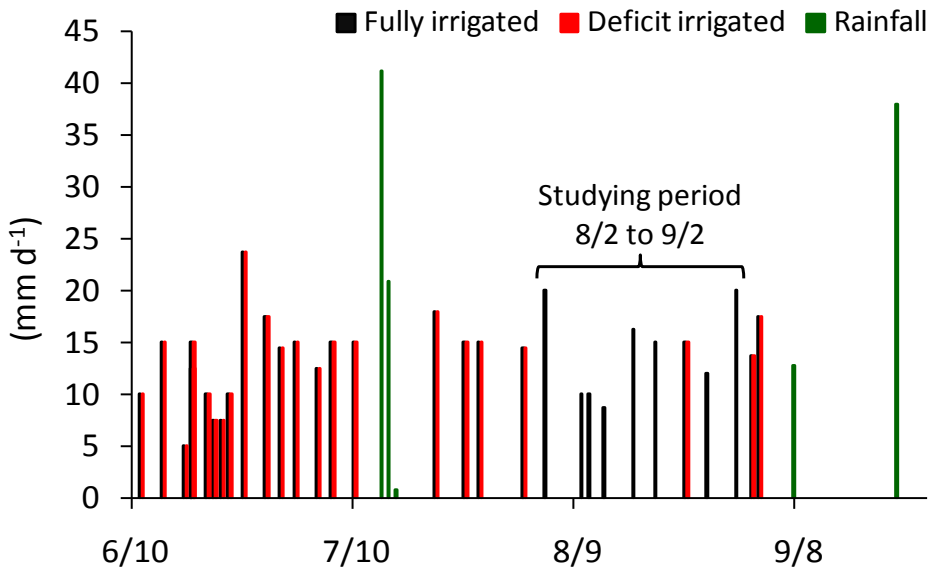

Figure 3 – Irrigation (mm d^{-1}) and rainfall (mm d^{-1}) during the field experiment as a function of date (m/dd/2010)

2.2.2 Bean crop in the field and agronomic operations

Before the experiment, the area was covered by several weed species; to eliminate them, a cutting, two plowings and three harrowing were performed before sowing. On May 18 a pre-planting herbicide was applied (Premerlin 600 EC®) at a dose of 4.0 l ha^{-1}.

The bean seeds were previously treated with fungicides Carbendazim and Tiram (Desoral Plus®), 200 ml per 100 kg of seed. The area was mechanically grooved with an interrow distance of 0.45 m, and a fertilizer was applied: 25 kg of N, 85 kg of P_2O_5 and 50 kg of K_2O per hectare. The sowing was done manually on June 11 at a seed density of about 14 seeds per meter.

At 41 days after sowing, 65 kg ha^{-1} of N was applied and the next day the area was completely deweeded. At 49 days after sowing, the fungicide Mancozeb (Manzate 800®) was applied at a dose of 3 kg ha^{-1} and the insecticide Chlorfenapyr (Pirate®) at a dose of 1 l ha^{-1}. Harvest was done manually at 92 days after sowing, on September 23.

2.2.3 Meteorological data

The weather station of ESALQ/USP provided data of rainfall (mm), photosynthetic active radiation (*PAR*, W m^{-2}), net radiation (R_n, W m^{-2}), wet bulb temperature (t_{wb}, °C) and wind speed (u, m s^{-1}). The daily maximum of the last four variables are shown in Figures 4 and 5. Although measurements of relative humidity and air temperature (psychrometry) were available from the weather station, they were also performed in the center of each of the experimental treatments. Psychrometers manufactured by Campbell Scientific, model CS215L9®, were connected to a data-logger CR1000®. Measurements of relative humidity were carried out instantaneously every 30 minutes, while the reported air temperatures are the average of measurements during the corresponding time interval.

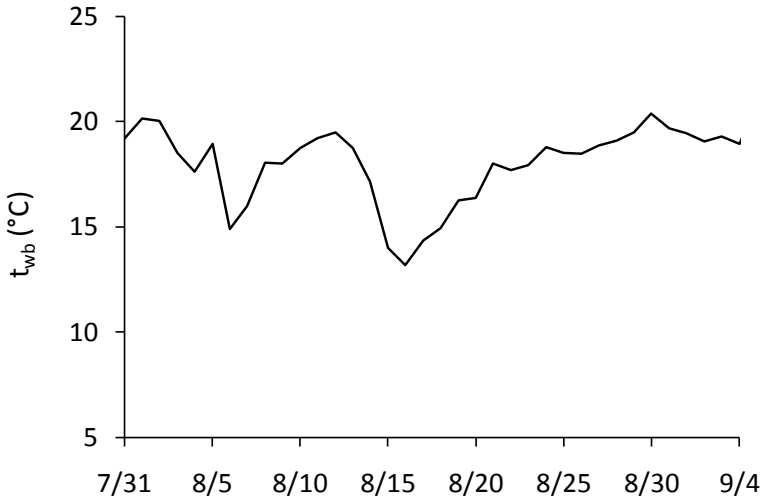

Figure 4 – Maximum daily values of wet bulb temperature (t_{wb}) measured at ESALQ/USP meteorological station as a function of date (m/dd/2010)

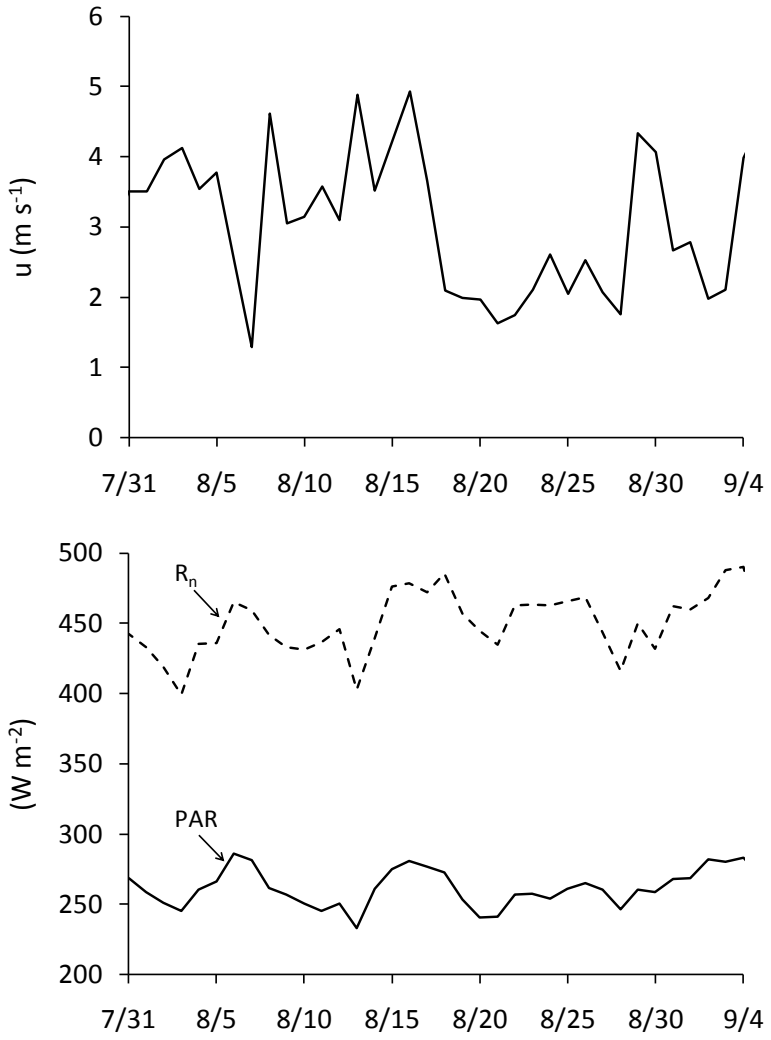

Figure 5 – Maximum daily values of wind speed (*u*) (above), net radiation (R_n) and photosynthetically active radiation (*PAR*) (below) measured at ESALQ/USP meteorological station as a function of date (m/dd/2010).

2.2.4 Leaf area

The leaf area index (*LAI*) was estimated by an indirect and nondestructive method with a ceptometer called Plant Canopy Analyser, model LAI-2000® from Li-Cor. This equipment consists of two parts: a control unit (LAI-2070®), which collects data, performs calculations of *LAI* and stores data, and an optical sensor (LAI-2050®), in which a lens projects the radiation inside the instrument which is then reflected by a mirror in the direction of silicon detectors, arranged in concentric rings. In this optical sensor, radiation focuses each of the rings in five different zenith angles (7°, 23°, 38°, 53° and 68°), obtaining a quantitative measurement of radiation penetrating the canopy.

The sensor collects the diffuse solar radiation that reaches above and below the canopy at five different angles simultaneously, and the *LAI* is estimated using the attenuation of radiation in these different angles.

The measuring procedure consisted of a reading above the crop canopy followed by five internal readings (below the canopy) in the center of each treatment. Measurements at five locations along the rows, with the sensor in the same direction, were taken as follow: one between the rows and the other four at plant lines of each treatment, in order to avoid the same plants to be overrepresented. A measure was taken using five repetitions of the above described procedure. A mask of 45° which directs or restricts entry of radiation was used to cover the lens of the optical sensor, in order to avoid interferences, for example, the influence of the operator's body. According to the manual of the equipment, it is recommend to be used with cloudy sky and scattered radiation, when there is little scattering of electromagnetic radiation by the leaves. Therefore, on clear days the measurements were made in the early morning or late afternoon when the solar elevation angle is low and there is less direct radiation.

The *LAI* was estimated five times during the experimental period, on August 4, 12, 19 and 27 and on September 2. The dots and asterisks of Figure 6 represent the five measurements, while lines shows the daily values of *LAI* obtained from a linear interpolation of measured data. It is observed in this figure that at the beginning of the sampled period the values of *LAI* of the two treatments were similar because both treatments were being irrigated. At later stages, the *LAI* of plants of the deficit irrigated treatment was reduced. The daily values of *LAI* measured by the ceptometer and obtained by linear interpolation are presented in Table 1.

Table 1 – Daily values of leaf area index (*LAI*). Bold-font values were measured; non-bold-font values were obtained by linear interpolation of measured values

Date	*LAI* (m^2 m^{-2})		Date	*LAI* (m^2 m^{-2})	
	Fully irrigated	Deficit irrigated		Fully irrigated	Deficit irrigated
8/4/2010	**3.37**	**3.55**	**8/19/2010**	**4.56**	**3.74**
8/5/2010	3.47	3.67	8/20/2010	4.63	3.58
8/6/2010	3.58	3.79	8/21/2010	4.69	3.43
8/7/2010	3.68	3.90	8/22/2010	4.76	3.27
8/8/2010	3.78	4.02	8/23/2010	4.82	3.12
8/9/2010	3.88	4.14	8/24/2010	4.89	2.96
8/10/2010	3.99	4.26	8/25/2010	4.95	2.80
8/11/2010	4.09	4.37	8/26/2010	5.02	2.65
8/12/2010	**4.19**	**4.49**	**8/27/2010**	**5.08**	**2.49**
8/13/2010	4.24	4.38	8/28/2010	5.18	2.55
8/14/2010	4.30	4.28	8/29/2010	5.29	2.61
8/15/2010	4.35	4.17	8/30/2010	5.39	2.68
8/16/2010	4.40	4.06	8/31/2010	5.49	2.74
8/17/2010	4.45	3.95	9/1/2010	5.60	2.80
8/18/2010	4.51	3.85	**9/2/2010**	**5.70**	**2.86**

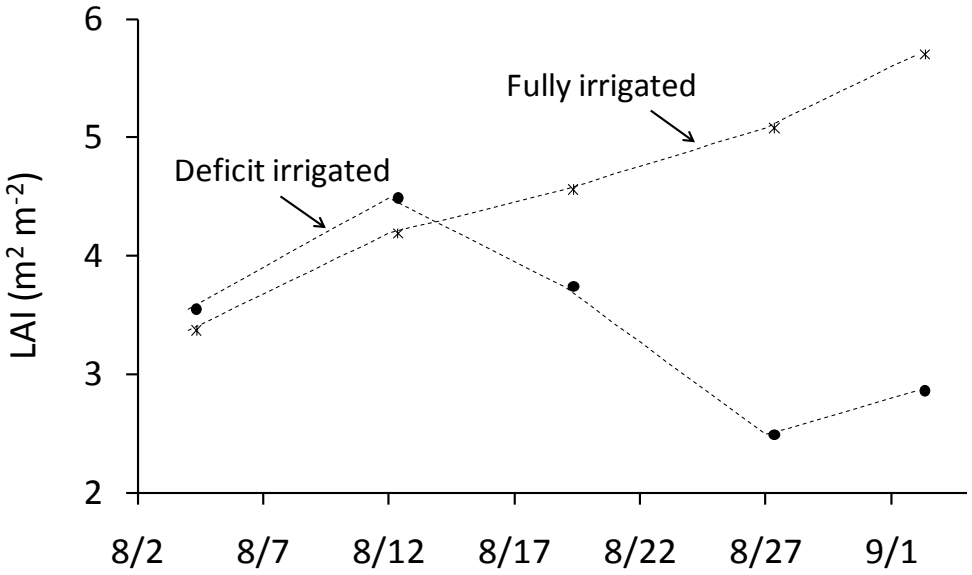

Figure 6 – Leaf area index (*LAI*) measured by a ceptometer (dots and asterisks) and linearly interpolated (dashed lines) as a function of date (m/dd/2010)

2.2.5 Detection of water stress

Canopy temperature, used as an indicator of water stress, was measured by two automated infrared thermometers (one at a central location at each treatment) of Apogee Instruments, model SI-111®, which were connected to the data-logger CR1000®. These sensors have an accuracy of ±0.2°C and a measuring range from -10°C to 65°C. The canopy temperature t_{canopy} is the result of an average of measurements over a time period of 30 minutes. In order to eliminate the effects of application of irrigation on temperature difference between canopy and air ($\Delta t_{canopy\text{-}air}$), *VPD* and soil properties, data obtained during the night and during irrigation application were eliminated.

The methodology applied in this study to identify water stress in plants of the non-fully irrigated treatment is based on three procedures. The first one consists of a linear regression between data of *VPD* and $\Delta t_{canopy\text{-}air}$. Such analysis was made due to the linear relationship between *VPD* and $\Delta t_{canopy\text{-}air}$ observed in plants without water stress as reported in literature (e.g., ERHLER, 1973; IDSO et al., 1981; SHIMODA; OIKAWA, 2006). The *VPD* is calculated from the difference between the water vapor saturation pressure e_s and the actual water vapor pressure e_a in the atmospheric air. Using the

Tetens (1930) equation, e_s is calculated from air temperature measured in each irrigation treatment; and from that e_a is calculated knowing the relative humidity.

In the second stage of water stress detection, t_{canopy} of both treatments was compared to the wet bulb temperature t_{wb} (°C), which represents the temperature at which a free water surface evaporates adiabatically. The temperature of a healthy transpiring crop to which sufficient water is supplied (i.e., a non-stressed canopy) is greater than the wet bulb temperature, but follows t_{wb} variations (WANJURA; UPCHURCH, 1997; MAHAN et al., 2005). When water supply to plants is limiting transpiration, t_{canopy} progressively increases in relation to t_{wb}.

Finally, the onset of plant water stress in the deficit irrigated treatment was determined by analyzing the difference $(\Delta t_{canopy-air})_{DI}$- $(\Delta t_{canopy-air})_{FI}$ and the difference VPD_{DI} - VPD_{FI}. When both differences became positive and did not return to negative values, plants of the deficit irrigated treatment were supposed to be under water stress.

The detection of water stress in plants of both irrigation treatments were done using the Ag_s model proposed by Jacobs (1994) and Jacobs, Van Den Hurk and Bruin (1996). The main objective of this analysis is to evaluate if plants can suffer water stress at under high atmospheric demand, even when there is sufficient water supply to the plant roots, as in the fully irrigated treatment. The Ag_s model estimated A, g_s and T_{Ags} to identify a midday dip in photosynthesis and transpiration (also called the afternoon dip), as a consequence of increased water vapor pressure deficit between leaves and atmospheric air.

2.2.6 Transpiration rate and stomatal conductance measurements

Leaf transpiration and stomatal conductance were measured with a dynamic equilibrium porometer by Li-Cor equipments, model LI-1600®. Leaf transpiration rate (mg m^{-2} s^{-1}) and stomatal conductance to water vapor (mm s^{-1}) on both sides of fully expanded leaves directly exposed to solar radiation were measured. A complete reading consisted of 10 repetitions on different plants of the same treatment between 11:00 AM and 2:30 PM. Observations were made during 11 days between August 10 and 23. The stomatal conductance of each leaf was calculated by the sum of stomatal conductances obtained on each side of the same leave.

2.2.7 Soil water status

Soil water pressure head (*h*) was measured using polymer tensiometers (PoT) (BAKKER et al., 2007; VAN DER PLOEG et al., 2008; ROOIJ et al., 2009). PoTs were installed at depths of 0.05 m (representing the soil layer between 0-0.1 m), 0.15 m (representing 0.1-0.2 m) and 0.3 m (representing 0.2-0.4 m) at two locations in each irrigation treatment. Measurements were written to memory every 30 minutes.

The polymer tensiometer is a novel instrument developed at WUR, The Netherlands, and allows automated measurements of soil water tension throughout the range of interest in environmental studies (*h* values of -160 m or less, with an accuracy of 0.2 m), far beyond the range covered by conventional tensiometers.

Although indirect measurements of water soil tension in dry soil are possible using, for example, TDR equipments to measure soil water content, there are serious restrictions in detailed studies on energy and water movement in soil because of hysteresis effects, and the introduction of errors associated with soil water retention curve, especially in drier soil. Especially within the rhizosphere, water contents are subject to frequent cycles of drying/wetting associated to hysteresis. The hysteretic discrepancy between *h* values at the same water content is a factor of great uncertainty when water content is determined to calculate *h*, as in the case of TDR measurements. Polymer tensiometers mitigate this problem by performing direct measurement of pressure head.

PoTs consist of a ceramic cone, stainless steel cup containing polymer, a pressure transducer and a data storage unit (Figure 7). A sensor measures the temperature at the base of polymer chamber in a range between 0 and 40°C with an accuracy of 0.01°C.

Figure 7 – Ceramic porous cone, stainless steel cup containing polymer and a pressure transducer of a polymer tensiometer (PoT) (approximate size indicated)

The operating principle of the polymer tensiometer is based on a concentrated hydrophilic polymer solution. Soluble polymer molecules are trapped in a steel reservoir by a ceramic cone that is permeable to the soil solution but impermeable to the polymer. The positive pressure in a PoT can easily be related to the negative soil water pressure head.

To determine the pressure head *h*, the positive pressure must be corrected for effects of temperature (BAKKER et al., 2007):

$$P_{cor} = P_m - \frac{t_m - t_{ref}}{Coef_t} \quad [32]$$

where P_{cor} (bar) is the temperature corrected pressure, P_m (bar) is the pressure measured by the PoT, t_m (°C) is the measured temperature, t_{ref} (°C) is the reference temperature obtained by the average temperature when the PoT are placed in water for 24 hours, and $Coef_t$ (bar °C^{-1}) is a coefficient of pressure variation as a function of temperature determined in the laboratory and specific to each tensiometer. Values of $Coef_t$ for the PoTs used in this study are presented in Table 2. The real pressure P_{real} (bar) is given by the difference between P_{cor} and the reference pressure P_{ref} (bar), obtained analogous to t_{ref}. The pressure head *h* is then given by the conversion of P_{real} in units of bar to units of m.

Table 2 – PoT temperature coefficients for tensiometers used in this study

Treatment	Observation point	Installation depth	PoT identification	Coefficient (bar °C^{-1})
Irrigated (FI)	1 (FI 1)	0.05 m	3Pb	0.173202324
	1 (FI 1)	0.15 m	3Kb	0.166866057
	1 (FI 1)	0.3 m	2Zf	0.182635154
	2 (FI 2)	0.05 m	2Kf	0.184305049
	2 (FI 2)	0.15 m	2Ed	0.158326915
	2 (FI 2)	0.3 m	3Oe	0.152656049
Deficit irrigated (DI)	1 (DI 1)	0.05 m	2Rb	0.194994297
	1 (DI 1)	0.15 m	6177	0.229699764
	1 (DI 1)	0.3 m	2843	0.196226960
	2 (DI 2)	0.05 m	6170	0.215976723
	2 (DI 2)	0.15 m	6180	0.214003910
	2 (DI 2)	0.3 m	6169	0.206374248

A correction in the final data of h is needed when an experiment with polymer tensiometers involves a longer period, as was the case of the field experiment conducted in this study. This procedure is necessary to mitigate the effect of small leaks of polymer or increase of salt content in the chamber containing polymer, which can be caused by the change of osmotic pressure with time. The correction is applied to the temperature and pressure reference values. t_{ref} and P_{ref}; they are determined before and after the experiment, and are then assumed to have changed linearly with time. Consequently, each value of h is determined from values of t_{ref} and P_{ref} that are a function of time.

2.2.8 Soil hydraulic properties

Soil hydraulic properties (hydraulic conductivity and soil water retention) for the soil from the experimental area were determined using the method of Wind (1966) and Schindler and Müller (2006). The method is based on the monitoring of pressure head at some depths within an evaporating soil sample accommodated in a volumetric ring. The method was adapted and conventional tensiometers were replaced by polymer tensiometers (DURIGON et al., 2011). Thus, the soil hydraulic properties could be determined over the entire range of pressure head down to the permanent wilting point.

The theory of the method can be described as follows: a vertical column is filled with porous material ("soil") with height L (m) and area A_r (m^2). The column is equipped with n tensiometers at depths z_1, z_2 ... z_n. The column with soil is closed at its bottom, losing water by evaporation only at its upper surface. At k different moments (t_1, t_2, ..., t_k), observations of pressure head at n positions equipped with tensiometers are made, and the pressure head $h_{i,j}$ is the value of h at depth z_i and time t_j. Similarly as Schindler and Müller (2006), a linear decrease of water content in the column from the bottom to the top is assumed. Based on the Darcy-Buckingham law, it is demonstrated that, under these conditions, the soil hydraulic conductivity K (m d^{-1}) at the average pressure head h between depths z_i and z_{i+1} during the time interval t_j to t_{j+1} is equal to:

$$K(h) = \frac{V_E}{A_r \nabla \Delta t}\left[1 - \frac{z_i + z_{i+1}}{2L}\right] \quad [33]$$

where $\Delta t = t_{j+1} - t_j$ (s) is the observation time interval, V_E (m^3) is the evaporated water volume during Δt, and ∇ is the mean hydraulic gradient at Δt given by

$$\nabla = \frac{(h_{i,j} - h_{i+1,j}) + (h_{i,j+1} - h_{i+1,j+1})}{2\Delta z} - 1 \quad [34]$$

with $\Delta z = z_{i+1} - z_i$ (m).

At k instants (t_1, t_2, ..., t_k) at which pressure head is measured, the total mass of the experimental setup is made, enabling the calculation of mass variation between observation times. At the end of the experiment, the mass of the water remaining in the soil column is determined by the gravimetric method, drying the soil at 105°C. This mass of remaining water, together with mass variations between observations, allows to calculate the k water masses (m_1, m_2, ..., m_k) (kg) for each observation time.

To mathematically describe the soil water retention curve, a functional relation $\theta = \theta(h)$ and $K = K(h)$ must be chosen. We used the Van Genuchten (1980) equation system given by

$$\Theta_{i,j} = [1 + |\alpha h_{i,j}|^{n}]^{(1/n)-1} \quad [35]$$

$$ln\, K_{i,j} = ln\, K_s + \lambda\ ln\, \Theta_{i,j} + 2\, ln[1 - [1 - \Theta^{1/m}]]^{m} \quad [36]$$

where $\Theta_{i,j} = (\theta_{i,j} - \theta_r)/(\theta_s - \theta_r)$, $\theta_{i,j}$ is the soil water content at depth z_i and time t_j, θ_s and θ_r are the saturated and residual soil water contents, respectively, K_s (m d^{-1}) is the saturated soil hydraulic conductivity, and α (m^{-1}), n, m and λ are empirical parameters of the equations.

Using an iterative procedure, parameter values that best matched the experimental observations were adjusted. Initially, arbitrary values are assigned to the parameters, i.e., $\theta_s = 0.5$ m^3 m^{-3}, $\theta_r = 0.1$ m^3 m^{-3}, $\alpha = 1.5$ m^{-1} and $n = 2.0$. By eq. 35, each observation of pressure head was converted into water content and the water contents estimated this way for the n tensiometers positions allowed an estimate of total water mass $\hat{m}_j$ (kg) in the soil at time j by

$$\hat{m}_j = \rho_w \frac{A_r}{2}\left[\theta_{1,j}(z_1 + z_2) + \sum_{i=2}^{n-1}[\theta_{i,j}(z_{i+1} - z_{i-1})] + \theta_{n,j}(2L - z_{n-1} - z_n)\right] \quad [37]$$

where ρ_w (kg m^{-3}) is the density of water.

The n values of $\theta_{i,j}$ at t_j were then recalculated by

$$\theta_{i,j}^{\ l} = \theta_{i,j}^{\ l-1} \frac{m_j}{\hat{m}_j} \quad [38]$$

where l represents the iteration number. With the new data set ($h_{i,j}$, $\theta_{i,j}$), parameters of eq. 35 were estimated again. This procedure was repeated until convergence, when parameters of eq. 35 did not change between two iterations.

Soil material from the surface layer (0-0.25 m) and from the layer between 0.25-0.50 m from the experimental area (a Rhodic Kanhapludalf with a bulk density of approximately 1200 kg m^{-3}) was collected, dried and sieved. A PVC ring ($L = 0.1$ m; 0.145 m of internal diameter; $A_r = 1.64 \cdot 10^{-2}$ m^2) was filled with this soil material and slowly saturated with water from the bottom to the surface.

After saturation, three polymer tensiometers were horizontally inserted at depths of 0.023 (z_1), 0.049 (z_2) and 0.076 m (z_3) through previously made circular apertures.

The ring filled with soil material and mounted with polymer tensiometers was placed on a precision balance (Tecnal Mark K16®, capacity 16 kg, resolution 10^{-4} kg) and the bottom sealed with tape to avoid water leakage and to guarantee evaporation would occur only by the upper sample surface. Pressure head at three depths ($h_{i,j}$) and the total mass m_j were automatically registered every 30 minutes. Measurements were finished when the upper tensiometer reached a pressure head of approximately -150 m.

At each observation interval, V_E (eq. 33) was calculated by the total mass variation $\Delta m = m_j - m_{j-1}$ (kg) and water density ρ_w:

$$V_E = -\frac{\Delta m}{\rho_w}. \qquad [39]$$

The hydraulic conductivity was calculated by eq. 33 for each observation interval. Parameters of soil water retention curve (eq. 35) were obtained as described above.

The entire procedure was repeated three times for each soil layer.

2.2.9 Mechanistic models

Root water uptake rate as a function of pressure head (measured by PoTs), root system data and soil hydraulic properties was simulated by the model of Jong Van Lier et al. (2008). The Ag_s model proposed by Jacobs (1994) was used to estimate the CO_2 assimilation rate, the stomatal conductance and the transpiration rate using data of the atmospheric conditions, canopy temperature and leaf area index.

2.2.9.1 Root water uptake model of Jong van Lier et al. (2008)

The root uptake model proposed by Jong Van Lier et al. (2008) requires data of soil hydraulic properties, root length density R and pressure head h. Soil hydraulic properties can be described by the set of equations proposed by Van Genuchten (1980), with parameters residual soil water content θ_r and saturated soil water content θ_s, saturated hydraulic conductivity K_s, and empirical parameters α, n and λ. For Van Genuchten soils, Jong Van Lier, Dourado Neto and Metselaar (2009) derived an analytical expression for the matric flux potential which was used in this study to

determine *M* from *h* data measured in the field. As lower bound of *h* in the integral expression to calculate *M*, the minimum pressure head at the root surface h_0, assumed equal to -150 m was used. Following Jong Van Lier et al. (2008), we used root radius r_0 equal to 0.05 mm. For root length density *R* we used values obtained by Raid, Hashim and Gallagher (1984) for Common Bean. These authors reported values of 2200 m m^{-3} between 0 and 0.1 m, 1550 m m^{-3} between 0.1 and 0.2 m, and 1400 m m^{-3} between 0.2 and 0.4 m.

To test the model, observed root water uptake S_{exp} (m^3 m^{-3} d^{-1}) was calculated from the experimental data for the first two layers (*z*=1 and *z*=2), as illustrated in Figure 8 and compared to the extraction S_{mod} (m^3 m^{-3} d^{-1}) obtained by the model of Jong Van Lier et al. (2008). $S_{exp,z=1}$ was calculated from the water balance of the surface layer between day *n* and *n+1* by:

$$(S_{exp})_{z=1,n-(n+1)} = -(\Delta stor + q_1 + E_s)_{z=1,n-(n+1)} \quad [40]$$

where $\Delta stor$ is the variation in water storage in layer *z*, q_1 is the vertical water flux density between layers *z*=1 and *z*=2 (negative upwards or positive downwards), and E_s is the water evaporation from soil surface, all in units of mm d^{-1}. For the subsurface layer, $S_{exp,z=2}$ was calculated by:

$$(S_{exp})_{z=2,n-(n+1)} = -(\Delta stor + q_1 + q_2)_{z=2,n-(n+1)} \quad [41]$$

in which q_2 (mm d^{-1}) is the vertical water flux density between layers *z*=2 and *z*=3 (negative upwards or positive downwards). The variation in water storage between day *n* and day *n+1* for a layer is calculated by:

$$\Delta stor_{n-(n+1)} = \Delta\theta_{n-(n+1)} Z \quad [42]$$

where *Z* (m) is the layer thickness. The vertical water flux between layers is given by:

$$q_{n-(n+1)} = \overline{K}(h)\frac{\Delta h_{n-(n+1)}}{d} \quad [43]$$

where $\overline{K}(h)$ is the mean soil hydraulic conductivity between layers (mm d^{-1}), Δh is the pressure head difference for layer *z* between days *n* and *n+1*, and *d* is the vertical distance between tensiometers

The evaporation rate from the soil surface E_s (mm d^{-1}) was estimated by empirical relations described by Driessen and Konijn (1992):

$$E_s = E_n \, exp(-k_e \, LAI) \quad [44]$$

in which E_n (mm d^{-1}) is the evaporation rate from bare soil and k_e is the light extinction coefficient (equal to 0.39 for beans).

Black, Gardner and Thurtell (1969) proposed to estimate the cumulative evaporation rate of bare soil during a drying period by:

$$\sum E_n = \beta \, t^{0.5} \quad [45]$$

where β (m $d^{-0.5}$) is an empirical parameter and t is the time (d) after rainfall or irrigation. The parameter β represents the evaporation of the first day of the drying period and can be estimated as the water evaporation rate of bare under optimal (wet) conditions. In this study, β was determined by the relation of Driessen e Konijn (1992):

$$\beta = E\left(\frac{RH_s - RH}{1 - RH}\right) \quad [46]$$

where E is the evaporation rate of a free water surface (mm d^{-1}) as in a Class A pan, RH_s is the relative soil humidity, and RH is the relative air humidity. The estimated value of β following this procedure was equal to $3.8 \cdot 10^{-3}$ m $d^{-0.5}$.

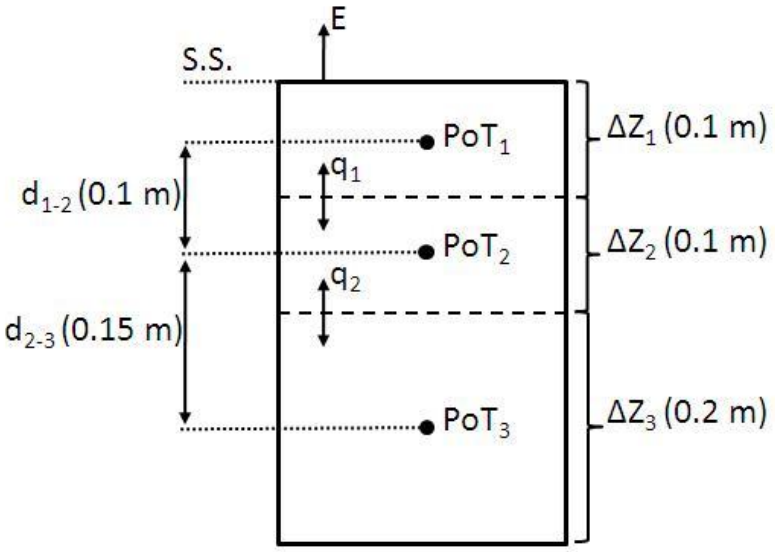

Figure 8 – Vertical distribution of PoTs in the field (S.S.: soil surface; E: evaporation; $d_{1\text{-}2}$: distance between tensiometers 1 and 3; $d_{2\text{-}3}$: distance between tensiometers 2 and 3; Z_1: thickness of layer 1; Z_2: thickness of layer 2; Z_3: thickness of layer 3; q_1: vertical water flux between layers 1 and 2; q_2: vertical water flux between layers 2 and 3; PoT_1: polymer tensiometer in layer 1; PoT_2: polymer tensiometer in layer 2; PoT_3: polymer tensiometer in layer 3)

The parameter f_z was estimated by minimizing the squared error between S_{mod} and S_{exp}, and the sensitivity of this parameter to the pressure head at root surface h_0 was calculated by the sensitivity coefficient η given by:

$$\eta = \frac{(f_{z,2} - f_{z,1})h_{0,150}}{(h_0 - h_{0,150})f_{z,1}} \quad [47]$$

in which $f_{z,1}$ is the parameter f_z obtained with h_0 equal to -150 m ($h_{0,150}$), and $f_{z,2}$ is the parameter f_z obtained with h_0 slightly different from -150 m (h_0).

2.2.9.2 CO_2 assimilation model of Jacobs (1994)

A complete description of the parameterizations proposed by Jacobs (1994) is given in Appendix A. The CO_2 assimilation model by Jacobs (1994) was programmed in Fortran® programming language and the source code is available in Appendix B.

The model calculates a vertical profile of all parameters using a routine of vertical extinction of *PAR* within the canopy, as well as the overall parameter values at canopy scale using the *LAI*. In this thesis, only the overall values are presented. The input data for the model with vertical *PAR* extinction for both irrigation treatments are *PAR*, wind speed *u*, day of the year, time and local latitude. Besides these data, observed data from each treatment (fully irrigated and deficit irrigated) of t_{air}, t_{canopy}, actual water vapor pressure e_a, *LAI* and canopy height were used. Some other model parameters are required (Appendix A). For C3 species, Goudriaan et al. (1985) suggest to use D_{max} = 45 g kg^{-1}, while g_m is determined by a function described in Appendix A. This equation uses the g_m value under ideal water conditions at 25°C, equal to 7 mm s^{-1} according to Nobel (1991). Under water deficit, g_m at 25°C reduces and Flowers et al. (2007) reported a value of 3.9 mm s^{-1}. Both values were used in the simulations to calculate g_m. Parameters f_o and C_s were assumed to be constant and equal to 0.85 and 612.98 mg m^{-3}, respectively.

2.3 Results and discussion

Section 2.3.1 describes the results of the soil hydraulic characterization. Section 2.3.2 presents the experimental field data, as well as the identification of plant water stress and involved environmental variables. In sections 2.3.3 and 2.3.4 the results of simulations of root water uptake and plant transpiration rate are presented.

2.3.1 Soil hydraulic properties

The determination of hydraulic properties of the soil from the experimental site was done following a laboratory procedure previously described. A first analysis of pressure head data from the laboratory evaporation experiment showed that during the first few days of evaporation water movement in the soil samples was not unidirectional, i.e., while at the top of cylinder the water movement was upward due to evaporation, at the bottom the water was moving downward by the gravitational action. These conditions did not allow the reliable calculation of *K(h)* by eq. 33. For this reason, data were used only from the moment water was moving upwards in the entire, as detected by tensiometer readings. This occurred 2 to 3 days after the beginning of the evaporation experiment, when pressure heads were between -1 to -3 m. Therefore, the evaporation method showed inefficient for determining soil hydraulic properties in the very wet range (h > -1 m). Other experimental factors agree to this observation: the resolution of polymer tensiometer measurements, which is around 0.2 m, makes observations in very wet range cumbersome. Furthermore, the use of sieved and disturbed soil material changes the nearly saturated and saturated hydraulic properties.

The bulk density in the disturbed samples used in the evaporation experiments with surface layer material was 1163, 1193 and 1105 kg m^{-3} for the three repetitions. For the layer between 0.25-0.5 m, these densities were 1081, 1030 e 1080 kg m^{-3}. These densities are markedly lower than the undisturbed field density of the soil, determined to be 1560 kg m^{-3} between 0-0.2 m, and 1380 kg m^{-3} between 0.2-0.76 m by Jong Van Lier and Libardi (1999). A difference of this order affects the hydraulic properties near saturation but can be supposed not to affect the hydraulic properties of the drier soil.

The soil water contents obtained at different pressure heads are shown in Figure 9, together with the corresponding fit of the Van Genuchten (1980) equation to the data. The figure also shows the 95% confidence interval. 36 iterations were necessary to reach convergence of eq. 35 for the 0-0.25 m layer, and 38 iterations were needed for the 0.25-0.5 m layer.

The fitting results for soil hydraulic conductivity K versus pressure head h are shown in Figure 10. In this figure, values of K obtained by eq. 33 with data from the evaporation experiment fitted by eq. 36 are plotted, together with the 95% confidence interval obtained with the upper limit of K_s combined to the lower limit of λ, and the lower limit of K_s combined to the upper limit of λ. The decrease of K with h is similar in the two soil layers. The 95% confidence interval is larger for the 0-0.25 m layer, which showed a greater dispersion of experimental data. The range in K covered by the confidence interval represents a little more than a factor of 10 in the layer between 0-0.25 m, and slightly less in the 0.25-0.5 m layer. In Table 3 the parameters of the Van Genuchten equation system fitted for both soil layers are presented. These values were used as input in the root water uptake model.

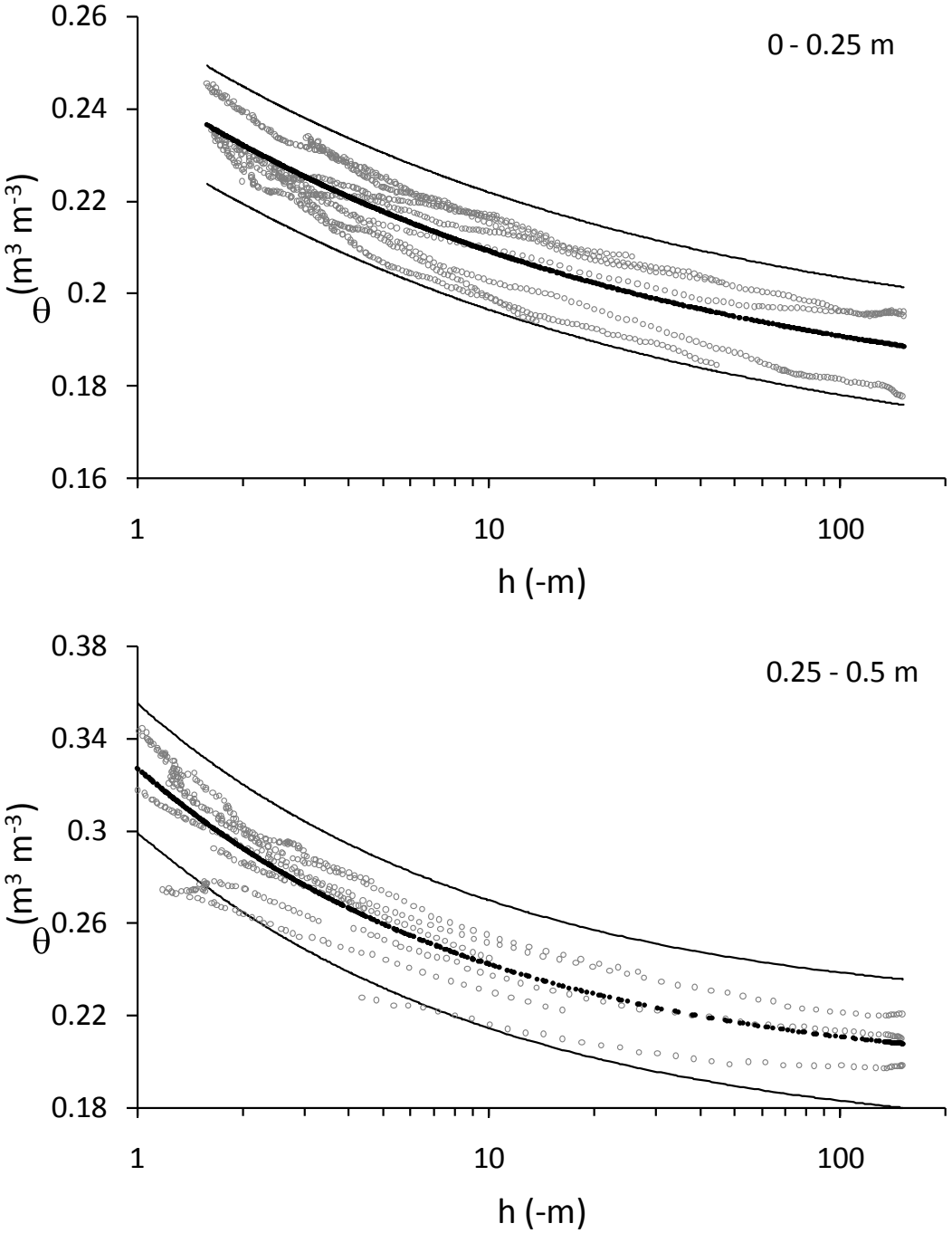

Figure 9 – Water content as a function of pressure head (soil water retention curves) in the layer between 0 and 0.25 m (above) and in the layer between 0.25 and 0.50 m (below). Grey dots represent experimentally obtained data and black dots represent fitted eq. 35. Thin lines delimit the 95% confidence interval

Table 3 – Parameters of Van Genuchten equations (eq. 35 and 36) fitted for the interval between -150 < h < -1 m, and lower and upper 95% confidence limits

Depth	Parameter	Fitted value	Lower limit (95%)	Upper limit (95%)
0-0.25 m	θ_s (m^3 m^{-3})	0.333338	-0.683255	1.349681
	θ_r (m^3 m^{-3})	0.172544	0.160314	0.184682
	α (m^{-1})	13.0085	-274.5302	300.5481
	K_s (m d^{-1})	0.37005	0.22278	0.614662
	n	1.30324	1.17209	1.43364
	λ	-2.88719	-3.26327	-2.54177
0.25-0.5 m	θ_s (m^3 m^{-3})	0.702592	-6.069214	7.474404
	θ_r (m^3 m^{-3})	0.192665	0.179261	0.206058
	α (m^{-1})	21.1517	-648.1561	690.4684
	K_s (m d^{-1})	0.18414	0.13913	0.24371
	n	1.43491	1.29182	1.57791
	λ	-3.22127	-3.35212	-3.09042

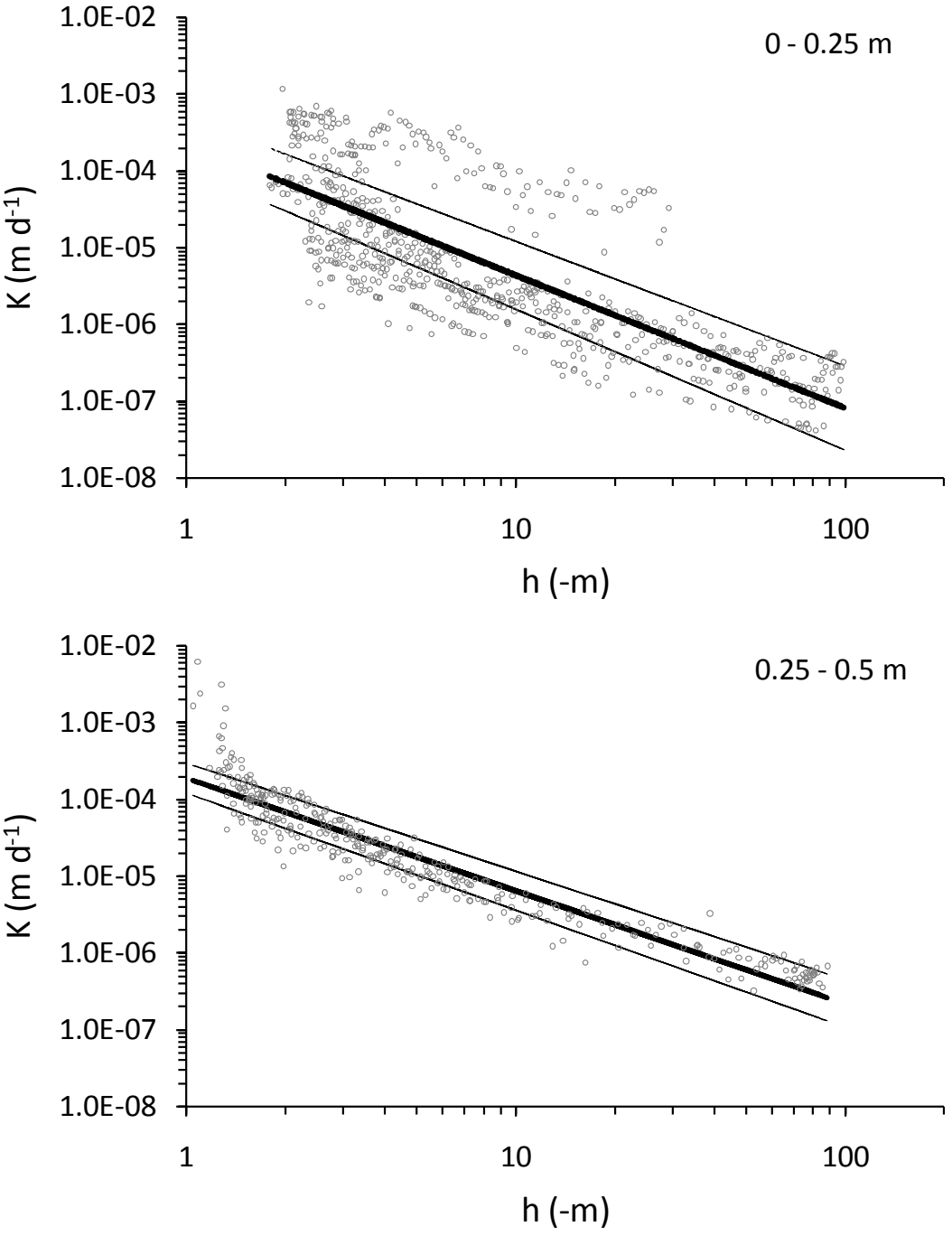

Figure 10 – Soil hydraulic conductivity as a function of pressure head for layer between 0 and 0.25 m (above) and for the layer between 0.25 and 0.50 m (below). Grey dots represent experimentally obtained data (eq. 33) and black line (bold) represents fitted eq. 36. Thin black lines represent the fit obtained with the upper limit of K_s combined to the lower limit of λ, and the lower limit of K_s combined to the upper limit of λ

2.3.2 Plant water stress related to environmental parameters

2.3.2.1 Atmospheric parameters

The detection of water stress in the bean plants of the deficit irrigated treatment was performed by analyzing and comparing the canopy temperature of this treatment with the canopy temperature of the fully irrigated treatment, together with the *VPD* (atmospheric demand) and the wet bulb temperature, following the studies of Ehrler (1973) and Shimoda and Oikawa (2006), and Wanjura and Upchurch (1997) and Mahan et al. (2005), respectively. The onset of water stress was determined by analysis of canopy and air temperature difference and difference in *VPD* ($(\Delta t_{canopy\text{-}air})_{DI}$ - $(\Delta t_{canopy\text{-}air})_{FI}$ and VPD_{DI} - VPD_{FI}).

Air temperature was measured at a central location in each irrigation treatment plot and showed to be very similar for both treatments (Figure 11). In the last weeks of the experiment, the air temperature in the deficit irrigated treatment tends to be around 0.5°C higher than in the fully irrigated treatment. The mean air temperature in the fully irrigated treatment was equal to 21.77°C while in the deficit irrigated treatment it was 22.15°C; maximum temperatures were 32.93°C and 33.46°C, respectively. On the other hand, canopy temperature of the deficit irrigated treatment tended to increase during the interval of analysis (Figure 12). In the fully irrigated treatment, this tendency was not observed and t_{canopy} presented a constant tendency over the course of the month. In the fully irrigated treatment, the mean and maximum t_{canopy} were 20.14°C and 29.94°C, in the deficit irrigated treatment they were 22.97°C and 38.34°C.

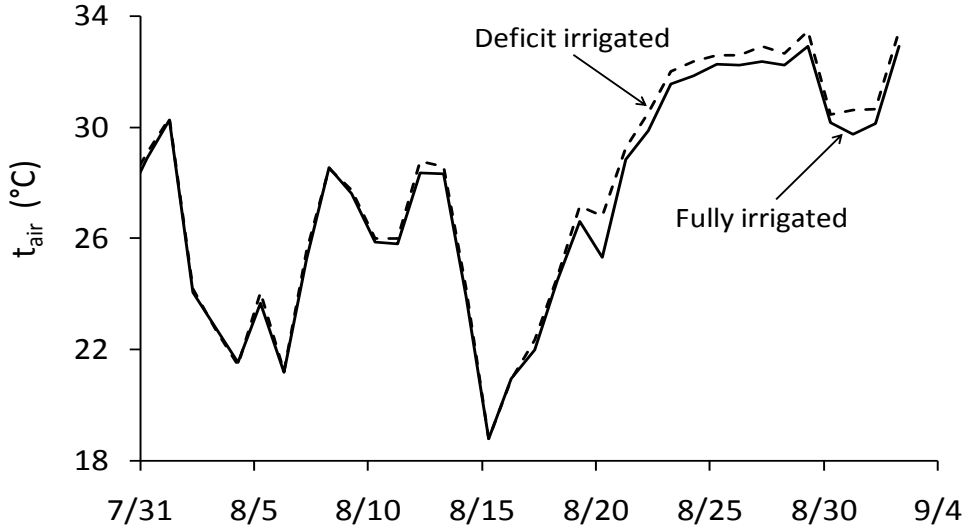

Figure 11 – Maximum daily air temperature during the interval of analysis for both treatments as a function of date (m/dd/2010)

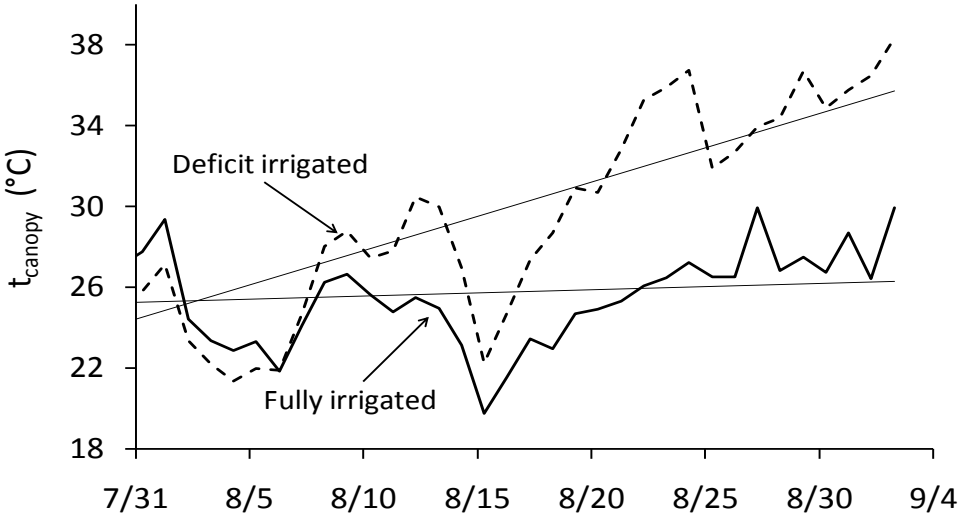

Figure 12 – Maximum daily canopy temperature during the interval of analysis for both treatments as a function of date (m/dd/2010). Straight lines are the tendency lines

There is a clear difference in the relationship between $\Delta t_{canopy\text{-}air}$ and *VPD* between treatments (Figure 13). In the fully irrigated treatment, a linear correlation between *VPD* (hPa) and $\Delta t_{canopy\text{-}air}$ (°C) was observed that can be described by $\Delta t_{canopy\text{-}air} = a\ VPD + b$, with $a = -0.19 \pm 0.013$ and $b = 1.78 \pm 0.27$ ($R^2 = 0.54$, intervals at a confidence level of 95%). This regression shows that an increase in *VPD*

decreased canopy temperature by enhancing the transpiration rate. Reduction in t_{canopy} and t_{air} difference depends on an increase in *VPD* at ideal water conditions and under clear sky. If a canopy is able to take up sufficient water to maintain the transpiration rate near the potential rate, the canopy temperature is reduced, therefore an increase in *VPD* reduces $\Delta t_{canopy\text{-}air}$ (IDSO et al., 1981; JACKSON et al., 1981).

In the deficit irrigated treatment, on the other hand, the fit was insignificant and the slope became practically zero ($a = 6.7 \cdot 10^{-3} \pm 0.02$ and $b = 0.78 \pm 0.41$; $R^2 = 7 \cdot 10^{-4}$). These results corroborate with the observations of Ehrler (1973) and Shimoda and Oikawa (2006). These authors found the relationship between *VPD* and $\Delta t_{canopy\text{-}air}$ to be $\Delta t_{canopy\text{-}air} = -0.79\ VPD + 0.42$ ($R^2 = 0.58$) for a rainy period and $\Delta t_{canopy\text{-}air} = -0.58\ VPD + 0.73$ ($R^2 = 0.27$) for a dry period in a grassland.

Figure 13 shows data of $\Delta t_{canopy\text{-}air}$ as a function of the observation time according to three time intervals: between 7:00 AM and 10:30 AM (black), between 11:00 AM and 2:30 PM (grey), and between 3:00 PM and 6:00 PM (light grey). During the first hours of the day, between 7:00 AM and 10:30 AM, the *VPD* was low in both treatments and the difference in temperature between air and canopy was close to zero. During other times of the day there were significant differences between treatments. In the fully irrigated treatment, between 11:00 AM and 2:30 PM, t_{canopy} was higher than t_{air} for values of *VPD* below 20 hPa, and for greater *VPD* values t_{canopy} was smaller than t_{air}. On the other hand, between 3:00 PM and 6:00 PM, t_{air} was always higher than t_{canopy}, independent of the *VPD* value.

For the deficit irrigated treatment, t_{canopy} was higher than t_{air} for almost all values of *VPD* between 11:00 AM and 2:30 PM, and smaller than t_{air} between 3:00 PM and 6:00 PM. At the middle of the day, t_{canopy} is higher than t_{air} independent of the water vapor pressure deficit (*VPD*), probably because there was not enough water in the soil to maintain transpiration at potential rates, thus cooling the leaves. Between 3:00 PM and 6:00 PM, when t_{air} and radiation was lower, plant transpiration was sufficient to reduce the leaf temperature below t_{air}.

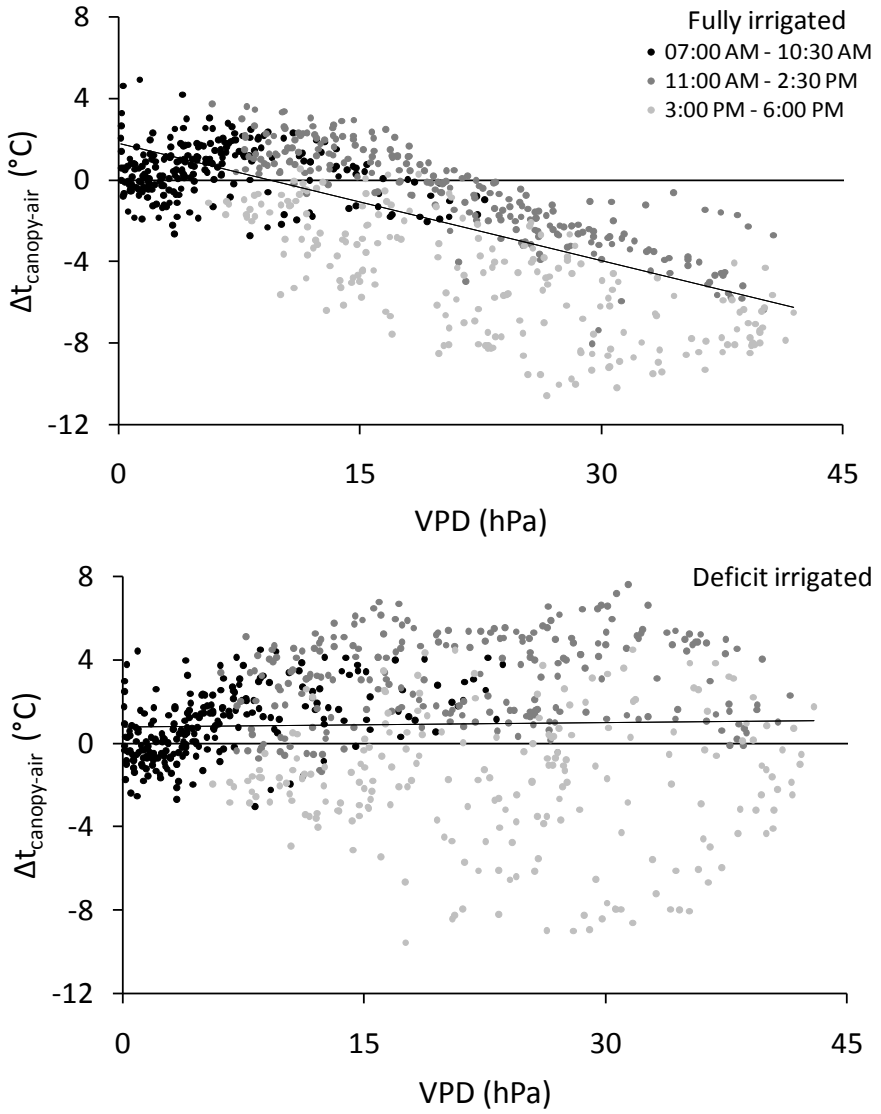

Figure 13 – Difference between canopy and air temperature ($\Delta t_{canopy\text{-}air}$) as a function of water vapor pressure deficit (*VPD*) for the fully irrigated (above) and deficit irrigated (below) treatment. The color of the dots represent the period of the day of the respective observation. Straight lines are tendency lines

As the geometry of plant leaves is different from the geometry of a wet bulb thermometer and leaves are exposed to radiation, they do not cool purely adiabatic and temperatures never become as low as t_{wb}. The difference between t_{wb} and t_{canopy} ($t_{wb} < t_{canopy}$) is determined by environmental conditions and the canopy structure. Figure 14 shows that the difference between t_{wb} and t_{canopy} is approximately constant throughout the period in the fully irrigated treatment, with a maximum value of 12.23°C,

contrarily to the deficit irrigated treatment where temperature differences increase indicating an increase in stomatal resistance to transpiration in the deficit irrigated plants. The maximum difference between t_{wb} and t_{canopy} in this treatment was equal to 19.6°C.

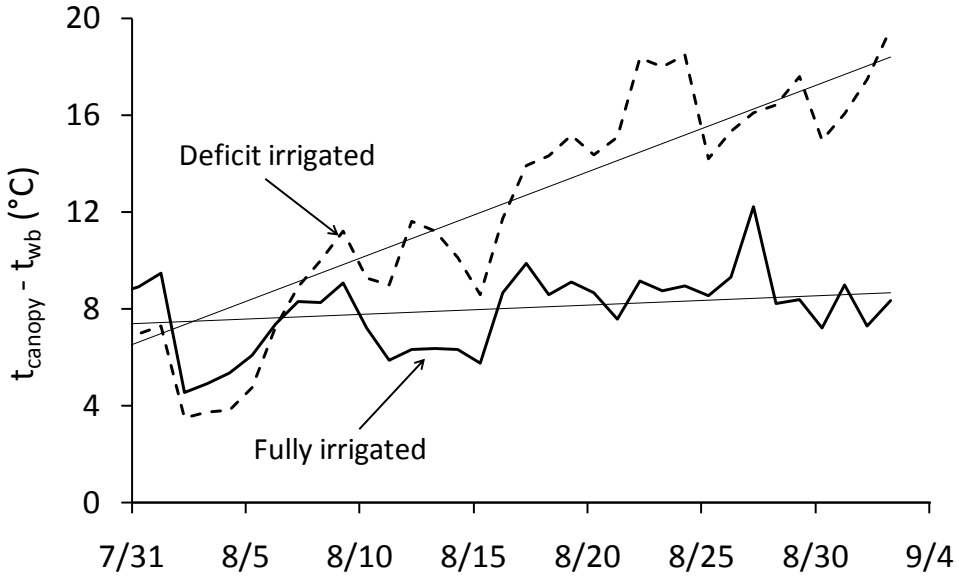

Figure 14 – Difference between canopy and wet bulb temperature (t_{canopy}-t_{wb}) for both treatments as a function of date (m/dd/2010). Straight lines are the tendency lines

A comparative analysis of the difference $(\Delta t_{canopy-air})_{DI}$ - $(\Delta t_{canopy-air})_{FI}$ and of the difference VPD_{NI} - VPD_{FI} was used to indicate the onset of water stress in the deficit irrigated treatment. Figure 15 shows this comparison. The value of $\Delta t_{canopy-air}$ between treatments showed its highest value (10.64°C) on September 2. By the analysis described for Figures 11 and 12, it can be concluded that $\Delta t_{canopy-air}$ is mainly determined by canopy temperature. $\Delta t_{canopy-air}$ of the deficit irrigated treatment increases in relation to the fully irrigated treatment due to a decrease in transpiration rate. The canopy temperature in the deficit irrigated treatment increased during the interval of analysis and when t_{canopy} became higher than t_{canopy} of the fully irrigated treatment, on August 5, plants were supposed to be water stressed.

Similar to the tendencies of air temperature, as both treatments were exposed to the same weather conditions, the average *VPD* calculated with t_{air} of each treatment was very similar during the interval of analysis (16.54 hPa for the deficit irrigated treatment

and 16.28 hPa for the fully irrigated treatment). However, the maximum daily *VPD* showed significant differences between treatments, as shown in Figure 15. On August 30, for example, the *VPD* in the deficit irrigated treatment was 4.76 hPa higher than in the fully irrigated plot. As the *VPD* was calculated based on observations made by psychrometers installed in each treatment, this can be considered to be a micrometeorological response to transpiration rate differences between treatments.

Four days (August 15, 23, 25 and 30, indicated by ellipses in Figure 15) were chosen for the simulations with the photosynthetic model because they represent different types of days that occurred during the field experiment. No irrigation was applied during these days and data from the entire day could be used as input in the CO_2 assimilation model. On August 15, the atmospheric water deficit decreased due to reduced demand due to overcast conditions. On August 23, one day before the application of irrigation in both treatments, both the atmospheric demand and the canopy temperature of deficit irrigated treatment were increasing. On August 25, the water stress had decreased as a result of the irrigation the day before and plants of the deficit irrigated treatment responded to the increased soil water content reducing canopy temperature and *VPD* in comparison with the fully irrigated treatment. On August 30, although the *VPD* in the deficit irrigated plot had been reduced, the canopy temperature increased to a value almost 8°C above the canopy temperature of the fully irrigated treatment.

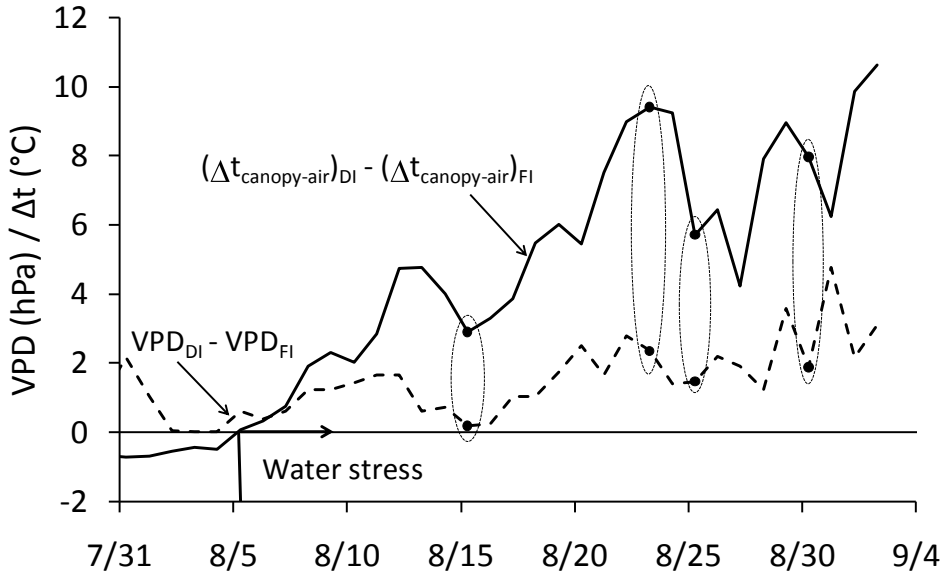

Figure 15 – Difference in *VPD* and difference in temperature ($\Delta t_{canopy\text{-}air}$) between deficit irrigated treatment and fully irrigated treatment as a function of date (m/dd/2010). Ellipses identify in a sequence the days August 15, 23, 25 and 30 which were analyzed in more details

The observed stomatal conductance and transpiration rate measured with the porometer are shown in Figure 16 for both treatments. On August 10, when the measurements started, the deficit irrigated treatment was in its 8th day without irrigation, and the effects of water stress could be observed in plants because the transpiration rate and stomatal conductance for plants in the deficit irrigated treatment were 191 mg m^{-2} s^{-1} and 10 mm s^{-1} lower, respectively, than for the plants in the fully irrigated treatment. Between August 14 and 16, a decrease in air temperature (Figure 12) caused a reduction of transpiration rate in both treatments. From day 16, however, observations in both treatments showed a different trend: in the deficit irrigated treatment, the transpiration rate increased following the increase in air temperature; in the fully irrigated treatment the transpiration rate was maintained at lower levels and approximately constant until the end of the month. It is also observed that, after the August 16, stomatal resistance of the deficit irrigated plants was high and approximately constant, while in the fully irrigated plants it decreased.

The closure of stomata is a mechanical process triggered due to the decrease of water content in the rhizosphere or to a high atmospheric demand. It can also be a response to a physiological process, a mechanism of the plant to defense itself against

water shortage. This process occurs through the formation of the hormone Abscisic Acid in the roots, which migrates to the leaves causing stomatal closure, reducing water loss by plants (TAIZ; ZIEGER, 2004). The effect of this hormone has been reported in plants of *Phaseolus vulgaris* L. (PARDOSSI; VERNIERI; TOGNONI, 1992).

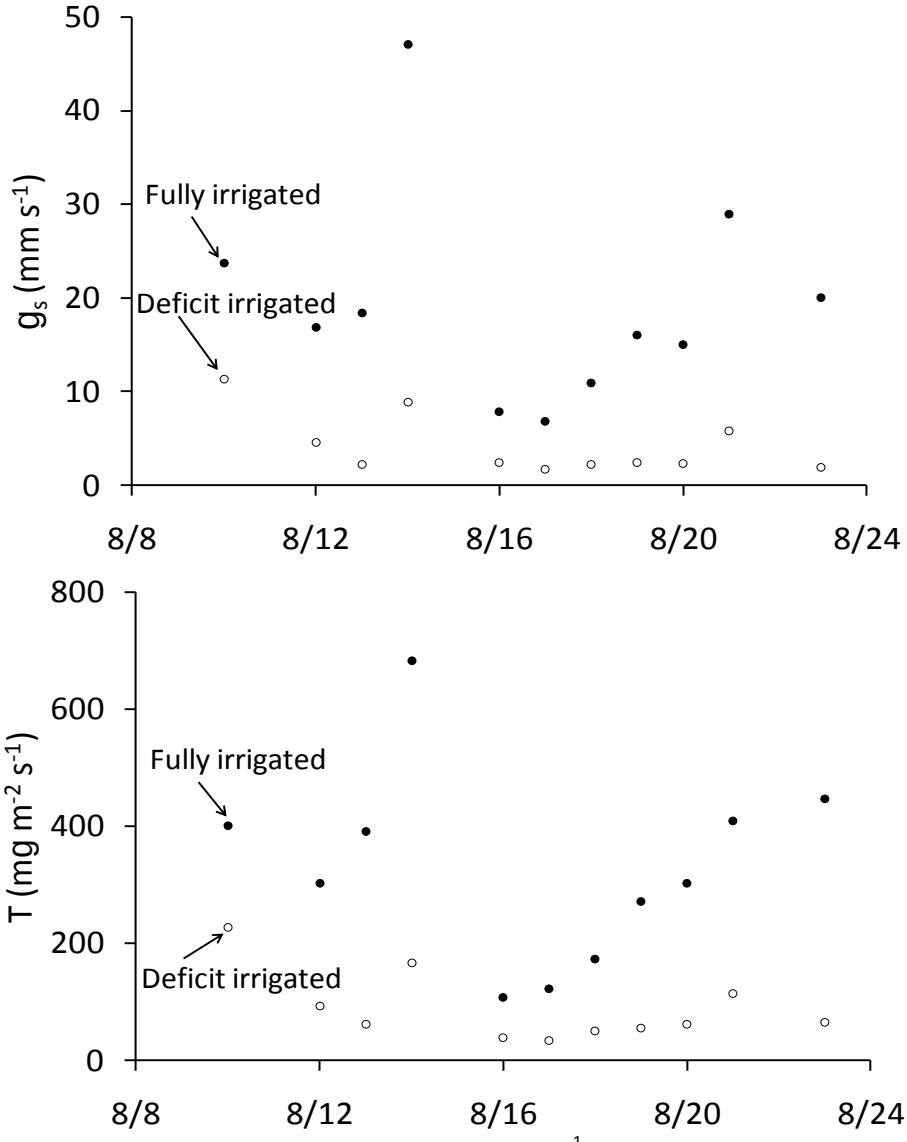

Figure 16 – Mean values of stomatal conductance g_s (mm s^{-1}) (above) and transpiration rate T (mg m^{-2} s^{-1}) (below) for both treatments as a function of date (m/dd/2010). Measurements were made between 11:00 AM and 2:30 PM by porometry

2.3.2.2 Soil parameters

The soil water pressure head was measured in three different soil layers (0-0.1 m, 0.1-0.2 m, and 0.2-0.4 m by polymer tensiometers. As expected, significant differences occurred between treatments. As can be seen in Figure 17, the pressure head decreased to below -160 m in the deficit irrigated treatment; at the same time t_{canopy} showed its highest values (~ 38°C) (Figure 12). Vertical lines in Figure 17 indicate the onset of plant water stress (August 5) determined by the criterion of temperature and *VPD* differences. It can be observed that this moment corresponds to a pressure head of a few meters negative in both observation points. Conceptually, there is no fixed value of pressure head at which water stress begins, since root water extraction depends on soil properties such as hydraulic conductivity, atmospheric demand and root system characteristics. However, under the conditions of this experiment, root water uptake was at its potential rates for pressure heads down to more or less -10 m.

In the fully irrigated treatment, data from PoT 3Pb, installed at a depth of 0.05 m were not used and are not shown in Figure 18. When the tensiometer data were collected, it was observed that the pressure head in this PoT was positive and increasing with time. This may have been caused by an electronic problem or a defect in the physical body of the tensiometer (porous cap or polymer chamber). For the other tensiometers, *h* remained high with values between 0 and -7 m, as shown in Figure 18. At observation point 1, *h* was higher than -0.1 m until August 16 at the depth of 0.15 m and until August 28 at the depth of 0.3 m.

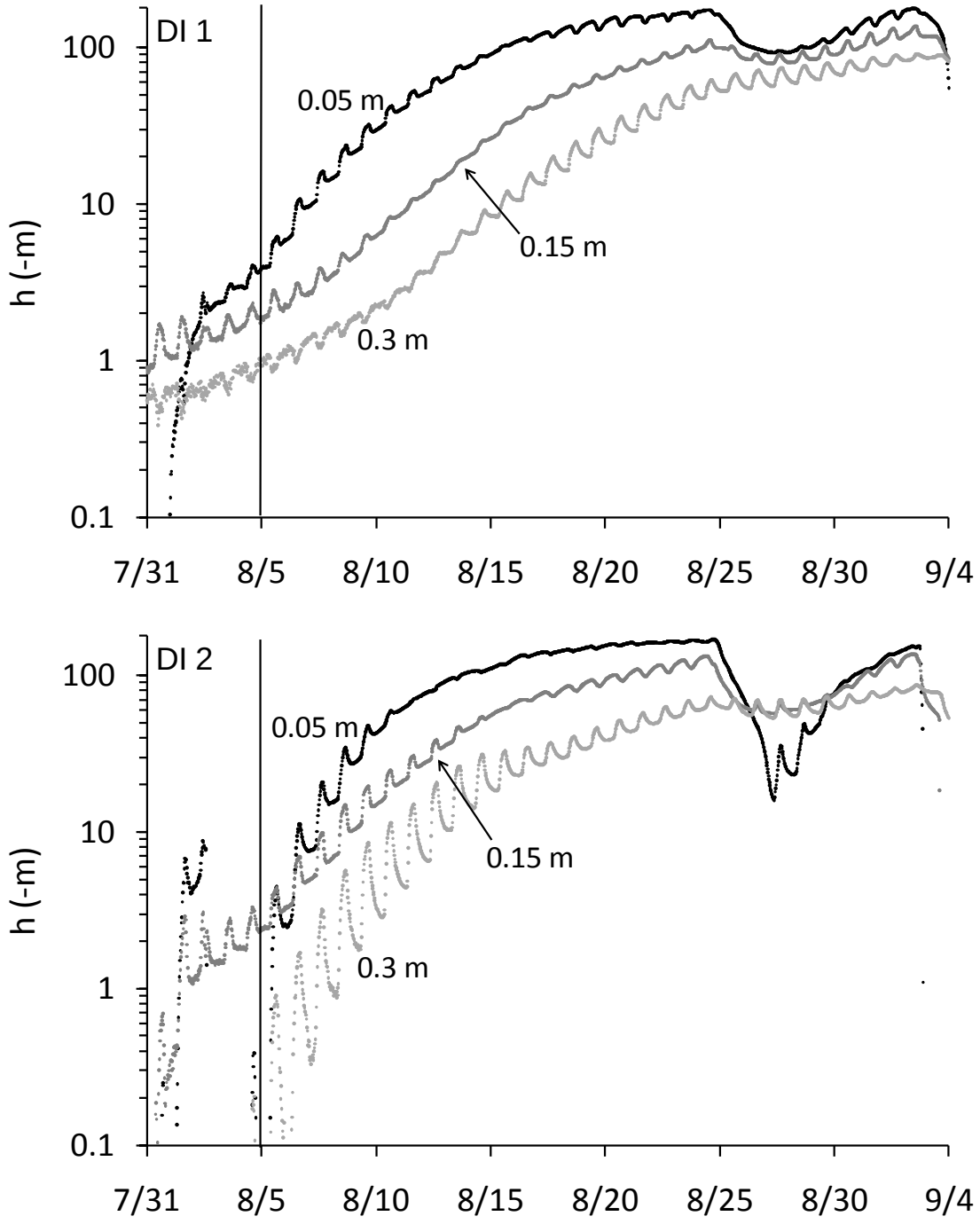

Figure 17 – Soil water pressure head *h* (m) for three depths in two observation points of the deficit irrigated treatment (DI 1 and DI 2) as a function of date (m/dd/2010). Vertical lines indicate the onset of water stress determined by the criterion of temperature and *VPD* differences

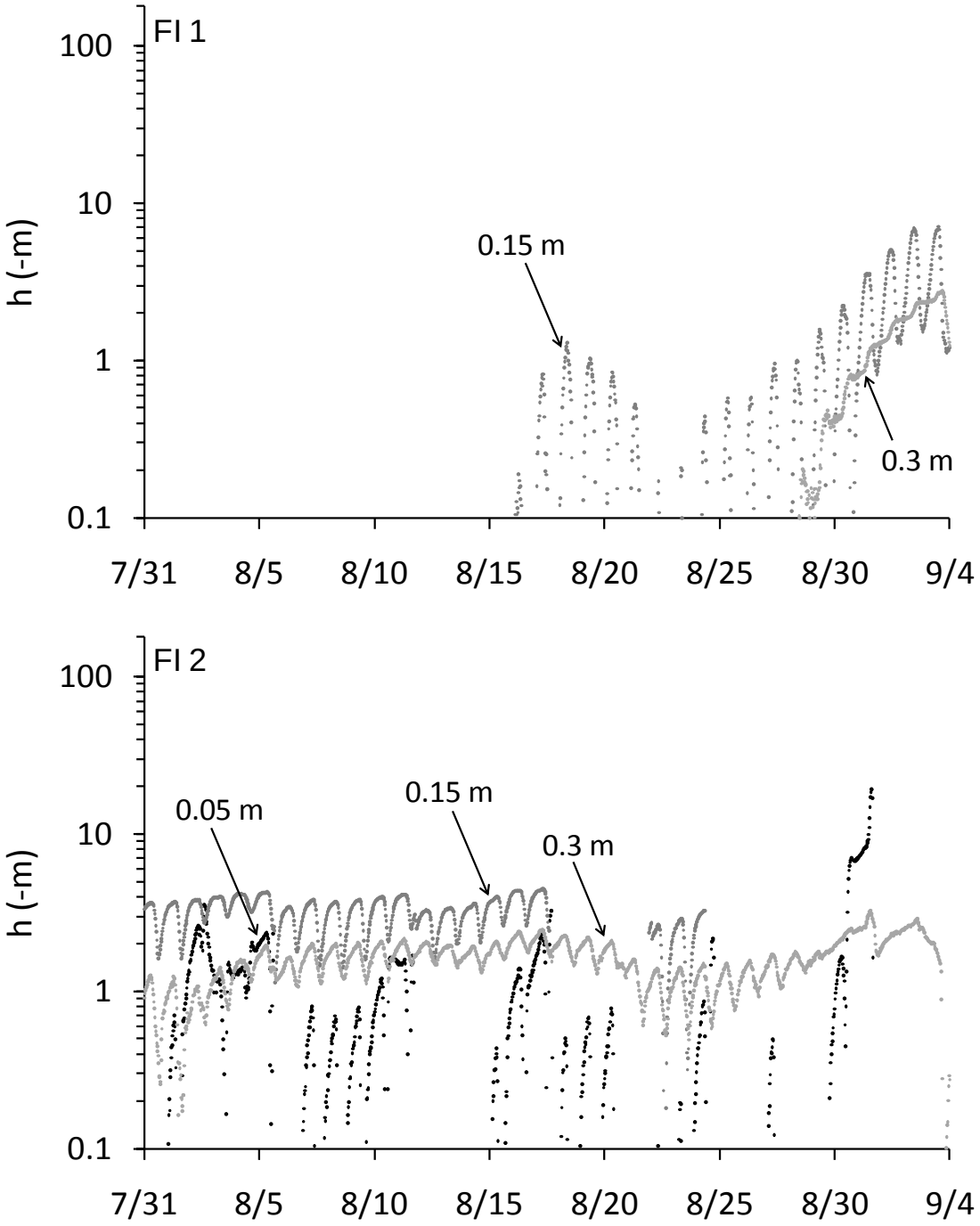

Figure 18 – Soil water pressure head *h* (m) at three depths in the two observation points in the fully irrigated treatment (FI 1 and FI 2) as a function of date (m/dd/2010)

2.3.2.3 Experimental data at detailed time scale

The most relevant experimental data were analyzed at the temporal resolution of the field measurements (one observation every 30 minutes) for four selected dates for which simulations were performed (August 15, 23, 25 and 30), and also for August 9 which represents a condition of soil water dynamics at the onset of the drying period. The *VPD* and t_{canopy} for both treatments and *h* in the two observation points of the deficit irrigated treatment are presented in the following. Previously, measurements of *PAR* at these days are shown (Figure 19). It is observed from the figure that only on August 15 the sky was overcast. For the other days, the observed *PAR* was characteristic for a day with clear sky at this time of the year, with maximum values near 260 W m^{-2}.

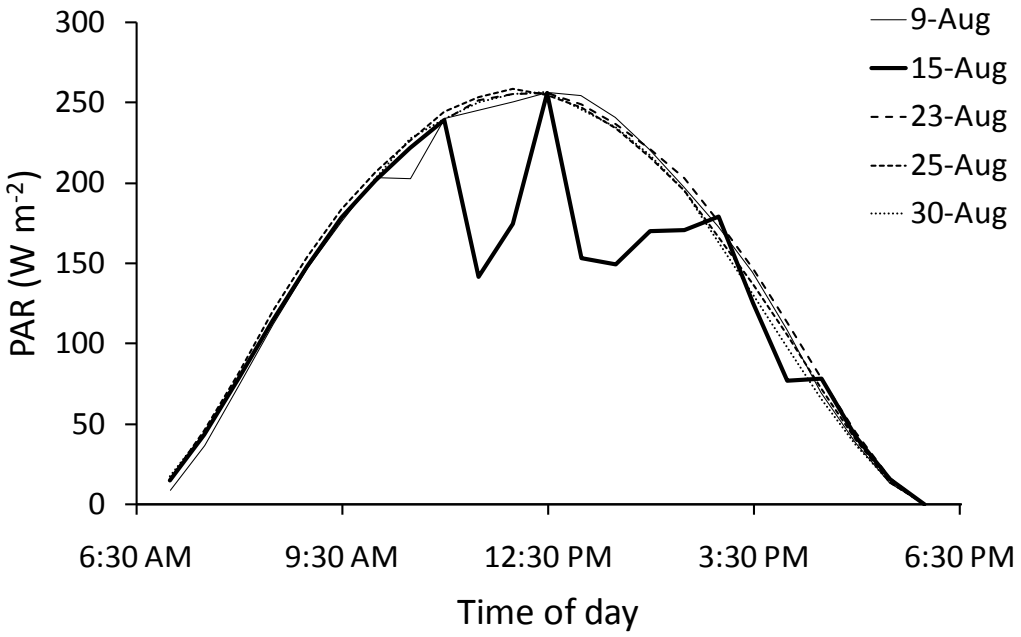

Figure 19 – Photosynthetically active radiation *PAR* (W m^{-2}) as a function of the time of the day for August 9, 15, 23, 25 and 30, 2010

On August 9 (Figure 20), the air temperature was high and *VPD* was similar in both treatments, reaching 25.5 hPa. The temperature of the deficit irrigated canopy showed an increase, indicating a reduction of the transpiration rate due to limiting soil hydraulic conditions, since irrigation had ceased a week before. The t_{canopy} of deficit irrigated treatment reached 26.5°C at 1:00 PM, 2°C above the t_{canopy} of the fully irrigated treatment. The pressure head of soil water was close to -50 m in the first layer in both

observation points, with a tendency to decrease with time. Except for the depth of 0.3 m at observation point 1, other *h* observations showed values to become lower at those times of the day during which the water uptake rate by roots was higher. This effect was most pronounced at the depth of 0.05 m, probably because this layer contains the highest root length density and loses water by evaporation. While *h* decreased from the bottom to the top of the soil profile, there was an upward vertical water flux. During the night, the pressure head increased in all layers because water loss by evapotranspiration stopped and ascension of water from below continued. It is interesting to observe that the soil at observation point 2 (DI 2) was drier than the soil of observation point 1 (DI 1), giving some indication of soil spatial variability.

On August 15 (Figure 21), plants of the deficit irrigated treatment were without irrigation for 13 days. The *VPD* was low with maximum values of 11.4 hPa and similar in both treatments due to the reduction of air temperature on that cloudy day. The canopy temperature of the deficit irrigated treatment was slightly higher (around 3°C) than in the fully irrigated treatment at the hottest time of the day. The pressure head of soil water was decreasing in the first two depths (0.05 m and 0.15 m), reaching -124 m. The low transpiration rate caused by lower atmospheric demand, together with the dry soil conditions made root water uptake to decrease. As a consequence, no reduction of pressure head in the first two layers was observed during this day. Due to the drier conditions, the water ascension also became lower and the pressure head of the upper layers was not increasing anymore during the night, except for the layer between 0.2-0.4 m from observation point 2.

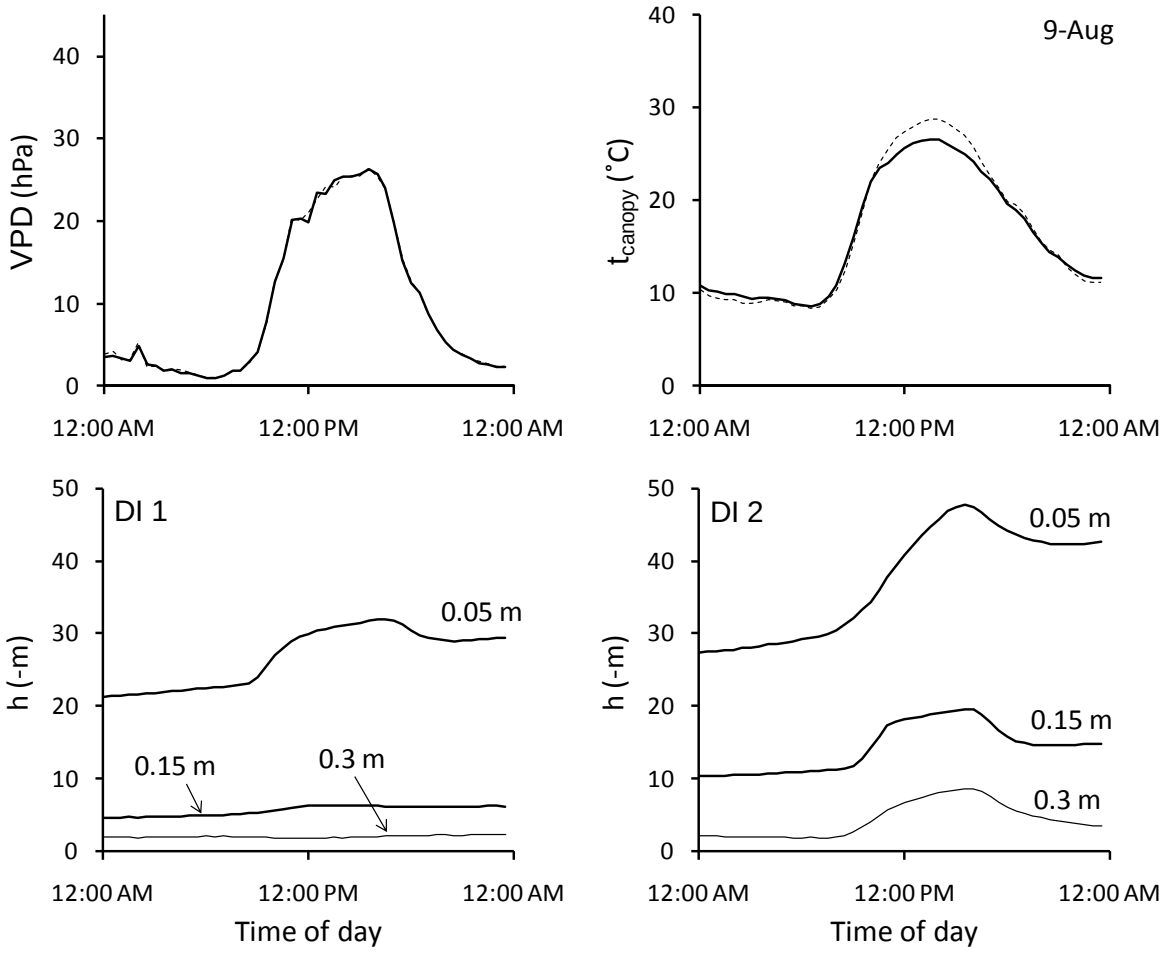

Figure 20 – Vapor pressure deficit (*VPD*) and canopy temperature (t_{canopy}) for the fully irrigated treatment (continuous line) and for the deficit irrigated treatment (dashed line), and soil water pressure head (*h*) at the two observation points in the deficit irrigated treatment (DI 1 and DI 2) on August 9, 2010

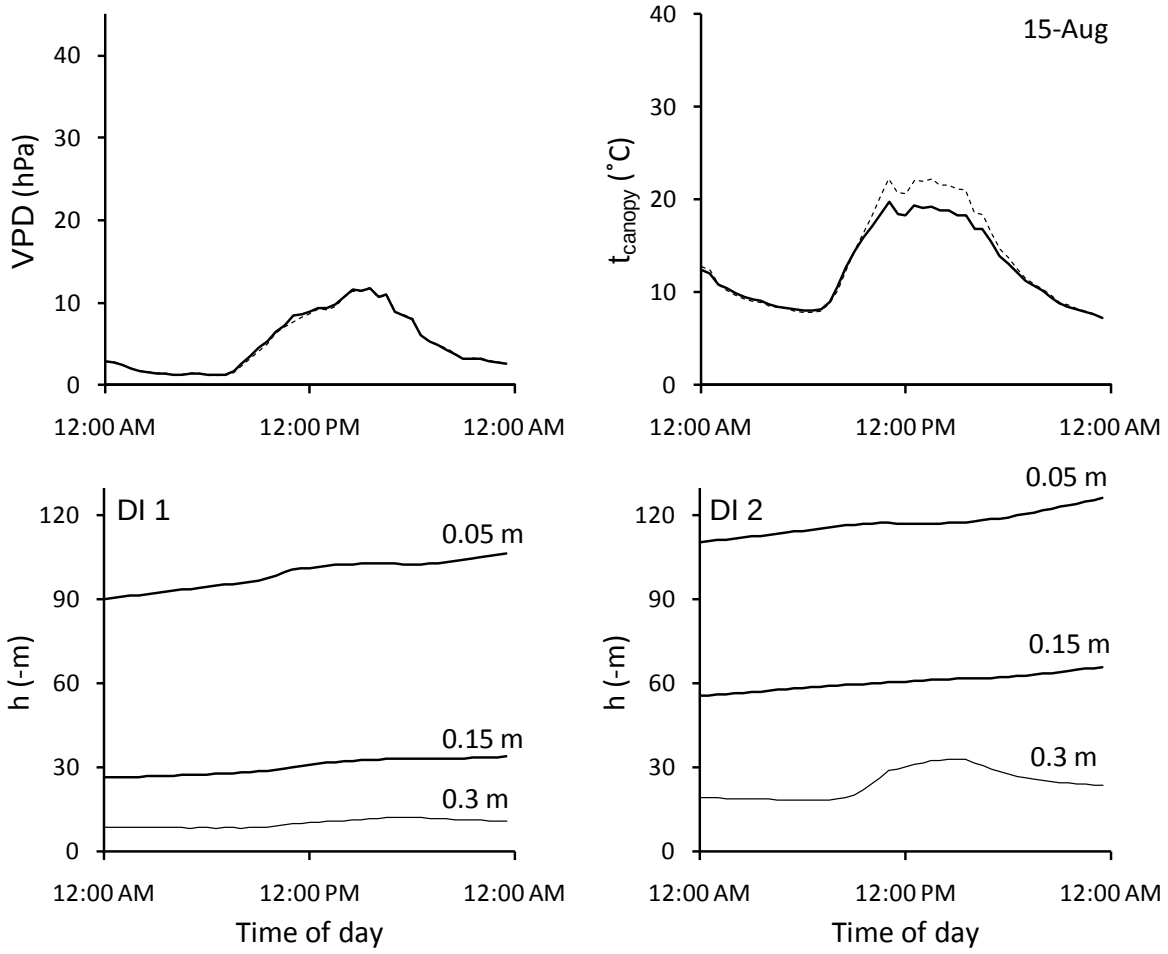

Figure 21 – Vapor pressure deficit (*VPD*) and canopy temperature (t_{canopy}) for the fully irrigated treatment (continuous line) and for the deficit irrigated treatment (dashed line), and soil water pressure head (*h*) at the two observation points in the deficit irrigated treatment (DI 1 and DI 2) on August 15, 2010

On August 23 (Figure 22), a clear day, plants of the deficit irrigated treatment were not receiving irrigation for 21 days. The atmospheric demand was high due to the higher air temperatures and the *VPD* of deficit irrigated plants was slightly higher than of the fully irrigated plants the warmest times of the day. At 2:00 PM, for example, *VPD* of the deficit irrigated treatment was 2.4 hPa higher than in the fully irrigated treatment. The canopy temperature significantly increased when compared to August 15. The soil water pressure head reached values below -160 m in the surface layer in both observation points. The effect of increasing root water extraction during the hottest hours of the day and reducing extraction in the afternoon can be observed in the tendencies of soil water pressure head values.

On August 24, plants of both treatments received an irrigation of 15 mm and this reflected in the observations for August 25 (Figure 23), when conditions were clearly different from August 23. The difference in *VPD* between the treatments was reduced, as well as the difference between t_{canopy}, with maximum values of approximately 5°C. The pressure head that at the beginning of the day was ~ -150 m in the 0-0.1 m layer of both observation points, increasing to -80 m at the end of the day. In the second soil layer *h* also tended to increase, although the drying effect of root water uptake can be observed during the afternoon hours.

On August 30 (Figure 24), although the atmospheric demand was reduced, the *VPD* in the deficit irrigated treatment was higher than in the fully irrigated treatment for the interval between 1:00 PM and 3:00 PM. The canopy temperature in the deficit irrigated treatment was higher than on August 25, while the canopy temperature of the fully irrigated treatment remained almost the same. The soil water pressure head further decreased in all layers, reaching -134 m at observation point 1 and -101 m at observation point 2. The effect of vertical water flux between layers was more evident at observation point 1; at observation point 2 this effect was less pronounced. The drier soil reduced root water uptake and transpiration rate, making the canopy temperature of deficit irrigated plants to increase.

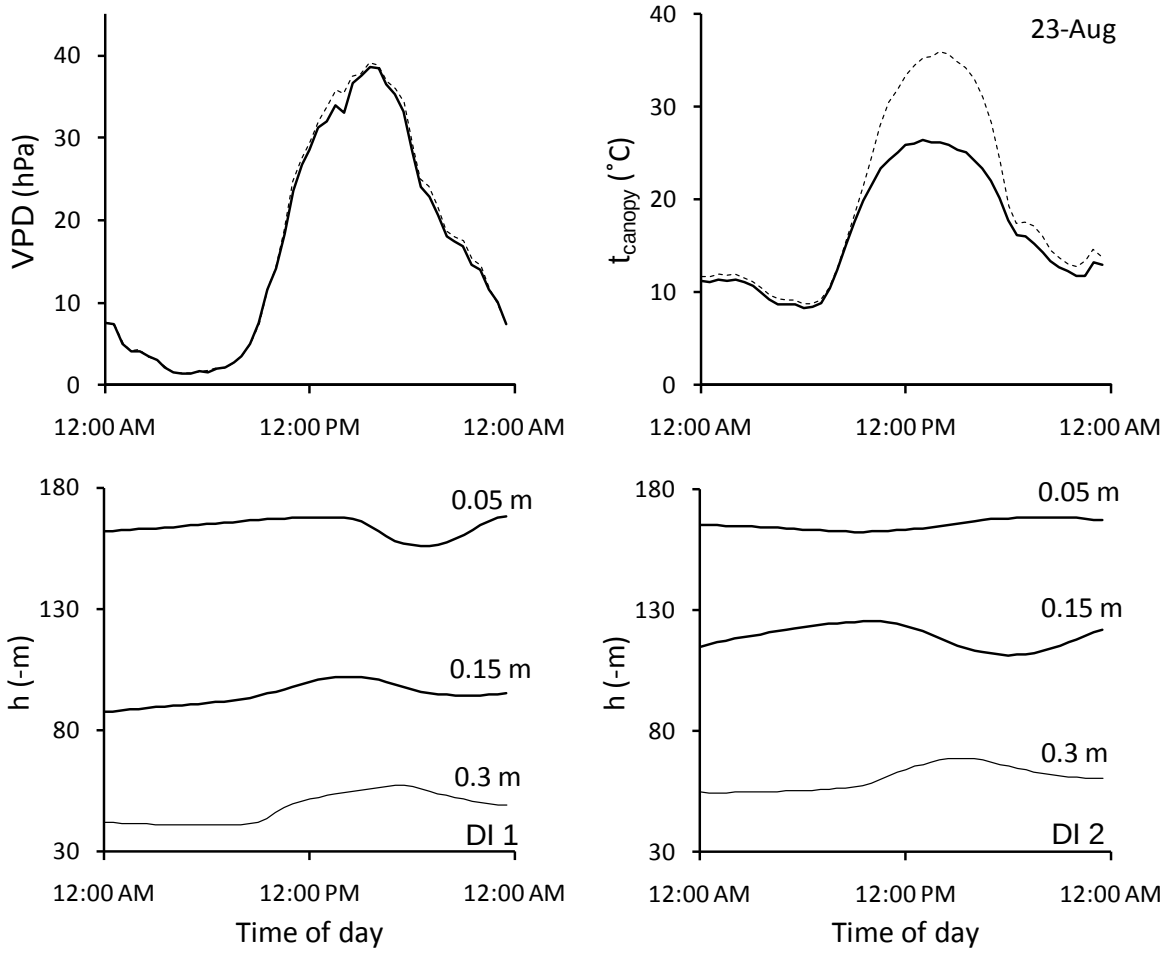

Figure 22 – Vapor pressure deficit (*VPD*) and canopy temperature (t_{canopy}) for the fully irrigated treatment (continuous line) and for the deficit irrigated treatment (dashed line), and soil water pressure head (*h*) at the two observation points in the deficit irrigated treatment (DI 1 and DI 2) on August 23, 2010

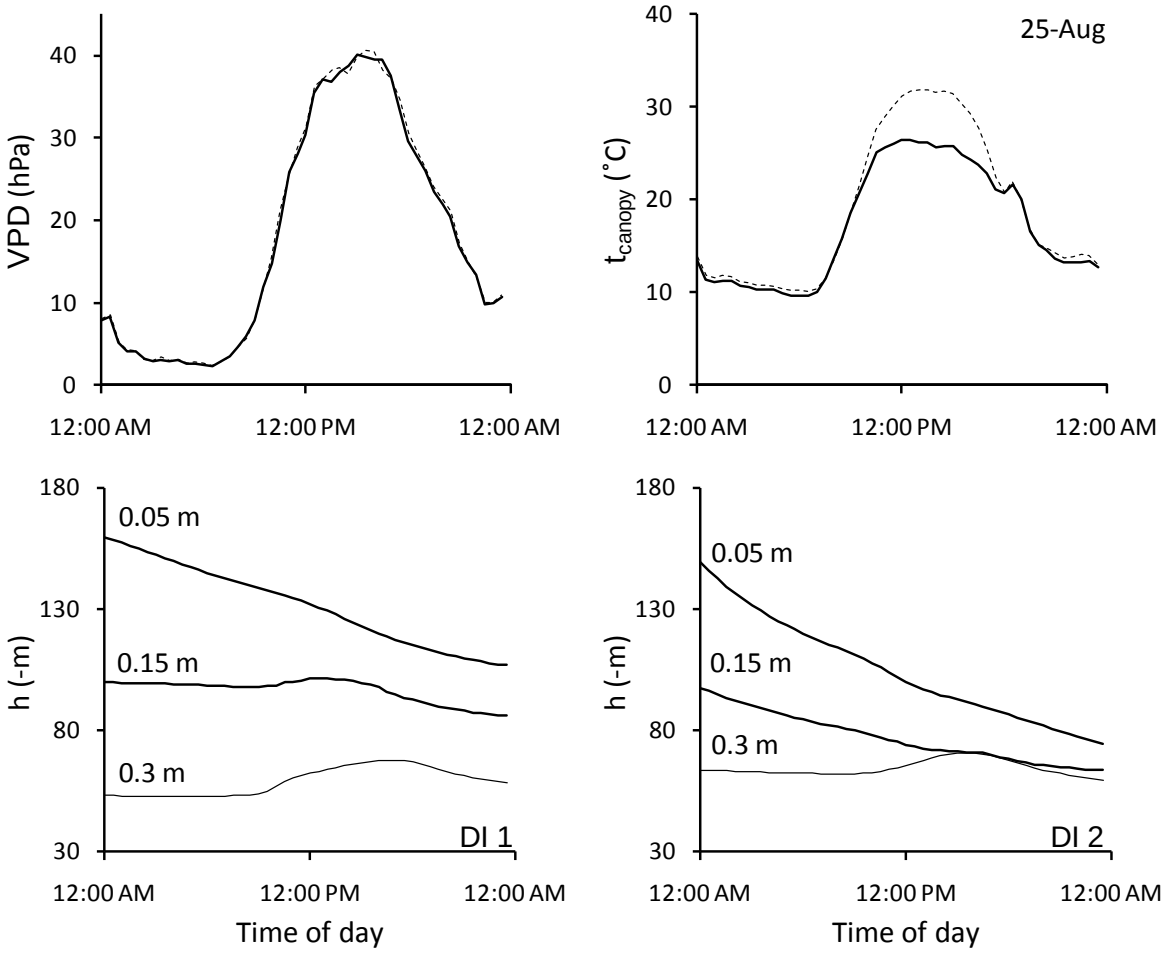

Figure 23 – Vapor pressure deficit (*VPD*) and canopy temperature (t_{canopy}) for the fully irrigated treatment (continuous line) and for the deficit irrigated treatment (dashed line), and soil water pressure head (*h*) at the two observation points in the deficit irrigated treatment (DI 1 and DI 2) on August 25, 2010

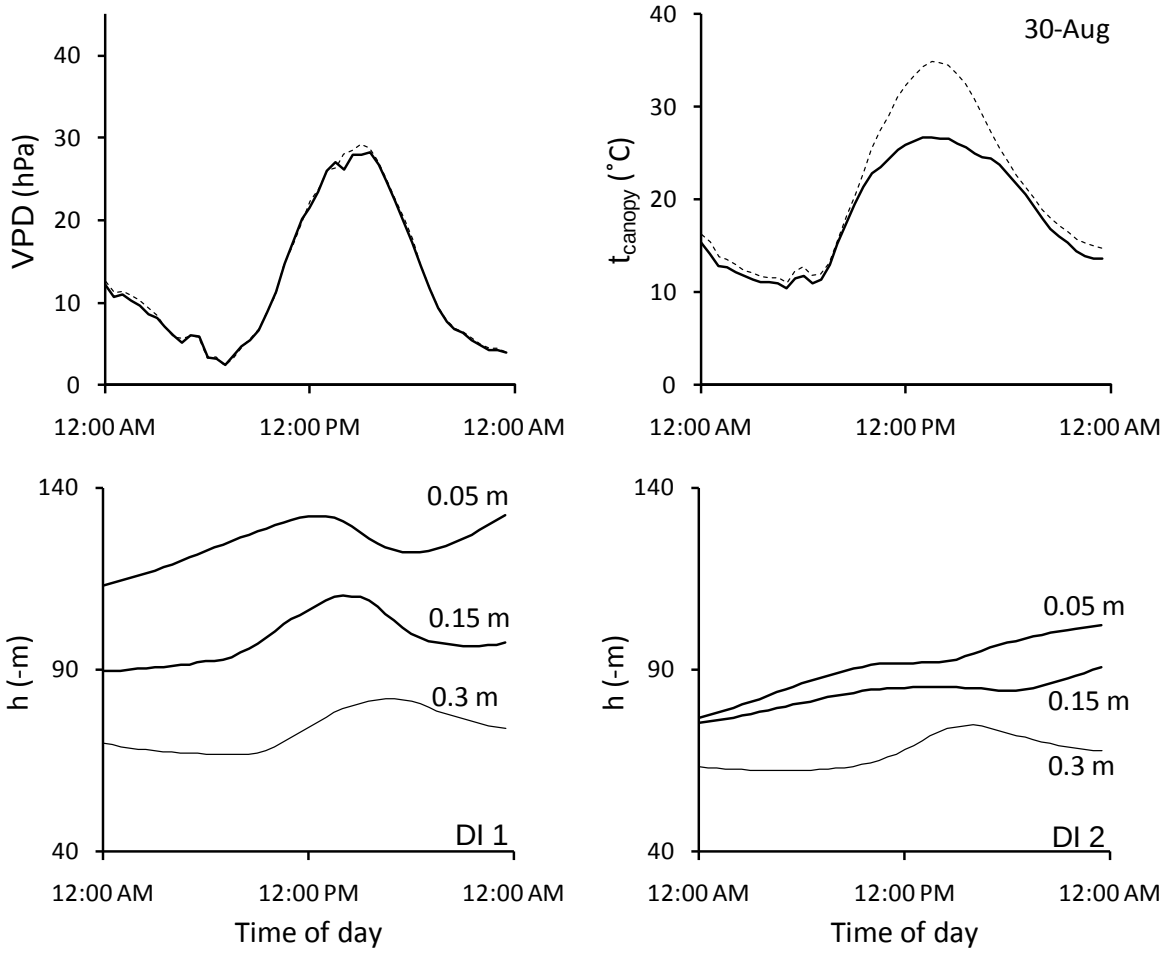

Figure 24 – Vapor pressure deficit (*VPD*) and canopy temperature (t_{canopy}) for the fully irrigated treatment (continuous line) and for the deficit irrigated treatment (dashed line), and soil water pressure head (*h*) at the two observation points in the deficit irrigated treatment (DI 1 and DI 2) on August 30, 2010

2.3.3 Root water uptake estimated by modeling

The soil water uptake by roots was estimated by the model at a daily scale; the analysis with a temporal resolution of 30 minutes showed inefficient because of the bias in individual observations. The soil water uptake estimated from the experimental data was also calculated on a daily scale. Both estimates were made for the deficit irrigated treatment.

The root water uptake model is sensitive to the root length density of plant, as shown by Jong Van Lier et al. (2008). Values obtained in the literature and mentioned in item 2.2.9.1 were used in the calculations. Following Faria et al. (2010), the empirical parameter f_z was fitted to each observation point and to combinations of K_s and λ

(Table 4). The data set of the layer between 0.1-0.2 m from observation point 1 did not converge and the values of f_z for this layer presented in Table 4 and used in Figure 26 are the same obtained to the point observation 2. In addition, data between 24 and 27 of August were excluded from analysis because in this period the plots were irrigated, reducing the reliability of measurements.

The different fitting combinations of λ and K_s (the upper limit of K_s combined to the lower limit of λ, and the lower limit of K_s combined to the upper limit of λ) were used to determine the range of parameter f_z. Faria et al. (2010) found f_z = 0.049, while in this study the fitted values of f_z were between 0.00143 and 0.00975, values around 10 times smaller. The experiment de Faria et al. (2010) was conducted with a disturbed soil material of medium texture, allowing more homogeneous root distribution increasing the efficiency of roots to take up water from the soil. The field experiment described in this thesis, on the other hand, was in a Rhodic Kanhapludalf, a soil type known for its high structural degree. The root system of plants is very heterogeneously distributed in this type of soil, making root water extraction less efficient an explaining the low values of f_z observed.

To check the sensitivity of f_z to the permanent wilting pressure head at the root surface h_0, the corresponding sensitivity coefficient η was calculated (eq. 47). To determine η, the original value used for h_0 (-150 m) was reduced by 0.1% (-150.15 m) (Table 5). With this new value, the procedure of f_z determination was done again. The η values were between 0.07 and 0.7, being f_z little to moderately sensitive to h_0.

Table 4 – Fitted values of parameter f_z to different combinations of K_s and λ for observation points in the deficit irrigated treatment

Observation point	Depth	f_z		
		K_s 95% lower	K_s adjusted	K_s 95% upper
		λ 95% upper	λ adjusted	λ 95% lower
DI 1	0-0.1 m	0.00168269	0.00305961	0.00321475
	0.1-0.2 m	0.00722595	0.00469817	0.00282977
DI 2	0-0.1 m	0.00974938	0.00360748	0.00143127
	0.1-0.2 m	0.00722595	0.00469817	0.00282977

Table 5 – Sensitivity coefficient η (eq. 47) of parameter f_z to the pressure head at root surface for different combinations of K_s and λ for observation points in the deficit irrigated treatment

Observation point	Depth	η		
		K_s 95% lower	K_s adjusted	K_s 95% upper
		λ 95% upper	λ adjusted	λ 95% lower
DI 1	0-0.1 m	-0.7411	-0.2308	-0.1548
DI 2	0-0.1 m	-0.1187	-0.1373	-0.1026
	0.1-0.2 m	-0.0752	-0.1164	-0.1710

The comparison between the root water uptake estimated by the model and by experimental data for the first soil layer (0-0.1 m) is shown in Figure 25, and for the soil layer between 0.1-0.2 m in Figure 26. The horizontal axis represents the root water uptake obtained from the experimental data (S_{exp}) and the vertical axis estimated by the model of Jong van Lier et al. (2008) (S_{mod}). After adjusting f_z, the water uptake in both observation points of the surface layer (Figure 25) is similar, with maximum values of approximately 0.018 $m^3\ m^{-3}\ d^{-1}$. Considering the soil depth (0.2 m), the uptake rate corresponds to an extraction of 3.6 mm d^{-1}. These values were obtained in both cases with the upper limit of K_s and lower λ. Most of the extraction, however, is close to zero

during the period from August 2 to September 2, confirming the results presented in Section 2.3.2 that indicated the reduction in soil water content and the occurrence of water stress.

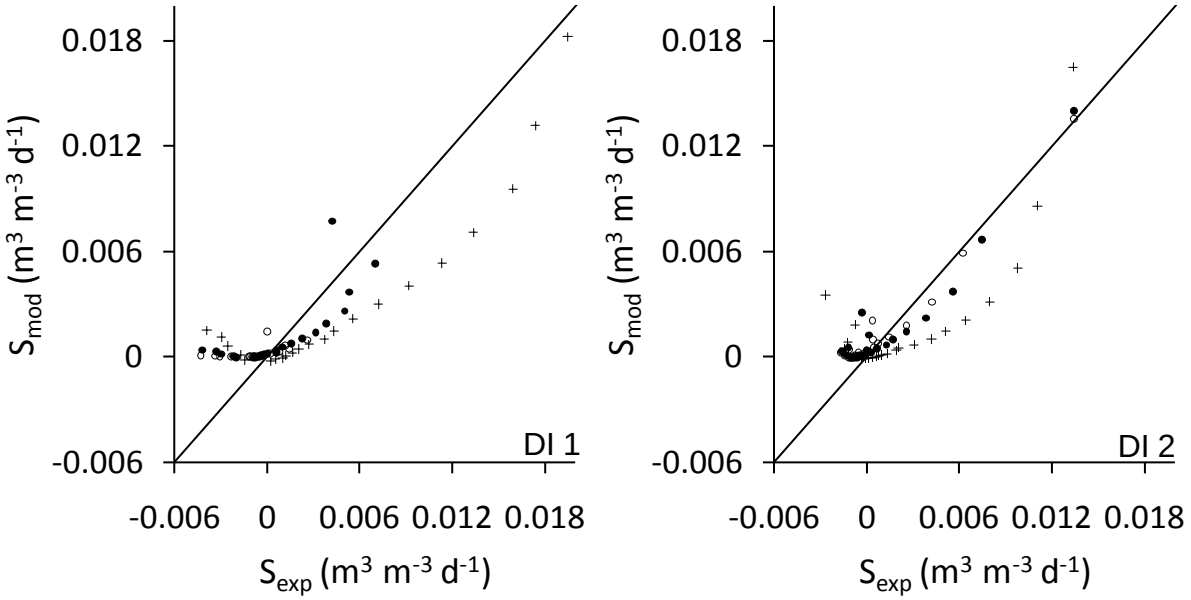

Figure 25 – Root soil water uptake calculated with experimental data (S_{exp}) and estimated by the model proposed by Jong Van Lier et al. (2008) (S_{mod}) for the soil layer between 0-0.1 m, two observation points (DI 1 e DI 2) in the deficit irrigated treatment. Black circles represent values calculated with fitted values of K_s and λ, open circles are calculated with the lower 95% limit of K_s and the upper 95% limit of λ, and crosses are calculated with the upper 95% limit of K_s and the lower 95% limit of λ

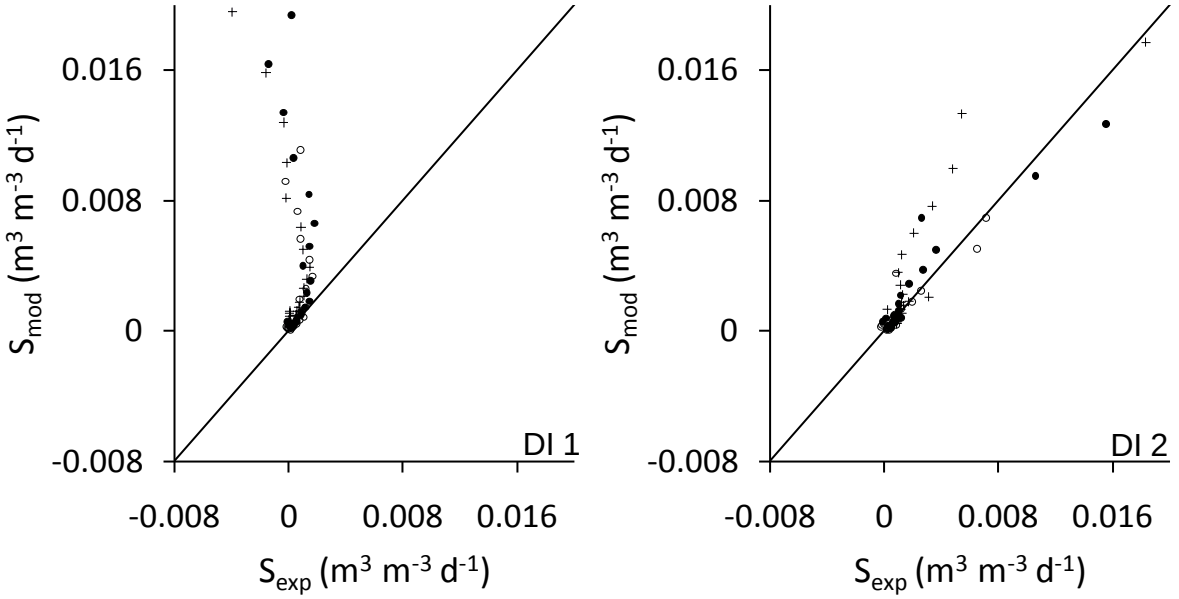

Figure 26 – Root soil water uptake calculated with experimental data (S_{exp}) and estimated by the model proposed by Jong Van Lier et al. (2008) (S_{mod}) for the soil layer between 0.1-0.2 m, two observation points (DI 1 e DI 2) in the deficit irrigated treatment. Black circles represent values calculated with fitted values of K_s and λ, open circles are calculated with the lower 95% limit of K_s and the upper 95% limit of λ, and crosses are calculated with the upper 95% limit of K_s and the lower 95% limit of λ

Figures 27 and 28 show water uptake as a function of time for the first soil layer; Figures 29 and 30 show the same for the soil layer between 0.1-0.2 m. For both surface layers of the two observation points and for the second layer of observation point 2, S_{mod} was higher at the beginning of August, when the soil water content was higher. As soil dries out, the water uptake decreases significantly reaching zero or even negative values in all layers. Different combinations of λ and K_s show the sensitivity of water uptake to the confidence interval of hydraulic conductivity. For August 7, for example, water uptake obtained for the surface layer of observation point 1 is equal to 0.007 m^3 m^{-3} d^{-1} if calculated with the fitted values of λ and K_s and 0.25 m^3 m^{-3} d^{-1} higher if calculated by combining the higher 95% limit of K_s to the lower 95% limit of λ. At the end of August, when it was considerably drier compared to the beginning of the month, soil hydraulic conductivity was reduced, also reducing the absolute difference between the water uptake obtained with different combinations of λ and K_s.

One aspect to be observed in water uptake obtained from the model as well as from the experimental data is the water release from roots to the soil, expressed by negative values of water extraction. The phenomenon of water loss by the roots, referred as hydraulic lift (CALDWELL; DAWSON; RICHARDS, 1998) or reverse flux (XU; BLAND, 1993), was reported in the literature for different species, including beans (SCHIPPERS; SCHROTH; HILDEBRAND, 1967). In case of water stress, the release of water by roots is a consequence of the pressure head difference between soil and root surface in which roots act as water conductors. In Figures 25 and 26, it is observed that at some occasions negative values were simulated for S_{mod} and estimated for S_{exp}. According to the model by Jong van Lier et al. (2008), in order to occur water release by the roots $\overline{M}_0$ must be smaller than $M_{0,z}$, in other words, the mean pressure head in the soil must be smaller (more negative) than the pressure heat at permanent wilting point (h_w). In the model, the value of h_w was kept constant and equal to -150 m for all simulations, but h in the soil became even more negative resulting in the water release. On the other hand, negative values of S_{mod} and S_{exp} can also be caused by imprecision in the determination of soil hydraulic properties, mainly $K(h)$, and of field measurements. As shown in Section 2.3.1, $K(h)$ was determined by the evaporation method and presented a relative imprecision (assessed by the 95% confidence interval) of an order of 10 times.

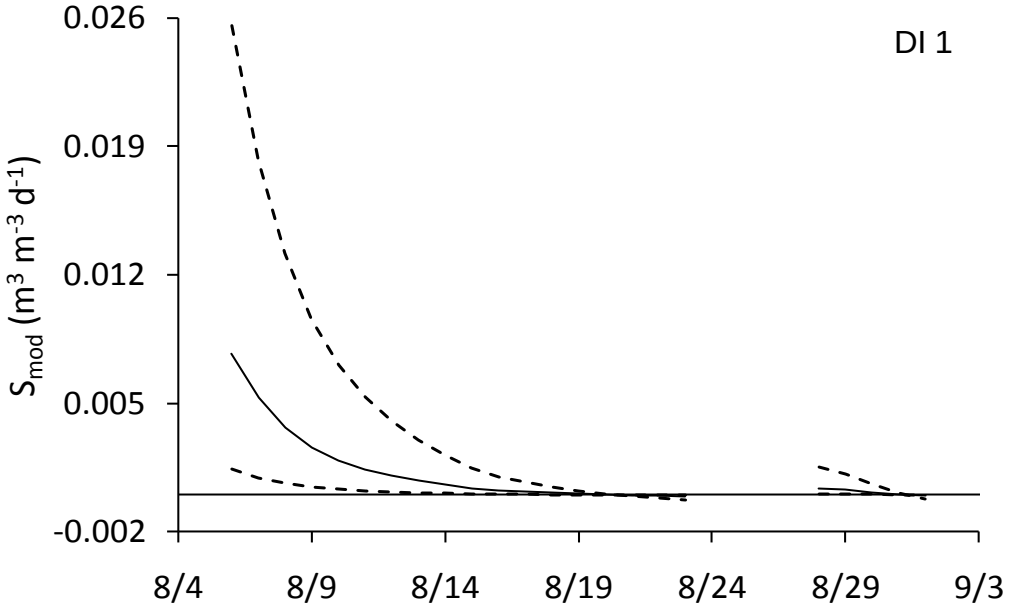

Figure 27 – Root soil water uptake (S_{mod}) in the soil layer between 0-0.1 m at observation point 1 (DI 1) of the deficit irrigated treatment as a function of date (m/dd/2010). Dashed lines represent estimates using the upper and lower limits of K_s and λ with 95% confidence interval

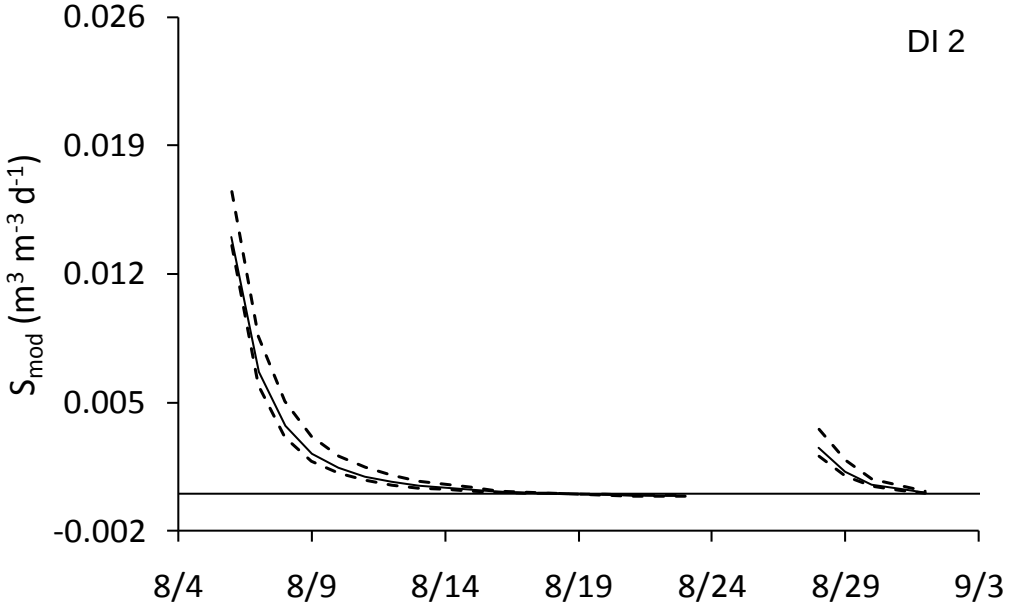

Figure 28 – Root soil water uptake (S_{mod}) in the soil layer between 0-0.1 m at observation point 2 (DI 2) of the deficit irrigated treatment as a function of date (m/dd/2010). Dashed lines represent estimates using the upper and lower limits of K_s and λ with 95% confidence interval

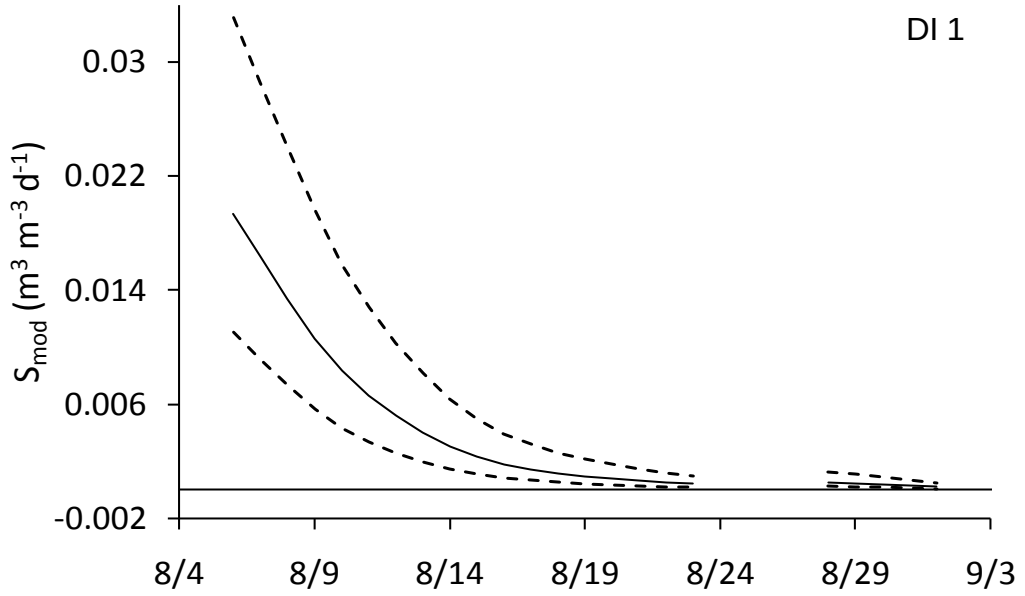

Figure 29 – Root soil water uptake (S_{mod}) in the soil layer between 0.1-0.2 m at observation point 1 (DI 1) of the deficit irrigated treatment as a function of date (m/dd/2010). Dashed lines represent estimates using the upper and lower limits of K_s and λ with 95% confidence interval

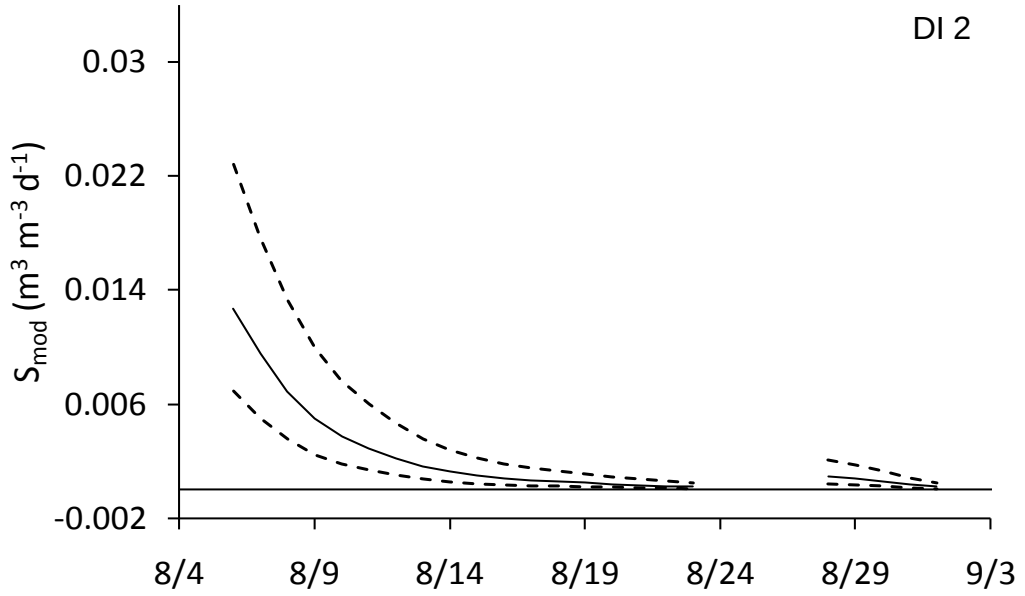

Figure 30 – Root soil water uptake (S_{mod}) in the soil layer between 0.1-0.2 m at observation point 2 (DI 2) of the deficit irrigated treatment as a function of date (m/dd/2010). Dashed lines represent estimates using the upper and lower limits of K_s and λ with 95% confidence interval

2.3.4 Plant transpiration rate estimated by modeling

2.3.4.1 Analysis on a detailed temporal scale

The transpiration rate was estimated by the Ag_s model for August 15, 23, 25 and 30, 2010. As mentioned before, these days were chosen based on the analysis of Figure 15 and represent different environmental conditions. Table 6 presents values of g_s, A and T observed by other authors that were used, together with measurements of T and g_s from the field experiment (Figure 16), for comparison with the simulations. By comparison of the values in Table 6, it appears that the values observed in this study corroborate in part with the measurements obtained in other studies, since the maximum values of g_s and T are up to 13 mm s^{-1} and 322 mg m^{-2} s^{-1} higher than those observed by Comstock and Ehleringer (1993), for example.

Table 6 – Stomatal conductance, CO_2 net assimilation and transpiration rate of bean plants (*Phaseolus vulgaris* L.) obtained by some authors and in this study

Reference	Water stress	Growing conditions	g_s (mm s^{-1})	A (mg m^{-2} s^{-1})	T (mg m^{-2} s^{-1})
Comstock and Ehleringer (1993)	Yes	Greenhouse	12.8-33.34	1.23-1.58	72 - 360
Lopes (1999)	No	Greenhouse	10.3-31	0.59-0.81	-
Paiva et al. (2005)	Yes	Field	6.56-20.12	-	-
Santos et al. (2006)	Yes	Greenhouse	5.1-23.08	0.17-1.27	-
Present study	Yes	Field	1.66-47.12	-	34.2 - 682.72

Figure 31 shows the simulations with the Ag_s model for August 15. The specific humidity deficit D_s, calculated by the model from the difference between the specific humidity at saturation at canopy temperature and air specific humidity, was higher during the warmest periods of the day in the deficit irrigated treatment. The simulations of CO_2 assimilation, stomatal conductance and transpiration rate showed a consistent pattern for the environmental conditions of that day, although the values were higher than

expected when compared to other studies (Table 6). Both simulated variables were higher for the fully irrigated treatment plants, showing that the deficit irrigated plants, without irrigation for 13 days, already were suffering the effect of reduced soil water content availability. No dip in transpiration rate during the warmest times of the day was observed, possibly because of the relatively low air temperature.

Figure 32 shows simulation results for August 23. The D_s in the deficit irrigated treatment reached values 16 g kg^{-1} higher than in the fully irrigated treatment. The simulation of *A* for plants of the deficit irrigated treatment showed a significant reduction during the warmest hours of the day, at the same time that fully irrigated plants maintained a nearly constant rate. The afternoon dip in transpiration rate was observed in plants of the fully irrigated treatment since the air temperature was high, and stomatal resistance increased after 9:30 AM. The transpiration rate of deficit irrigated plants suffered a greater reduction during the warmest hours of the day in response to the air temperature and to the reduced soil water content.

Results for August 25 are shown in Figure 33. The day before, on August 24, plants of both treatments were irrigated (15 mm). The D_s of the deficit irrigated treatment decreased on August 25 and as a consequence the difference of D_s between the two treatments was reduced. As shown by the simulation of *A*, the deficit irrigated plants recovered and their assimilation of CO_2 exceeded the levels estimated for day 23. The values of g_s and transpiration rate of the deficit irrigated treatment, obtained from *A*, also increased in relation to day 23. For the fully irrigated treatment, the assimilation of CO_2 and other variables decreased during the warmest hours of the day in relation to day 23 due to the increase of air temperature.

The simulation results for August 30 are shown in Figure 34, and show signs of severe plant water stress. The D_s in the deficit irrigated treatment was again slightly higher than in the fully irrigated treatment during most of the day. According to the simulations, the deficit irrigated plants absorbed less CO_2 and the stomatal conductance and transpiration rate presented the lowest values of all days. In the fully irrigated treatment, there was an afternoon dip in transpiration rate, which occurred around 2:00 PM.

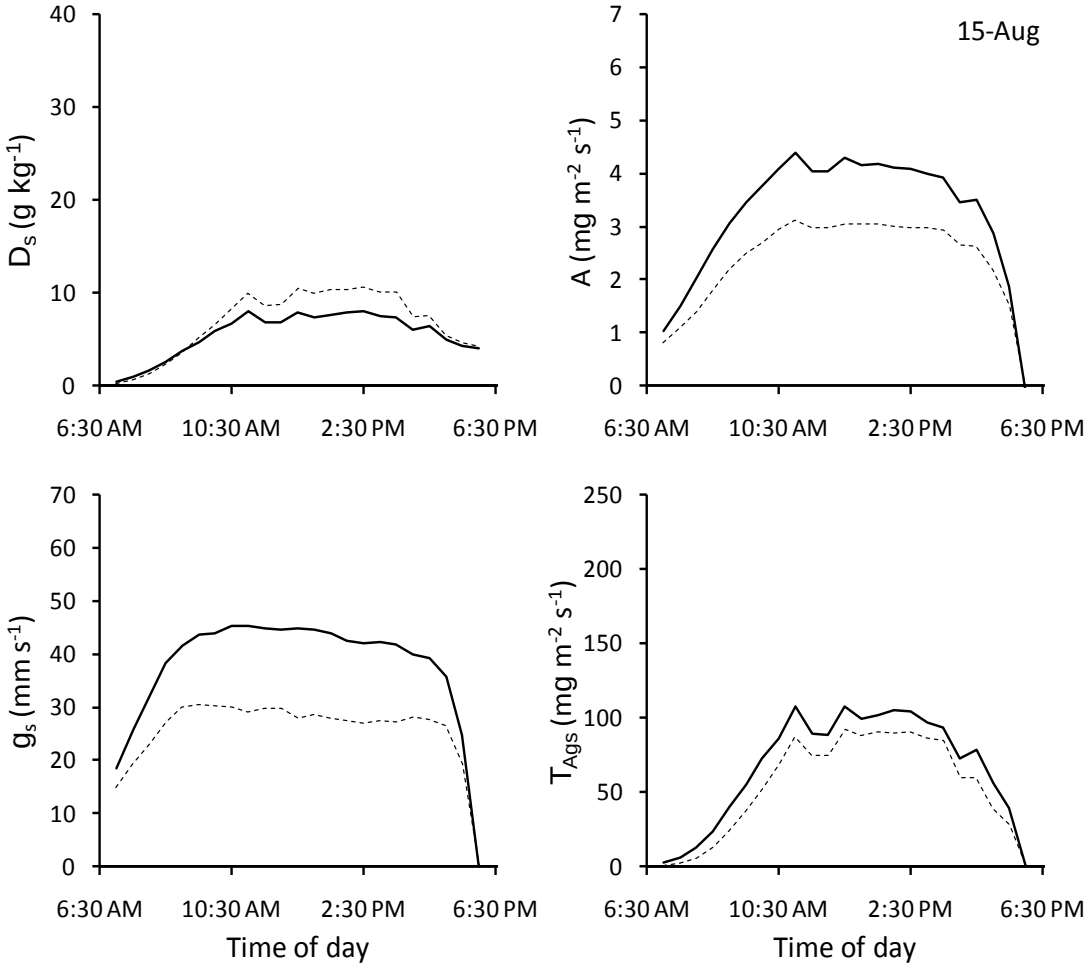

Figure 31 – Specific humidity deficit (D_s), CO_2 net assimilation (A), stomatal conductance for water vapor (g_s) and transpiration rate (T_{Ags}) between 7:00 AM and 6:00 PM of August 15, 2010. Solid lines represent the fully irrigated treatment and dashed lines represent the deficit irrigated treatment

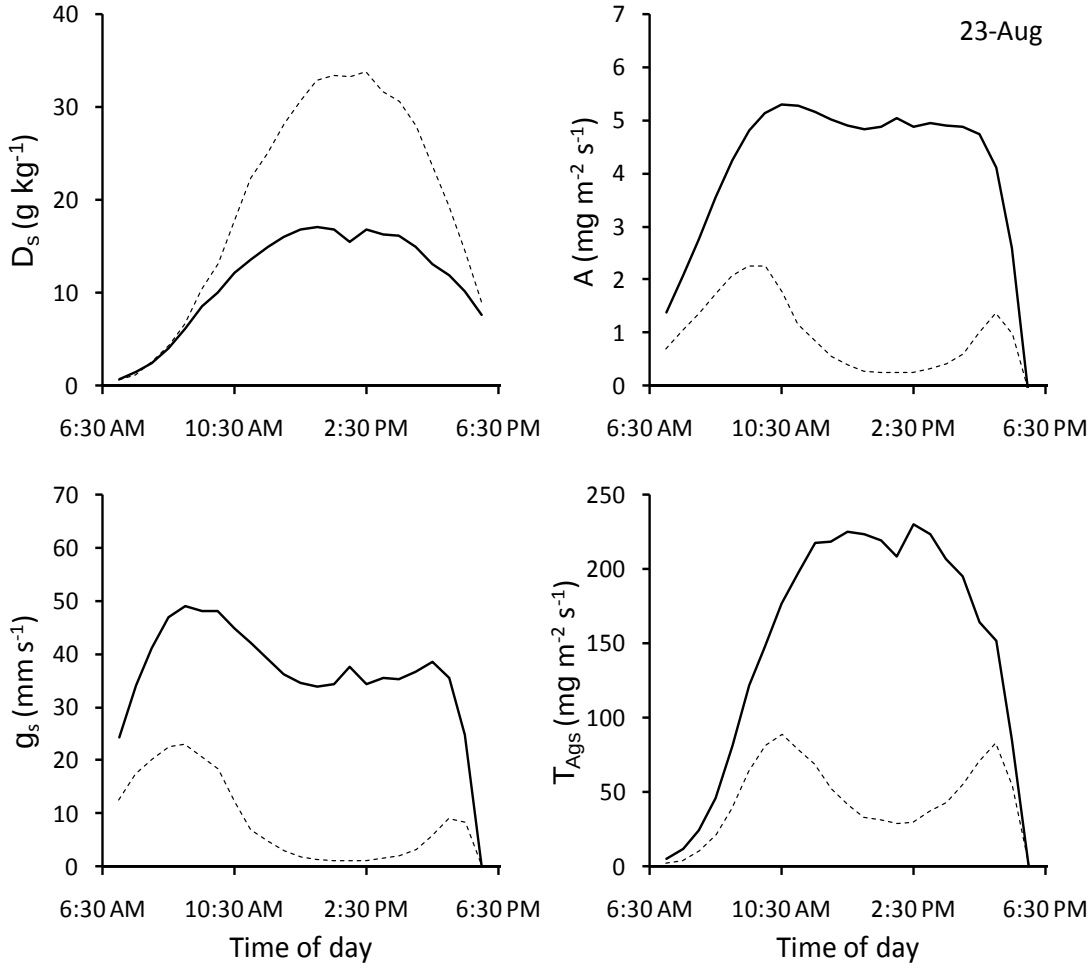

Figure 32 – Specific humidity deficit (D_s), CO_2 net assimilation (A), stomatal conductance for water vapor (g_s) and transpiration rate (T_{Ags}) between 7:00 AM and 6:00 PM of August 23, 2010. Solid lines represent the fully irrigated treatment and dashed lines represent the deficit irrigated treatment

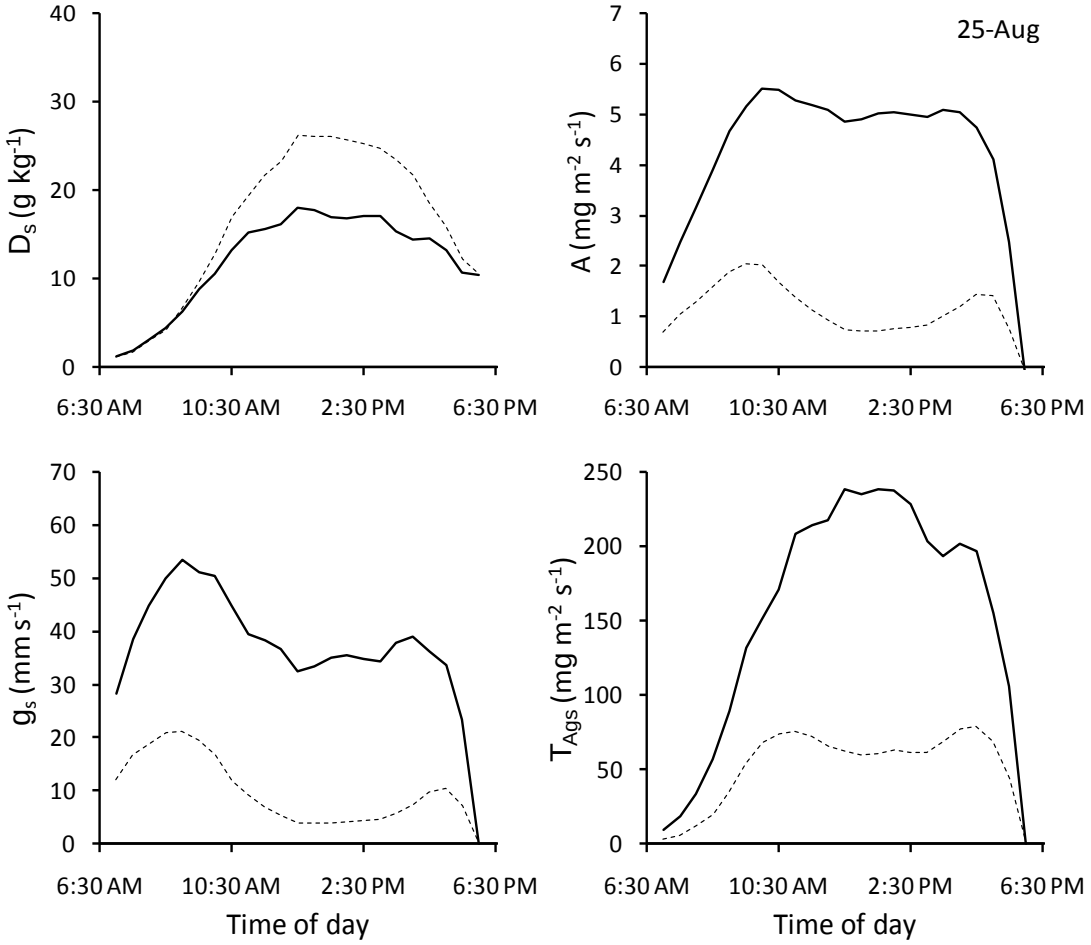

Figure 33 – Specific humidity deficit (D_s), CO_2 net assimilation (A), stomatal conductance for water vapor (g_s) and transpiration rate (T_{Ags}) between 7:00 AM and 6:00 PM of August 25, 2010. Solid lines represent the fully irrigated treatment and dashed lines represent the deficit irrigated treatment

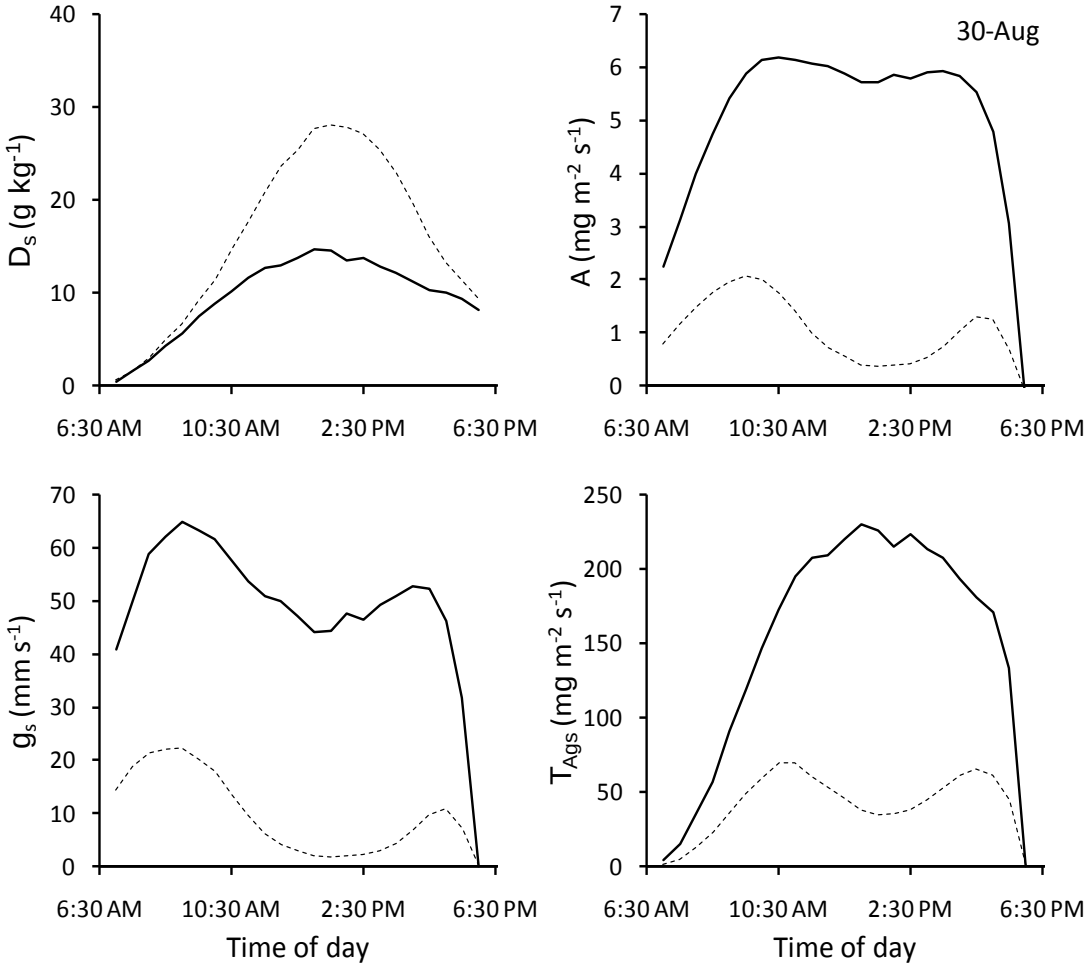

Figure 34 – Specific humidity deficit (D_s), CO_2 net assimilation (A), stomatal conductance for water vapor (g_s) and transpiration rate (T_{Ags}) between 7:00 AM and 6:00 PM of August 30, 2010. Solid lines represent the fully irrigated treatment and dashed lines represent the deficit irrigated treatment

2.3.4.2 Analysis on a daily time scale

The simulations with Ag_s model were also made on a daily time scale for the entire period between August 5 and September 2, and the maximum daily values of D_s, A, g_s and T_{Ags} are shown in Figure 35 for both treatments. The specific humidity deficit of the fully irrigated treatment slightly increased (~ 8.2 g kg^{-1}) during the month, contrarily to the deficit irrigated plants, in which D_s in early September was approximately 31.2 g kg^{-1} greater than at the beginning of August. The cultivar Pérola used in this experiment is of indeterminate growth, the rate of leaf area in the fully irrigated treatment increasing until the end of the experiment, while the *LAI* of the deficit irrigated treatment

increased until August 12 and then decreased due to the partial loss of leaves as a result of water stress. On the whole, from the simulations of *A* plants in the fully irrigated treatment increased the maximum CO_2 assimilation during the month because of the increasing air temperature and *LAI*. As a result, g_s and T_{Ags} also tended to increase until the beginning of September. On the other hand, while D_s in the deficit irrigated treatment increased significantly during the month, the maximum assimilation rate of CO_2 increased only until August 12 in agreement to the increase in leaf area. From then on the assimilation showed a downward tendency until the end of the month, together with g_s and T_{Ags}.

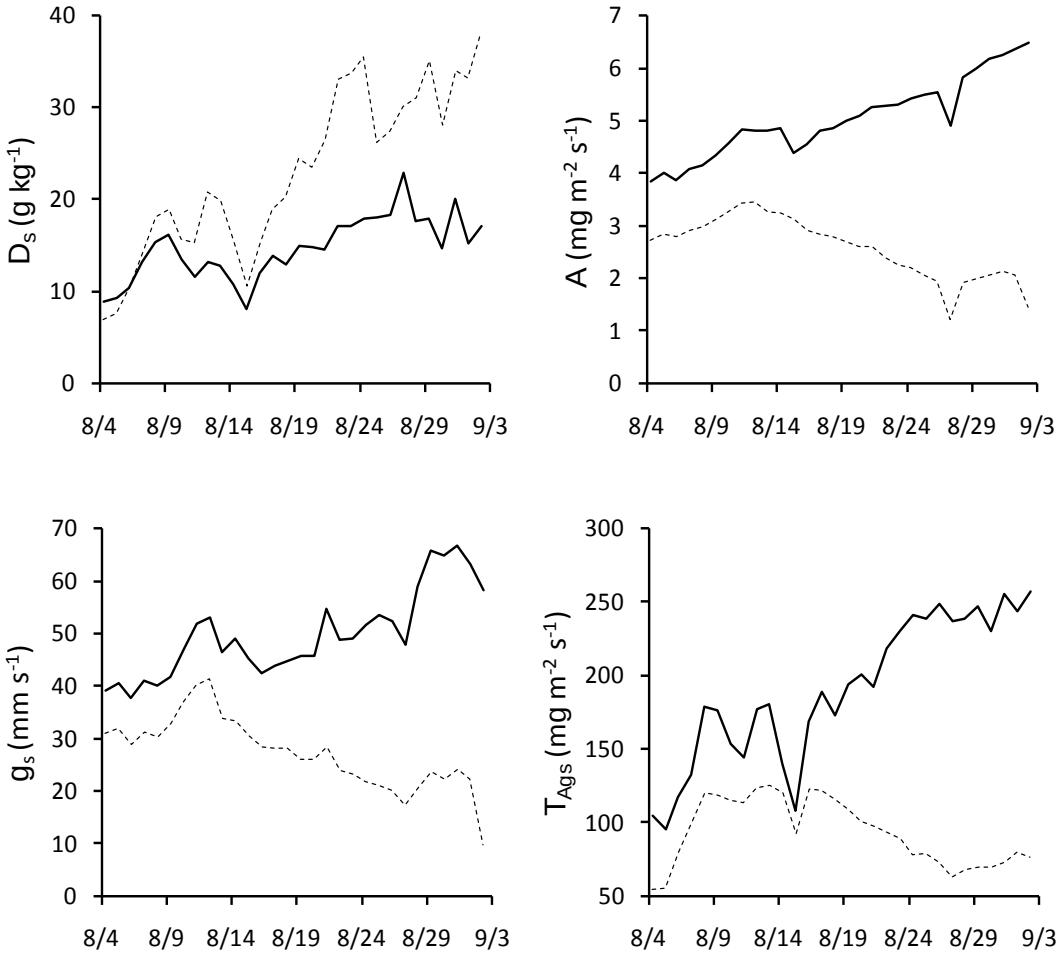

Figure 35 – Maximum daily values of specific humidity deficit (D_s), CO_2 net assimilation (A), stomatal conductance for water vapor (g_s) and transpiration rate (T_{Ags}) simulated by Ag_s model for the fully irrigated (continuous line) and deficit irrigated (dashed line) treatments as a function of date (m/dd/2010)

3 CONCLUSIONS

The methodology used in this study allowed confirming the hypothesis that water stress in plants is caused by environmental factors related to the soil-root and leaf-atmosphere interfaces. Regarding the soil-root interface, the most important environmental factors are the soil hydraulic properties, especially the hydraulic conductivity, and the root length density; on the leaf-atmosphere interface the vapor pressure deficit of atmospheric air is of highest importance. Both interfaces must be somehow considered in crop water stress modeling.

The detection of water stress occurrence in the deficit irrigated plants was made by comparisons between *VPD* and $\Delta t_{canopy\text{-}air}$ and between t_{canopy} and t_{wb} of the two irrigation treatments. The deficit irrigated plants did not show a linear relationship between *VPD* and $\Delta t_{canopy\text{-}air}$ and the canopy temperature tended to increase in relation to t_{wb} during the drying period. These patterns were not observed for plants in the fully irrigated treatment. The onset of water stress in deficit irrigated plants was on August 5. From that day on, the difference $\Delta t_{canopy\text{-}air}$ between treatments, as well as the difference between *VPD*, continuously remained positive until the beginning of September. It could be shown experimentally that plants in the deficit irrigated treatment suffered from water stress for about a month. On a time scale of 30 minutes, it could be shown that the transpiration rate was reduced even though the vapor pressure deficit was low in the atmosphere if the soil water content was reduced.

The simulations with the mechanistic model of soil water root uptake proposed by Jong van Lier et al. (2008) and of CO_2 assimilation by Jacobs (1994) were compared to observations of the two treatments. The soil water uptake model was sensitive to soil hydraulic parameters, especially hydraulic conductivity and root length density. The soil hydraulic conductivity determined by evaporation experiments in laboratory presented a large statistical deviation, propagating into the values obtained from the water uptake model. The root length density had not been measured in the field experiment and literature values were used. However, it was possible to fit an empirical factor to represent the difference between the literature values of root length density and those that matched in the experiment. The inclusion of this empirical factor is necessary to

correct for the effect of heterogeneous distribution of roots in soil on root water uptake due to, since the model without correction factor supposes a homogeneous distribution of the root system.

The transpiration rate estimated by the Jacobs (1994) model showed to be dependent on the canopy temperature used to calculate the specific humidity deficit between leaves and air D_s and the mesophyll conductance, on the mesophyll conductance, on D_s (on its turn also dependent on air temperature), and on the leaf area index. These parameters were evaluated by comparing the simulations with the data of fully irrigated and deficit irrigated treatment. However, the relative importance of each of them could not be identified clearly in this study. The characteristics of simulated A, g_s and T proved consistent with the expected diurnal time scale. On the other hand, the maximum values of A and g_s were overestimated by the model, while the values of transpiration rate were underestimated when compared to those obtained by observational studies. Being a mechanistic model, the Ag_s model requires and is sensitive to several parameters. The use of values from literature obtained under conditions that are not always comparable with the real experimental conditions may not fully represent the processes that occurred. Simulations showed that at some days even plants in the fully irrigated treatment showed signs of water stress at the warmest times of the day.

CITED LITERATURE

AGELE, S.O.; COHEN, S. Within plant resistance to water flow in tomato and sweet melons. **African Crop Science Journal**, Kampala, v. 15, n. 1, p. 127-138, Jan. 2007.

ALLEN, R.G.; PEREIRA, L.S.; RAES, D. **Crop evapotranspiration**. Roma: FAO 1998. 297 p. (FAO. Irrigation and Drainage Paper, 56).

ANGELOCCI, L.R. **Água na planta e trocas gasosas/energéticas com a atmosfera:** introdução ao tratamento biofísico. Piracicaba: O autor, 2002. 272 p.

AMATO, M.; PARDO, A. Root length and biomass losses during sample preparation with different screen mesh sizes. **Plant and Soil**, Dordrecht, v. 161, p. 299-303, Sept. 1994.

BAKKER, G.; VAN DER PLOEG, M.J. VAN DER; ROOIJ, G.H. DE; HOOGENDAM, C.W.; GOOREN, H.P.A.; HUISKES, C.; KOOPAL, L.K.; KRUIDHOF, H. New polymer tensiometers: measuring matric pressures down to the wilting point. **Vadose Zone Journal**, Madison, v. 6, n. 1, p. 196-202, Feb. 2007.

BALL, J.T. Calculations related to gas exchange. In: ZEIGER, E.; FARQUHAR, G.D.; COWAN, I.R. (Ed.). **Stomatal function**. Stanford: Stanford University Press, 1987. p. 445-476.

BERGAMASCHI, G.; VIEIRA, H.J.; OMETTO, J.C.; ANGELOCCI, L.R.; LIBARDI, P.L. Deficiência hídrica em feijoeiro. I. Análise de crescimento e fenologia. **Pesquisa Agropecuária Brasileira**, Brasília, v. 23, n. 7, p. 733-743, out. 1988.

BERGAMASCHI, G.; VIEIRA, H.J.; LIBARDI, P.L.; OMETTO, J.C.; ANGELOCCI, L.R. Deficiência hídrica em feijoeiro. III. Evapotranspiração máxima e relações com a evapotranspiração calculada pelo método de Penman e com a evaporação do tanque "Classe A". **Pesquisa Agropecuária Brasileira**, Brasília, v. 24, n. 4, p. 387-392, abr. 1989.

BERLATO, M.A.; MATZENAUER, R.; BERGAMASCHI, H. Evapotranspiração máxima da soja relações com a evapotranspiração calculada pela equação de Penman, evaporação de tanque "classe A" e radiação solar global. **Agronomia Sulriograndense**, Porto Alegre, v. 22, n. 2, p. 243-259, fev. 1986.

BETTS, R.A.; COX, P.M.; LEE, S.E.; WOODWARD, F.I. Contrasting physiological and structural vegetation feedbacks in climate change simulations. **Nature**, London, v. 387, n. 5, p. 796-799, May 1997.

BLACK, T.A.; GARDNER, W.R.; THURTELL, G.W. The prediction of evaporation, drainage and soil water storage for a bare soil. **Soil Science Society of America Journal**, Madison, v. 33, p. 655-660, June 1969.

BLIZZARD, W.E.; BOYER, J.S. Comparative resistance of the soil and the plant to water transport. **Plant Physiology**, Waterbury, v. 66, n. 5, p. 809-814, Mar. 1980.

BOCCARA, M.; BOUÉ, C.; GARMIER, M.; PAEPE, R. de; BOCCARA, A.-C. Infra-red thermography revealed a role for mitochondria in pre-symptomatic cooling during harpin-induced hypersensitive response. **The Plant Journal**, New York, v. 28, n. 6, p. 663-670, June 2001.

BOWDEN, R.L.; ROUSE, D.I.; SHARKEY, T.D. Mechanism of photosynthesis decrease by *Verticillium dahliae* in potato. **Plant Physiology**, Waterbury, v. 94, n. 13, p. 1048-1055, May 1990.

BRINGHAM, I. J.Soil-root-canopy interactions. **Annals of Applied Biology**, San Francisco, v. 138, n. 2, p. 243-251, June 2001.

BROADLEY, M.J.; ESCOBAR-GUTIERREZ, A.J.; BURNS, A.; BURNS, I.G. Nitrogen limited growth of lettuce is associated with lower stomatal conductance. **New Phytologist Journal**, Lancaster, v. 152, n. 1, p. 97-106, Apr. 2001.

BROWN, H.T.; ESCOMBE, F. Researches on some of the physiological processes of green plants with special references to the interchange of energy between the leaf and the surroundings. **Proceedings of the Royal Society**, London, v. 76, n. 1, p. 29-111, Feb. 1905.

BUNCE, J.A. Effect of boundary layer conductance on the response of stomata to humidity. **Plant, Cell and Environment**, Logan, v. 8, n. 1, p. 55-57, Sept. 1985.

CALDWELL, M.M.; DAWSON, T.E.; RICHARDS, J.H. Hydraulic lift: consequences of water efflux from the roots of plants. **Oecologia**, Berlin, v. 113, p. 151-161, Oct. 1998.

CALVET, J.-C.; NOILHAN, J.; ROUJEAN, J.-L.; BESSEMOULIN, P.; CABELGUENNE, M.; OLIOSO, A.; WIGNERON, J.-P. An interactive vegetation SVAT model tested against data from six contrasting sites. **Agricultural and Forest Meteorology**, Amsterdam, v. 92, p. 73–95, Sept. 1998.

CAMPBELL, G.S.; NORMAN, J.M. **An introduction to environmental biophysics.** New York: Spring-Verlag, 1998. 286 p.

CARBON, B.A. Diurnal water stress in plants grown on a course soil. **Australian Journal of Soil Research**, Melbourne, v. 11, n. 1, p. 33-42, Jan. 1973.

CASAROLI, D. **Transpiração de plantas e condições hidráulicas do solo.** 2008. 145 p. Tese (Doutorado em Física do Ambiente Agrícola) - Escola Superior de Agricultura “Luiz de Queiroz”, Universidade de São Paulo, Piracicaba. 2008.

CHAERLE, L.; VAN CAENEGHEN, V.; MESSENS, E.; LAMBERS, H.; VAN MONTAGU, M.; VAN DER STRAETEN, D. Presymptomatic visualization of plant-virus interactions by thermography. **Nature Biotechnology**, San Francisco, v. 17, n. 7, p. 813-816, Sept. 1999.

CLAWSON, K.L.; BLAD, B.L. Infrared thermometry for scheduling irrigation of corn. **Agronomy Journal**, Madison, v. 74, n. 2, p. 311-316, May 1982.

COLLATZ, G.J.; BALL, J.T.; GRIVET, C.; BERRY, J.A. Physiological and environmental regulation of stomatal conductance, photosynthesis and transpiration: a model that includes a laminar boundary layer. **Agricultural and Forest Meteorology**, Amsterdam, v. 54, n. 2/4, p. 107-136, July 1991.

COMSTOCK, J.; EHLERINGER, J. Stomatal response to humidity in common bean (*Phaseolus vulgaris*): implications for maximum transpiration rate, water-use efficiency and productivity. **Australian Journal of Plant Physiology**, Melbourne, v. 20, p. 669-691, July 1993.

COSTA, R.C.L.; LOPES, F.N.; OLIVA, M.A. Crescimento, morfologia, partição de assimilados e produção de matérica seca em *Phaseolus vulgaris* L. submetido a três níveis de nitrogênio e dois regimes hídricos. **Pesquisa Agropecuária Brasileira**, Brasília, v. 29, n. 9, p. 1453-1465, jul. 1991.

COWAN, I.R. Transport of water in the soil-plant-atmosphere system. **Journal of Applied Ecology**, London, v. 2, n. 1, p. 221-239, Jan. 1965.

DIRKSEN, C.; RAATS, P.A.C. Water uptake and release by Alfalfa roots. **Agronomy Journal**, Madison, v. 77, n. 4, p. 621-626, June 1985.

DOORENBOS, J.; KASSAM, A.H. **Yield response to water**. Rome: FAO, 1979. 306 p. (Irrigation and Drainage Paper, 33).

DOORENBOS, J.; PRUITT, W.O. **Guidelines for predicting crop water requirements**. Rome: FAO, 1976. 196 p. (FAO. Irrigation and Drainage Paper, 24).

DRIESSEN, P.M.; KONIJN, N.T. **Land-use systems analysis**. Wageningen: Wageningen Agricultural University, 1992. 210 p.

DURIGON, A.; JONG VAN LIER, Q. DE; GOOREN, H.P.A.; METSELAAR, K. Measuring hydraulic conductivity down to wilting point using polymer tensiometers in an evaporation experiment. **Vadose Zone Journal**, Madison, v. 10, p. 741-746, Mar. 2011.

EHRLER, W.L. Cotton leaf temperatures as related to soil water depletion and meteorological factors. **Agronomic Journal**, Madison, v. 65, p. 404-409, Jan. 1973.

EL-SHARKAWY, M.A.; COCK, J.H.; HELD, K.A.A. Water use efficiency of Cassava. II. Differing sensitivity of stomata to air humidity in Cassava and other warm-climate species. **Crop Science**, Madison, v. 24, p. 503–507, Dec. 1984.

ENCARNAÇÃO, C.R.F. **Estudo da demanda de água do feijoeiro (*Phaseolus vulgaris* L.) var. Goiano Precoce.** 1980. 62 p. Tese (Doutorado em Irrigação e Drenagem) - Escola Superior de Agricultura “Luiz de Queiroz”, Universidade de São Paulo, Piracicaba, 1980.

FARIA, L.N.; ROCHA, M.G. da; JONG VAN LIER, Q. de; CASAROLI, D. A split-pot experiment with sorghum to test a root water uptake partitioning model. **Plant and Soil**, Dordrecht, v. 331, p. 299-311, Aug. 2010.

FARIAS, J.R.B.; ASSAD, E.D.; ALMEIDA, I.R.; EVANGELISTA, B.A.; LAZZAROTTO, C.; NEUMAIER, N.; NEPOMUCENO, A.L. Caracterização de risco de déficit hídrico nas regiões produtoras de soja no Brasil. **Revista Brasileira de Agrometeorologia**, Santa Maria, v. 9, n. 3, p. 415-421, mar. 2001.

FARQUHAR, G.D.; CAEMMERER, S. VON; BERRY, J.A. A biochemical model of photosynthetic CO_2 assimilation in leaves of C3 species. **Planta**, Berlin, v. 149, n. 1, p. 78-90, July 1980.

FEDDES, R.A.; KABAT, P.; VAN BAKEL, P.J.T.J.; BRONSWIJK, J.B.; HALBERTSMA, J. Modelling soil water dynamics in the unsaturated zone-state of the art. **Journal of Hydrology**, Tucson, v. 100, n. 1. p. 69-111, Mar. 1988.

FLEXAS, J.; RIBAS-CARBÓ, M.; DIAZ-ESPEJO, A.; GALMÉS, J.; MEDRANO, H. Mesophyll conductance to CO_2: current knowledge and future prospects. **Plant, Cell and Environment**, Logan, v. 31, p. 602-621, May 2008.

FLOWERS, M.D.; FISCUS, E.L.; BURKEY, K.O.; BOOKER, F.L.; DUBOIS, J.-J.B. Photosynthesis, chlorophyll fluorescence, and yield of snap bean (*Phaseolus vulgaris* L.) genotypes differing in sensitivity to ozone. **Environmental and Experimental Botany**, Amsterdam, v. 61, p. 190-198, Aug. 2007.

GARDNER, W.R. Dynamic aspects of water availability to plants. **Soil Science**, Baltimore, v. 89, n. 2, p. 63-73, Oct. 1960.

GEIGER, R. Klassifikation der Klimate nach W. Köppen. **Landolt-Börnstein Zahlenwerte und Funktionen aus Physik, Chemie, Astronomie, Geophysik und Technik (alte Serie), Band III (Astronomie und Geophysik)**. Berlin, v. 3, p. 204-235, Aug. 1954.

GOUDRIAAN, J.; VAN LAAR, H.H. Calculation of daily totals of the gross CO_2 assimilation of leaf canopies. **Netherlands Journal of Agricultural Science**, Wageningen, v. 26, n, 2, p. 373-382, Feb. 1978.

_____. **Modelling potential crop growth processes**. Dordrecht: Kluwer Academic, 1994. 238 p.

GOUDRIAAN, J.; VAN LAAR, H.H.; VAN KEULEN, H.; LOUWERSE, W. Photosynthesis, CO_2 and plant production. In: DAY, W.; ATKIN, R.K. (Ed.). **Wheat growth and modeling**. New York: Plenum Press, 1985. chap. 3, p. 107-122.

GROSSNICKLE, S.C.; RUSSEL, J.H. Gas exchange processes of yellow-cedar (*Chamaecyparis nootkatensis*) in response to environmental variables. **Canadian Journal of Botany**, Guelph, v. 69, p. 2684-2691, Apr. 1991.

GUILIONI, L.; JONES, H.G.; LEINONEN, I.; LHOMME, J.P. On the relationships between stomatal resistance and leaf temperatures in thermography **Agricultural and Forest Meteorology**, Amsterdam, v. 148, n. 11, p. 1908-1912, June 2008.

HATFIELD, J.L.; PINTER JR., P.J.; CHASSERAY, E.; EZRA, C.E.; REGINATO, R.J.; IDSO, S.B.; JACKSON, R.D. Effects of panicles on infrared thermometer measurements of canopy temperature in wheat. **Agricultural and Forest Meteorology**, Amsterdam, v. 32, n. 2. p. 97-105, Oct. 1984.

HEINEN, M. **Dynamics of water and nutrients in closed, recirculating cropping systems in glasshouse horticulture:** with special attention to lettuce grown in irrigated sand beds. 1997. 270 p. Thesis - Agricultural University, Wageningen, 1997.

HUGHES, D.F.; JOLLEY, V.D.; BROWN, J.C. Role for potassium in the iron-stress response mechanism of iron-efficient oat. **Soil Science Society of America Journal**, Madison, v. 53, p. 830-835, Sept. 1992.

HULUGALLE, N.R.; WILLATT, S.T. The role of soil resistance in determining water uptake by plant root systems. **Australian Journal of Soil Research**, Melbourne, v. 24, n. 4, p. 571-574, Sept. 1983.

IDSO, S.B. Non-water stressed baselines: a key to measuring and interpreting plant water stress. **Agricultural Meteorology**, Amsterdam, v. 27, p. 59-70, July 1982.

IDSO, S.B.; JACKSON, R.D.; REGINATO, R.J. Remote sensing of crop yields. **Science**, Washington, v. 196, p. 19-25, July 1977.

IDSO, S.B.; JACKSON, R.D.; PINTER, P.J.; REGINATO, R.J.; HATFIELD, J.L. Normalizing the stress-degree-day parameter for environmental variability. **Agricultural Meteorology**, Amsterdam, v. 24, p. 45-55, Oct. 1981.

JACKSON, R.D.; REGINATO, R.J.; IDSO, S.B. Wheat canopy temperature: a practical tool for evaluating water requirements. **Water Resources Research**, Washington, v. 13, n. 3, p. 651-656, Sept. 1977.

JACKSON, R.D.; IDSO, S.B.; REGINATO, R.J.; PINTER JR., P.J. Canopy temperature as a crop water stress indicator. **Water Resources Research**, Washington, v. 17, n. 5, p. 1133-1138, June 1981.

JACOBS, C.M.J. **Direct impact of atmospheric CO_2 enrichment on regional transpiration.** 1994. 177 p. Thesis - Agricultural University, Wageningen, 1994.

JACOBS, C.M.J.; VAN DEN HURK, B.M.M.; BRUIN, H.A.R. DE. Stomatal behavior and photosynthetic rate of unstressed grapevines in semi-arid conditions. **Agricultural and Forest Meteorology**, Amsterdam, v. 80, n. 2, p. 111-134, Mar. 1996.

JARVIS, A.J.; DAVIES, W.J. The coupled response of stomatal conductance to photosynthesis and transpiration. **Journal of Experimental Botany**, Lancaster, v. 49, p. 399-406, June 1998.

JARVIS, P.G. The interpretation of the variations in leaf water potential and stomatal conductance found in canopies in the field. **Philosophical Transactions of Royal Society - Biological Science**, London, v. 273, n. 1, p. 593-610, Sept. 1976.

JONES, H.G. Use of infrared thermometry for estimation of stomatal conductance as a possible aid to irrigation scheduling. **Agricultural and Forest Meteorology**, Amsterdam, v. 95, n. 3, p. 139-149, Sept. 1999.

_____. Application of thermal imaging and infrared sensing in plant physiology and ecophysiology. **Advances in Botanical Research**, Birminghan, v. 41, n. 1, p. 107-163, Mar. 2004.

JONES, H.G.; STOLL, M.; SANTOS, T.; SOUSA, C. DE; CHAVES, M.M.; GRANT, O.M. Use of infrared thermography for monitoring stomatal closure in the field: application to grapevine. **Journal of Experimental Botany**, Lancaster, v. 53, n. 378, p. 2249-2260, Nov. 2002.

JONG VAN LIER, Q. DE. **Física do solo.** Viçosa: Sociedade Brasileira de Ciência do Solo, 2010. 298 p.

JONG VAN LIER, Q. DE; LIBARDI, P.L. Variabilidade dos parâmetros da equação que relaciona a condutividade hidráulica com a umidade do solo no método do perfil instantâneo. **Revista Brasileira de Ciência do Solo**, Campinas, v. 23, p. 1005-1014, dez. 1999.

JONG VAN LIER, Q. DE; METSELAAR, K.; VAN DAM, J.C. Root water extraction and limiting soil hydraulic conditions estimated by numerical simulation. **Vadose Zone Journal**, Madison, v. 5, p. 1264-1277, Nov. 2006.

JONG VAN LIER, Q. DE; VAN DAM, J.C.; METSELAAR, K. Root water extraction under combined water and osmotic stress. **Soil Science Society of America Journal**, Madison, v. 73, n. 5, p. 862-875, Oct. 2009.

JONG VAN LIER, Q. DE; DOURADO NETO, D.; METSELAAR, K. Modeling of transpiration reduction in van Genuchten-Mualem type soils. **Water Resources Research**, Washington, v. 45, n. 2, p. W02422, Sept. 2009.

JONG VAN LIER, Q. DE; VAN DAM, J.C.; METSELAAR, K.; JONG, R. DE; DUIJNISVELD, W.H.M. Macroscopic root water uptake distribution using a matric flux potential approach. **Vadose Zone Journal**, Madison, v. 7, p. 1065-1078, Aug. 2008.

JORGE, L.A.C. **SIARCS 3.0 para Windows:** manual do usuário. São Carlos: EMBRAPA, 1996. 30 p.

KÖPPEN, W. Versuch einer Klassifikation der Klimate, vorzugsweise nach ihren Beziehungen zur Pflanzenwelt. **Geographic Zeitschrift**, Berlin, v. 6, p. 593-611, 1900.

KUIPER, P.J.C. The effects of environmental factors on the transpiration of leaves, with special reference to stomatal light response. **Landbouwhogeschool Wageningen**, Wageningen, v. 7, p. 1-49, Nov. 1961.

KLUTE, A.; PETERS, D.B. Water uptake and root growth. In: WHITTINGTON, W.J. (Ed.). **Root growth**. London: Butterworths, 1969. p. 105-132.

LASCANO, R.J.; VAN BAVEL, C.H.M. Root water uptake and soil water distribution: test of an availability concept. **Soil Science Society of America Journal**, Madison, v. 48, p. 233-237, June 1984.

LEFFLER, A.J.; PEEK, M.S.; RYEL, R.J.; IVANS, C.Y.; CALDWELL, M.M. Hydraulic redistribution through the root systems of senesced plants. **Ecology**, London, v. 86, n. 6, p. 633-642, Sept. 2005.

LEGATES, D.R.; MCCABE, G.J. Evaluating the use of “goodness-of-fit” measures in hydrologic and hydroclimatic model validation. **Water Resources Research**, Washington, v. 35, p. 233-241, July 1999.

LEINONEN, I.; GRANT, O.M.; TAGLIAVIA, C.P.P.; CHAVES, M.M.; JONES, H.G. Estimating stomatal conductance with thermal imagery. **Plant, Cell & Environment**, Logan, v. 29, n. 7, p. 1508-1517, Apr. 2006.

LEUNING, R. A critical appraisal of a combined stomatal-photosynthesis model for C3 plants. **Plant, Cell and Environment**, Logan, v. 18, n. 2, p. 339-355, Oct. 1995.

LOPES, D.B. **Photosyntetic competence of bean leaves with rust and anthracnose**. 1999. 166 p. Thesis - University of Florida, Florida, 1999.

MAHAN, J.R.; YEATER, K.M. Agricultural applications of a low-cost infrared thermometer. **Computers and Electronics in Agriculture**, London, v. 64, n. 2, p. 262-267, June 2008.

MAHAN, J.R.; BURKE, J.J.; WANJURA, D.F.; UPCHURCH, D.R. Determination of temperature and time thresholds for BIOTIC irrigation of peanut on the Southern High Plains of Texas. **Irrigation Science**, Heidelberg, v. 23, p. 145-152, May 2005.

MATERECHERA, S.A.; ALSTON, A.M.; KIRBY, J.M.; DEXTER, A.R. Influence of root diameter on the penetration of seminal roots into a compacted subsoil. **Plant and Soil**, Dordrecht, v. 144, n. 1, p. 297-303, July 1992.

METSELAAR, K.; JONG VAN LIER, Q. DE. The shape of the transpiration reduction function under plant water stress. **Vadose Zone Journal**, Madison, v. 6, p. 124-139, Jan. 2007.

MOLDRUP, P.; ROLSTON, D.E.; HANSEN, J.A.A.; YAMAGUCHI, T. A simple, mechanistic model for soil resistance to plant water uptake. **Soil Science**, Baltimore, v. 153, n. 2, p. 87-93, Feb. 1992**.**

MONTEITH, J.L. A reinterpretation of stomatal responses to humidity. **Plant, Cell and Environment**, Logan, v. 18, n.4, p. 357-364, June 1995.

MORAN, M.S.; CLARKE, T.R.; INOUE, Y.; VIDAL, A. Estimating crop water deficit using the relation between surface-air temperature and spectral vegetation index. **Remote Sensing of Environment**, Sydney, v. 49, n. 2, p. 249-263, July 1994.

NIMAH, M.N.; HANKS, R.J. Model for estimating soil water, plant, and atmospheric interrelations: I Description and sensitivity. **Soil Science Society of America Proceedings**, Madison, v. 37, n. 1, p. 522-527, Feb. 1973.

NIYOGI, N.; RAMAN, S. Comparison of four different stomatal resistance schemes using FIFE observations. **Journal of Applied Meteorology**, Boston, v. 36, n. 7, p. 903-917, Apr. 1997.

NOILHAN, J.; MAHFOUF, J.-F. The ISBA land surface parameterization scheme. **Global and Planetary Change**, New York, v. 13, p. 145-159, Sept. 1996.

NOILHAN, J.; PLANTON, S. A simple parameterization of land surface processes for meteorological models. **Monthly Weather Review**, Washington, v. 117, p. 536-549, Sept. 1989.

OZIER-LAFONTAINE, H.; LAFOLIE, F.; BRUCKLER, L.; TOURNEBIZE, R.; MOLLIER, A. Modelling competition for water in intercrops: theory and comparison with field experiments. **Plant and Soil**, Dordrecht, v. 204, n. 1, p. 183-201, Jan. 1998.

PAIVA, A.S.; FERNANDES, E.J.; RODRIGUES, T.J.D.; TURCO, J.E.P. Condutância estomática em folhas de feijoeiro submetido a diferentes regimes de irrigação. **Engenharia Agrícola**, Jaboticabal, v. 21, n. 1, p. 161-169, abr. 2005.

PARDOSSI, A; VERNIERI, P; TOGNONI, T. Involvement of abscisic acid in regulating water status in *Phaseolus vulgaris* L. during chilling. **Plant Physiology**, New York, v. 100, p. 1243-1250, Oct. 1992.

PASSOS, E.E.M.; PRADO, C.H.B.A.; ARAGÃO, W.M. The influence of vapor pressure deficit on leaf water relations of *Cocos nucifera* in Northeast Brazil. **Experimental Agriculture**, Cambridge, v. 45, n. 1, p. 93-106, Oct. 2009.

PETERS, R.T.; EVETT, S.R. Modeling diurnal canopy temperature dynamics using one-time-of-day measurements and a reference temperature curve. **Agronomy Journal**, Madison, v. 96, n. 11, p. 1553-1561, Nov. 2004.

PINTER, P.J.; HATFIELD, J.L.; SCHEPERS, J.S.; BARNES, E.M.; MORAN, M.S.; DAUGHTRY, A.; UPCHURCH, D.R. Remote sensing for crop management. **Photogrammetric Engineering & Remote Sensing**, Bethesda, Maryland, v. 69, n. 6, p. 647-664, Apr. 2003.

PORTES, T.A. Ecofisiologia. In: ARAUJO, R.S.; RAVA, C.A.; STONE, L.F.; ZIMMERMANN, M.J.O. (Ed.). **Cultura do feijoeiro comum no Brasil.** Goiânia: Potafós, 1996. p. 101-137.

RAATS, P. Uptake of water from soils by plant roots. **Transport in Porous Media**, Berlin, v. 68, n. 1, p. 5-28, Aug. 2007.

RADIN, J.W. Genetic variability for stomatal conductance in Pima cotton and its relation to improvements of heat adaptation. **Proceedings of the National Academy of Sciences of the United States of America**, Washington, v. 91, n. 15, p. 7217-7221, Sept. 1994.

REID, J.B.; HASHIM, O.; GALLAGHER, J.N. Relations between available and extractable soil water and evapotranspiration from a bean crop. **Agricultural Water Management**, Amsterdam, v. 9, p. 193-209, Sept. 1984.

RICHARDS, J.H.; CALDWELL, M.M. Hydraulic lift: substantial nocturnal water transport between soil layers by *Artemisia tridentata* roots. **Oecologia**, Berlin, v. 73, n. 3, p. 486-489, Mar. 1987.

RICHARDS, L.A. The usefulness of capillary potential to soil moisture and plant investigators. **Journal of Agricultural Research**, Washington, v. 37, p. 719-742, Oct. 1928.

RODRIGUEZ, D.; SADRAS, V.O.; CHRISTENSEN, L.K.; BELFORD, R. Spatial assessment of the physiological status of wheat crops as affected by water and nitrogen supply using infrared thermal imagery. **Australian Journal of Agricultural Research**, Melbourne, v. 56, n. 9, p. 983-993, Sept. 2005.

RONDA, R.J.; BRUIN, H.A.R.; HOLTSLAG, A.A.M. Representation of canopy conductance in modeling the surface energy budget for low vegetation. **Journal of Applied Meteorology**, Boston, v. 40, p. 1431-1443, Jan. 2001.

ROOIJ, G. DE; VAN DER PLOEG, M.; GOOREN, H.P.A.; BAKKER, G.; HOOGENDAM, C.W.; HUISKES, C.; KRUIDHOF, H.; KOOPAL, L.K. Measuring very negative water potentials with polymer tensiometers: principles, performance and applications. **Biologia**, Bratislava, v. 64, n. 3, p. 438-442, June 2009.

ROOSE, T.; FOWLER, A.C. A model for water uptake by plant roots. **Journal of Theoretical Biology**, Boston, v. 228, n. 2, p. 155-171, Oct. 2004.

ROUJEAN, J.-L. A tractable physical model of shortwave radiation interception by vegetative canopies. **Journal of Geophysical Research**, Boulder, v. 101, n. 5, p. 9523-9532, May 1996.

SADRAS, V.O.; WILSON, L.J. Growth analysis of cotton crops infested with spider-mites. I. Light interception and radiation-use efficiency. **Crop Science Journal**, Madison, v. 37, n. 4, p. 481-491, July 1997.

SANTOS, M.G.; RIBEIRO, R.V.; TEIXEIRA, M.G.; OLIVEIRA, R.F.; PIMENTEL, C. Foliar phosphorous supply and CO_2 assimilation in common bean (*Phaseolus vulgaris* L.) under water deficit. **Brazilian Journal of Plant Physiology**, Lavras, v. 18, n. 3, p. 407-411, July 2006.

SANTOS, R.Z.; ANDRÉ, R.G.B. Consumo da água nos diferentes estádios de crescimento da cultura do feijoeiro. **Pesquisa Agropecuária Brasileira**, Brasília, v. 27, n. 4, p. 543-548, jul. 1992.

SCHINDLER, U.; MÜLLER, L. Simplifying the evaporation method for quantifying soil hydraulic properties. **Journal of Plant Nutrition and Soil Science**, Berlin, v. 169, p. 623-629, Oct. 2006.

SCHIPPERS, B.; SCHROTH, M.N.; HILDEBRAND, D.C. Emanation of water from underground plant parts. **Plant and Soil**, Dordrecht, v. 27, p. 81-91, Jan. 1967.

SCHRÖDER, T.; JAVAUX, M.; VANDERBORGHT, J.; VEREECKEN, H. Comment on "Root water extraction and limiting soil hydraulic conditions estimated by numerical simulation". **Vadose Zone Journal**, Madison, v. 6, n. 3, p. 524-526, Mar. 2007.

SCHRÖDER, T.; JAVAUX, M.; VANDERBORGHT, J.; KORFGEN, B.; VEREECKEN, H. Effect of local soil hydraulic conductivity drop using a three-dimensional root water uptake model. **Vadose Zone Journal**, Madison, v. 7, n. 3, p. 1089-1098, Aug. 2008.

SHIMODA, S.; OIKAWA, T. Temporal and spatial variations of canopy temperature over a C3-C4 mixture grassland. **Hydrological Processes**, Malden, v. 20, p. 3503-3516, Sept. 2006.

SILVEIRA, P.M.; STONE, L.F. **Irrigação do feijoeiro**. Goiânia: Embrapa Arroz e Feijão, 1981. 230 p.

STEINMETZ, S. **Evapotranspiração máxima no cultivo do feijão de inverno**. Goiânia: Embrapa Arroz e Feijão, 1984. 4 p.

STEWART, J.B. Modelling surface conductance of pine forest. **Agricultural and Forest Meteorology**, Amsterdam, v. 43, n. 1, p. 19-35, Jan. 1988.

TAIZ, L.; ZEIGER, E. **Fisiologia vegetal**. Tradução de E.R. Santarém et al. 3. ed. Porto Alegre: Artemed, 2004. 719 p.

TARDIEU, F.; DAVIES, W.J. Stomatal response to abscisic acid is a function of current plant water status. **Plant Physiology,** Waterbury, v. 48, p. 540-545, Oct. 1992.

TARDIEU, F.; SIMMONNEAU, T. Variability among species of stomatal control under fluctuating soil water status and evaporative demand: modeling isohydric and anisohydric behaviours. **Journal of Experimental Botany**, Lancaster, v. 49, p. 419-432, Jun. 1998.

TAYLOR, H.M.; KLEPPER, B. Water uptake by cotton root systems: an examination of assumptions in the single root model. **Soil Science**, Baltimore, v. 120, n. 1, p. 57-67, Apr. 1975.

TETENS, V.O. Uber einige meteorologische. **Begriffe, Zeitschrift fur Geophysik**, Berlin, v. 6, p. 297-309, Sep. 1930.

THORNLEY, J.H.M. **Mathematical models in plant physiology**. London: Academic Press, 1976. 274 p.

TUZET, A.; PERRIER, A.; LEUNING, R. A coupled model of stomatal conductance, photosynthesis and transpiration. **Plant, Cell and Environment**, Logan, v. 26, p. 1097–1116, May 2003.

VAN DER PLOEG, M.J.; GOOREN, H.P.A.; BAKKER, G.; ROOIJ, G.H. Matric potential measurements by polymer tensiometers in cropped lysimeters under water-stressed conditions. **Vadose Zone Journal**, Madison, v. 7, n. 3, p. 1048-1054, Mar. 2008.

VAN GENUCHTEN, R. A closed-form equation for predicting the hydraulic conductivity of unsaturated soils. **Soil Science Society of America Journal**, Madison, v. 44, p. 892-898, Sept. 1980.

VAN HOVE, L.W.A. **The mechanism of NH_3 and SO_2 uptake by leaves and its physiological effects**. 1989. 134 p. Thesis - Agricultural University, Wageningen, 1989.

VERHOEF, A.; ALLEN, S.J.; BRUIN, H.A.R. DE; JACOBS, C.M.J.; HEUSINKVELD, B.G. Fluxes of carbon dioxide and water vapor from a Sahelian savanna. **Agricultural and Forest Meteorology**, Amsterdam, v. 80, n. 2/4, p. 231-248, Oct. 1996.

WANG, Y.P.; LEUNING, R. A two-leaf model for canopy conductance, photosynthesis and partitioning of available energy. I. Model description and comparison with a multi-layered model. **Agricultural and Forest Meteorology**, Amsterdam, v. 91, p. 89-111, June 1998.

WANG, Y.P.; YU, Q.; LI, J.; LI, L.-H.; LI, X.-G.; YU, G.-R.; SUN, X.-M. Simulation of diurnal variations of CO_2, water and heat fluxes over winter wheat with a model coupled photosynthesis and transpiration. **Agricultural and Forest Meteorology**, Amsterdam, v. 137, p. 194-219, Jan. 2006.

WANJURA, D.F.; MAHAN, J.R. Thermal environment of cotton irrigated using canopy temperature. **Irrigation Science**, Heidelberg, v. 14, n. 2, p. 199-205, May 1994.

WANJURA, D.F.; UPCHURCH, D.R. Accounting for humidity in canopy-temperature-controlled irrigation scheduling. **Agricultural Water Management**, Amsterdam, v. 34, p. 217-231, June 1997.

WANJURA, D.F.; UPCHURCH, D.R.; MAHAN, J.R. Control of irrigation scheduling using temperature-time thresholds. **Transactions of the ASAE**, St. Joseph, v. 38, p. 403-409, July 1995.

WILLIGEN, P. DE; VAN NOORDWIJK, M. **Roots, plant production, and nutrient use efficiency**. 1987. 282 p. Thesis - Agricultural University, Wageningen, 1987.

WILKS, D.S. **Statistical methods in the atmospheric sciences.** San Diego: Academic Press, 1995. 467 p.

WILLMOTT, C.J. On the validation of models. **Progress in Physical Geography**, London, v. 2, p. 184-194, June 1981.

WILLMOTT, C.J.; ACKLESON, S.M.; DAVIS, R.E., FEDDEMA, J.J.; KLINK, K.M.; LEGATES, D.R.; O'DONNELL, J.; ROWE, C.M. Statistics for the evaluation and comparison of Models. **Journal of Geophysical Research**, Boulder, v. 90, p. 8995-9005, Aug. 1985.

WIND, G.P. Capillary conductivity data estimated by a simple method. In: RIJTEMA, P.E.; WASSINK, H. (Ed.). **Water in the unsaturated zone.** Wageningen: IASH, 1968. v. 1. Proceedings of the Wageningen Symposium, p. 181–191.

XU, X.; BLAND, W.L. Reverse water flow in sorghum roots. **Agronomy Journal**, Madison, v. 85, p. 384-388, July 1993.

ZIMMERMANN, U.; MEINZER, F.; BENTRUP, F.W. How does water ascend in tall trees and other vascular plants? **Annals of Botany**, Oxford, v. 76, p. 545-551, July 1995.

APPENDICES

Appendix A: Parameterizations of Ag_s model

The CO_2 assimilation model proposed by Jacobs (1994) and Jacobs, Van Den Hurk and De Bruin (1996) consists of three parts. The first part describes the photosynthetic rate, the second one describes the stomatal responses and the third part describes the parameterization of stomatal responses as a function of air humidity. These three parts are detailed below.

1. The photosynthetic rate

a. CO_2 and light responses

The photosynthetic part of the Ag_s model is in essence the model of Goudriaan et al. (1985). This model describes most of the important response characteristics of photosynthesis. It can be used to evaluate photosynthesis of C3 and C4 plants. The modeling approach is based on two essentially different conditions:

i. light is the limiting factor (at high CO_2 concentrations);

ii. CO_2 is the limiting factor (at high light intensity).

A is linearly related to the absorbed PAR at very low light intensity:

$$A = \varepsilon PAR - R_d \qquad [48]$$

where ε denotes the initial quantum efficiency (mg J^{-1}) and e R_d is the dark respiration (mg m^{-2} s^{-1}). ε quantifies the slope of the light response curve and it is affected by photorespiration. It can be calculate by:

$$\varepsilon = \varepsilon_o \frac{C_s - \Gamma}{C_s + 2\Gamma} \qquad [49]$$

where ε_o represents the maximum quantum use efficiency (0.017 mg J^{-1} for C3 plants), C_s the CO_2 concentration at leaf surface (mg m^{-3}) and Γ the CO_2 concentration compensation (mg m^{-3}). Eq. 49 is derived from biochemical considerations and is similar to the result obtained by Farquhar, Caemmerer and Berry (1980).

At high light intensities and limiting CO_2 concentrations, it may be assumed that the photosynthetic rate coincides with the asymptotic value of the light response curve A_m (mg m^{-2} s^{-1}) (THORNLEY, 1976). Then, at low intercellular CO_2 concentration C_i, A_m is linearly related to the CO_2 concentration according to:

$$A_m = g_m(C_i - \Gamma) \qquad [50]$$

where g_m is the mesophyll conductance (mm s^{-1}) and quantifies the slope of the CO_2 response curve at high light intensities.

An empirical light response function of A is used to combine the effects of CO_2 and light described above. The asymptotic exponential is used here:

$$A = (A_m + R_d)\left(1 - exp\left(\frac{-\varepsilon PAR}{A_m + R_d}\right)\right) - R_d . \quad [51]$$

Goudriaan and Laar (1994) defined R_d as a function of canopy temperature t_{canopy}. R_d increases with temperature by a factor of 2 each 10°C. It can be calculated by a Q_{10} function (Q_{10} = 2):

$$R_d = 50 Q_{10}^{\frac{(t-20)}{10}} \quad [52]$$

The Q_{10} function is defined by a proportional increase in a parameter value as temperature increases 10°C.

The above equations predict an unlimited photosynthesis at high light intensities and high CO_2 concentrations. In reality, the photosynthetic rate will be bound to a maximum, $A_{m,max}$ (mg m^{-2} s^{-1}), which is related to the ability of plants to allocate the products of the Calvin cycle and to regenerate ribulose 1,5 biphosphate. A_m is accounted for using a saturation response, similar to eq. 51:

$$A_m = A_{m,max}\left(1 - exp\left(\frac{-g_m(C_i - \Gamma)}{A_{m,max}}\right)\right). \quad [53]$$

b. Temperature responses

The temperature dependence of photosynthesis is accounted for by the temperature dependence of Γ and $A_{m,max}$. The temperature response of these variables is based on a Q_{10} response function:

$$X(t) = X(@25) \cdot Q_{10}^{\frac{t-25}{10}} \quad [54]$$

where t is temperature (°C), $X(t)$ is the value of any variable X at temperature t, and $X(@25)$ the value of X at t = 25°C. This equation is directly used to describe the temperature response of Γ. In the case of $A_{m,max}$ and g_m, equation above is modified using the inhibition function:

$$X(t) = \frac{X(@25) \cdot Q_{10}^{\frac{t-25}{10}}}{(1+exp(0.3(t_1 - t)))(1+exp(0.3(t - t_2)))} \quad [55]$$

where t_1 and t_2 denote reference temperatures. t_1 and t_2 can be adjusted to mimic species-specific features (for instance, the lower temperature optimum of C3 species than C4 species). The resulting default values used in the present study are summarized in Table 7.

Table 7 – Parameter values used in the present study

Parameter (X)	X(@25)	Q_{10}	t_1 (°C)	t_2 (°C)
ε_0 (mg J^{-1})	0.017	-	-	-
f_0	0.85	-	-	-
Γ (mg m^{-3})	81.0	1.5	-	-
$A_{m,max}$ (mg m^{-2} s^{-1})	2.2	2	8	38
g_m (mm s^{-1})	3.9 or 7	2	5	28
g_c (mm s^{-1})	0	-	-	-

2. Stomatal responses

This section describes how CO_2 assimilation and stomatal control are related in the Ag_s model.

The assumption that stomatal behavior and CO_2 assimilation are coupled is based on the fundamental premise that plants will operate their stomata such that carbon gain is maximized while minimizing water loss. It is believed that it is this strategy which results in the strong observed correlation between A and g_s. The correlation is observed in the laboratory as well as in the field, including under such unfavorable conditions as senescence, water stress, nutrient shortage and air pollution (for example, GOUDRIAAN; VAN LAAR, 1978; VAN HOVE, 1989). It should be stressed that a correlation between A and g_s does not imply large stomatal control of A nor does it imply large stomatal control of A.

To calculate g_s from A (eq. 22), the concentration difference $C_s - C_i$ has to be known. The tendency to maintain a constant $C_i/C_s = k$ has been demonstrated experimentally (k is about 0.7 for C3 species). It implies in a linear relation between A and g_s.

However, the ratio between C_i and C_s will be constant only if environmental stimuli affect A and g_s in the same way. The humidity of the air directly affects g_s independently of A. As D_s increases, g_s can be reduced at a greater rate than A which results in a reduction of C_i/C_s. The ratio C_i/C_s is also affected by CO_2 concentration. Both effects are taken into account in eq. 23.

Eq. 23 allows calculating the intercellular CO_2 concentration which is used to estimate A_m as well as the difference between intercellular and environmental CO_2 concentrations. Moreover, eq. 23 allows minimizing the stomatal responses to humidity. These equations determine a simultaneous solution of A and C_i/C_s and avoid inefficient interactions or analytical solutions. The current approach needs two parameters to be determined, D_{max} (D_s when stomata are closed) and f_o. A typical value for D_{max} in agricultural crops is 45 g kg^{-1}. Assuming that the standard values of f (0.7 to C3 plants) are valid at $D_s \approx 10$ g kg^{-1}, it follows that f_o is about 0.85 for C3 plants.

To calculate the specific humidity deficit between leaves and environmental air D_s (eq. 21) the air specific humidity at saturation q_{sat} at canopy temperature t_{canopy}, (°C) and the air specific humidity q at air temperature t_{air} (°C) are needed. Expressing both in units of g kg^{-1}:

$$q_{sat}(t_{canopy}) = \frac{0.62197\, e_s}{P_{atm} - 0.337803\, e_s} \quad [56]$$

$$q(t_{air}) = \frac{0.62197\, e_a}{P_{atm} - 0.337803\, e_a} \quad [57]$$

where P_{atm} is the atmospheric pressure (kPa), e_a is the actual water vapor (kPa), e_s is the saturation pressure of water vapor (kPa) at t_{canopy}:

$$e_s = 0.6108 \cdot 10^{\frac{7.5 t_{canopy}}{237.3 + t_{canopy}}} . \quad [58]$$

3. Parameterization of stomatal responses to air humidity

The parameterization of stomatal humidity responses in the context of Ag_s model relies on the following observations and assumptions:

i. f decreases almost linearly with D_s, at least at low D_s;

ii. at the timescale of interest for this study (a day or less) the independent humidity effects do not affect the potential activity of photosynthetic apparatus, that is, g_m and $A_{m,max}$ remain constant;

iii. the minimum epidermal conductance is equal to g_c. This is the case if $PAR = 0$ or if $D_s = D_{max}$.

The last assumption defines D_{max}: a small transpiration rate and a minimum photosynthetic rate are allowed after stomatal closure (where $g_s = 0$). The minimum photosynthetic rate at full light intensity is denoted as A_{min} (mg m^{-2} s^{-1}). A_{min} will be established at a minimum internal CO_2 concentration C_{min} (mg m^{-3}) corresponding to a minimum value of f, f_{min}. f_{min} can be estimated as follows. It is assumed that A_{min} and the corresponding C_{min} are found in the quasi-linear part of the C_i-response curve. Then, A_{min} may be estimated by:

$$A_{min} = g_m(C_{min} - \Gamma) \qquad [59]$$

from which follows (using the first approximation to Ag_s and neglecting possible effects of transpiration):

$$C_{min} = \frac{g_c C_s + g_m \Gamma}{g_c + g_m}. \qquad [60]$$

and f_{min}, defined as f at D_{max} will be:

$$f_{min} = \frac{g_c}{g_c + g_m} \qquad [61]$$

while f (eq. 23) is written as a linear function of D_s:

$$f = f_o\left(1 - \frac{D_s}{D_{max}}\right) + f_{min}\left(\frac{D_s}{D_{max}}\right). \qquad [62]$$

4. Canopy scale

The above presented Ag_s model calculates CO_2 assimilation at a leaf scale. The calculated A is used to find the stomatal conductance so that g_s also applies at the leaf

scale. However the model requires canopy photosynthetic rate to drive CO_2 fluxes. It is assumed that t_s (equal to t_{canopy}), D_s and C_s are constant throughout canopy. The extinction of *PAR* by plants must be described in the model when it is upscaled to canopy. The leaves in upper layer of a canopy intercept the major quantity of solar radiation and the photosynthetic activity is reduced in the lowest layers. *PAR* extinction is described in the model by Roujean (1996) parameterization. Absorbed amount of *PAR* at a *z* level of canopy is given by:

$$PAR(z) = (1 - K(z))PAR(h) \quad [63]$$

where *h* is the canopy height and *K* is the extinction coefficient:

$$K(z) = f(Z_h)K_{df}(z) + (1 - f(Z_h))K_{dr}(z) \quad [64]$$

$K_{df}(z)$ and $K_{dr}(z)$ are the difuse and direct radiation extinction coefficients, respectively:

$$K_{df}(z) = 1 - exp(-0.8bLAI(h - z)/h) \quad [65]$$

$$K_{dr}(z) = 1 - exp\left(-\frac{G_n}{\cos\theta_s} bLAI(h - z)/h\right) \quad [66]$$

Z_h is the zenital angle and G_n is the parameter that describes leave distribution (a spherical angular distribution with $G_n = 0.5$ is assumed). $f(Z_h)$ is the portion of descendent short wave radiation that is diffused at the canopy top:

$$f(Z_h) = \frac{0.25}{0.25 + \cos Z_h} \quad [67]$$

and *b* is the scattering coefficient of leaves:

$$b = 1 - \frac{1 - \sqrt{1 - \omega}}{1 + \sqrt{1 - \omega}} \quad [68]$$

in which ω (= 0.2) is the single scattering albedo of leaves at *PAR*.

If a homogeneous vertical distribution of leaves is assumed, CO_2 net assimilation *A*, stomatal conductance g_s and transpiration rate T_{Ags} are given by:

$$A = \frac{LAI}{h}\int_0^h A dz$$
$$g_s = \frac{LAI}{h}\int_0^h g_s dz \quad [69]$$
$$T_{Ags} = \frac{LAI}{h}\int_0^h T_{Ags} dz$$

.

The integrals are solved by applying the five-point Gaussian integration scheme:

$$A = LAI\sum_{i=1}^{5} W_i A(z_i)$$
$$g_s = LAI\sum_{i=1}^{5} W_i g_s(z_i) \quad [70]$$
$$T_{Ags} = LAI\sum_{i=1}^{5} W_i T_{Ags}(z_i)$$

where z_i and W_i are distance and weight of point i, respectively, and values are presented in Table 8.

Table 8 – Weights and distances of five points integration method

Point	i = 1	i = 2	i = 3	i = 4	i = 5
Weight	0.1184635	0.2393144	0.2844444	0.2393144	0.1184635
Distance	0.0469101	0.2307534	0.5	0.7692465	0.9530899

Appendix B: Source code of CO_2 assimilation model

The Ag_s model was programmed in ForTran® programming language and the source code is presented below. The main program is called code_canopy_tese.f90. Four more files are needed to run the simulations: the ags_canopy.inp file which contains some input parameters and file names; the bean1.txt file with values of D_{max} and g_m at 25°C; the lai_nir.txt or lai_ir.txt files which contain *LAI* values; and dados_07_18_nir_modelo.txt or dados_07_18_ir_modelo.txt files with meteorological and canopy temperature data.

```
!*******************************************************************************
!*******************************************************************************

program ags_canopy_scale
implicit none

!*******************************************************************************
!****************************** D E C L A R A T I O N S **************
!*******************************************************************************

!Main program
real     ep0, cs, f0, gama25, ammax25, q10_gama, q10_ammax
real     gc, t1_am, t2_am, patm, lat, dmax, t1_gm, t2_gm, gm25
real     doy, horig, doy2, q10_gm
real     dados_exp(11), dados_est(12), dados2(4)
real     tar, tl, wind, part, nr, ea, lai,vpd, es_l
real     ds, gs_med, trans_med
real*8   rconst
real     gama, gm_mm, rd, am, ci, amg, amin, ep
real     par_ext, ch, zc
real     gs, gsc, an, transp
real     gs_tt, gsc_tt, an_tt, transp_tt
real     gs_m, trans_m

integer  i

character*50 plantfile, meteofile, laifile
character*40 output1, output2
character*12 chr
character*7  day, day2, daylai
character*6  hour
```

```
data      rconst /8.314472/   !Universal gas constant (m3Pa/molK)

!Gauss integration method
integer   igauss
real*8    wgauss(5), dist_gauss(5)
data      igauss /5/
data      wgauss /0.1184635, 0.2393144, 0.2844444, 0.2393144, 0.1184635/
data      dist_gauss /0.0469101, 0.2307534, 0.5, 0.7692465, 0.9530899/

!*******************************************************************************
!*******************************  M A I N   P R O G R A M   **********
!*******************************************************************************

!Read inputfile
!Open files and read data
open(unit=10,file='ags_canopy.inp',status='old')
read(10,*) chr
read(10,*) plantfile
read(10,*) meteofile
read(10,*) laifile
read(10,*) output1, output2
read(10,*) chr
read(10,*) chr
read(10,*) ep0
read(10,*) chr
read(10,*) chr
read(10,*) cs
read(10,*) chr
read(10,*) f0
read(10,*) chr
read(10,*) gama25
read(10,*) chr
read(10,*) ammax25
read(10,*) chr
read(10,*) chr
read(10,*) q10_gama
read(10,*) chr
read(10,*) q10_ammax
read(10,*) chr
read(10,*) q10_gm
read(10,*) chr
read(10,*) gc
read(10,*) chr
read(10,*) chr
```

```
read(10,*) t1_am, t2_am
read(10,*) chr
read(10,*) t1_gm, t2_gm
read(10,*) chr
read(10,*) patm
read(10,*) chr
read(10,*) lat
read(10,*) chr
read(10,*) ch
open(unit=11,file=meteofile,status='old')
open(unit=12,file=plantfile,status='old')
open(unit=23,file=laifile,status='old')
read(12,*) chr
read(12,*) chr
read(12,*) chr
read(12,*) dmax, gm25

!Output files
open(unit=21,file=output2,status='unknown')

!Read meteorological and experimental data (horig: 0.25, 0.5 and 0.75 of hour):
read(23,*) daylai, lai

200 read(11,*,end=203) day, hour, doy, horig, dados_exp, dados_est
202 continue

if(day.eq.daylai)then
        tar    = dados_exp(1)                  !Air temperature from plot (°C)
        tl     = dados_exp(2)                  !Leaf temperature (°C)
        vpd    = dados_exp(3)                  !Vapor pressure deficit at atmospher(hPa)
        ea     = dados_exp(5)                  !Actual vapor pressure (hPa)
        part   = dados_est(5)*0.21569          !PAR radiation at canopy top (W/m2)
        wind = dados_est(2)                    !Wind velocity (m/s)

        an_tt     = 0.
        gs_tt     = 0.
        gsc_tt    = 0.
        transp_tt = 0.

!Estimates Leaf-to-Air Specific Humidity Deficit (Ds, g/kg)
        call vegetation_ds(ds,es_l,tl,ea,patm,dmax)

!If Ds=0, go to the next meteorological data
        if(ds .eq. 0.)then
```

```
                print*,'Ds equal to zero!'
                go to 200
        endif

!Estimates some parameters for CO2 assimilation and stomatal conductance subroutine
        call          assim1(gama,gm_mm,rd,am,amg,amin,ci,ep,q10_gama,q10_ammax,tl,t1_am,
        t2_am,gc,ds,dm ax,cs,q10_gm,t1_gm,t2_gm,ep0,gama25,ammax25,f0,gm25)

!Number of LAI levels
        do i=1,igauss
                an     = 0.
                gs     = 0.
                 gsc    = 0.
                transp = 0.

    !Z height levels inside the canopy (m)
                zc = 0.
                zc = ch*dist_gauss(i)

!Estimates the PAR extinction within canopy
                call ext_par(par_ext,lat,doy,horig,part,ch,lai,zc)

 !Estimates CO2 net assimilation and stomatal concuctance
                call       assim2(gs,gsc,an,transp,gama,rd,am,ci,cs,amg,amin,ep,par_ext,ds,dmax,
                gc,wind, gm_mm)


!Integration of local CO2 assimilation rate, stomatal conductance and transpiration to canopy
scale
                an_tt     = an_tt     + (an*wgauss(i))
                gs_tt     = gs_tt     + (gs*wgauss(i))
                gsc_tt    = gsc_tt    + (gsc*wgauss(i))
                transp_tt = transp_tt + (transp*wgauss(i))

        enddo !Profile

!Write output file 2 - totals
        an_tt     = an_tt*lai
        gs_tt     = gs_tt*lai
        gsc_tt    = gsc_tt*lai
        transp_tt = transp_tt*lai

        write(21,101) day, hour, doy, horig, an_tt, gs_tt, transp_tt, vpd, ds, part, ea, es_l, tl
```

```
        go to 200
else
        read(23,*) daylai, lai
        go to 202
203 endif

close(10)
close(11)
close(12)
close(13)
close(21)
close(23)

101 format(a9,2x,a6,2x,11(f7.2,2x))
stop
end

!*******************************************************************************
!********************************  S U B R O U T I N E S ***********************
!*******************************************************************************

!1  Returns Leaf-to-Air VDP
!The vegetation-surface-layer model (Jacobs (1996))
!Cs (cs), Tl (t) and Ds (ds) are considered constants inside the canopy
subroutine vegetation_ds(ds,es_l,t,ea2,patm,dmax)
real   ds,t,patm,dmax,ea2
real   es_l,qr
real   qs

!qs=saturation specific humidity at leaf temperature
es_l = 0.
qs   = 0.
es_l = 6.108*(10.**((7.5*t)/(237.3+t)))                    !hPa
qs   = ((0.62197*es_l)/(patm-0.37803*es_l))*1000.          !g/kg

!qr=specific humidity at reference level
qr = 0.
qr = ((0.62197*ea2)/(patm-0.37803*ea2))*1000.              !g/kg

!Ds: specific humidity deficit at leaf surface (g/kg)
ds = 0.
ds = qs-qr
```

```
if(ds.lt.0.or.ds.gt.dmax)then
          ds = 0.
endif

end

!*************************************************************************
!*************************************************************************

!2  Returns the PAR extinction within canopy (Calvet et al., 1998)
subroutine ext_par(par_ext,lat,doy,horig,part,h,laic,z)
real par_ext, lat, doy, horig, part, h, laic
real lssa, ldist, fsca, sdecl, ha
real thetas, cthetas, f_thetas
real kdf, kdir, kt
real z

lssa  = 0.20        !leaf single scattering albedo (w)
ldist = 0.50        !parameter that describes the distribution of leaves (spherical distribution)

!Foliage scattering coefficient (b)
fsca = 0.
fsca = 1. - ((1.-sqrt(1.-lssa))/(1.+sqrt(1.-lssa)))

!Solar zenith angle
sdecl = 0.
ha    = 0.
sdecl = 23.45*sind((360./365.)*(doy-80.))                !solar declination (+-23.45°)
ha    = (horig-12.)*15.                                  !hourly angle (decimal hourly time)

thetas = 0.
thetas = sind(lat)*sind(sdecl)+cosd(lat)*cosd(sdecl)*cosd(ha)
thetas = acosd(thetas)

!Ratio of diffuse to total solar radiation at the top of the canopy
cthetas  = 0.
f_thetas = 0.
cthetas  = cosd(thetas)
f_thetas = 0.25/(0.25+cthetas)

!Extinction coefficients of diffuse and direct light
kdf   = 0.
kdir  = 0.
kdf   = 1. - exp(-0.8*fsca*laic*(h-z)/h)
```

```
kdir  = 1. - exp(-(ldist/cosd(thetas))*fsca*laic*(h-z)/h)

!Total extinction coefficient of light
kt = 0.
kt = f_thetas*kdf+(1.-f_thetas)*kdir

!Absorbed PAR (J/m2 s)
par_ext = 0.
par_ext = (1.-kt)*part

end

!************************************************************************
!************************************************************************

!3  Returns the CO2 assimilation and gs at each vertical level
subroutine                  assim1(gama,gm_mm,rd,am,amg,amin,ci,ep,q10_gama,q10_ammax,tl,
t1_am,t2_am,gc,ds,dmax,cs,q10_gm,t1_gm,t2_gm,ep0,gama25,ammax25,f0,gm25)
real gama,gm25,rd,am,ci,amg,amin,ep,q10_gama,q10_ammax,tl,t1_am,t2_am,gc
real ds,dmax,cs,q10_gm,t1_gm,t2_gm,ep0,gama25,ammax25,f0
real fmin,f2,f1,f
real const1,cmin

!Gama: CO2 compensation concentration (mg/m3)
gama = 0.
gama = gama25*q10_gama**((tl-25.)/10.)
gama = (gama*44.01)/24.45

!Am,max: leaf photosyntesis capacity (mg/m2s)
ammax = 0.
ammax = ammax25*q10_ammax**((tl-25.)/10.)
ammax = ammax/((1.+exp(0.3*(t1_am-tl)))*(1.+exp(0.3*(tl-t2_am))))

!gm: mesophyl conductance (mm/s)
gm_mm = 0.
gm_mm = gm25*q10_gm**((tl-25.)/10.)
gm_mm = gm_mm/((1.+exp(0.3*(t1_gm-tl)))*(1.+exp(0.3*(tl-t2_gm))))

!f: fraction Ci-Gama/Cs-Gama
 fmin = 0.
if(gc .eq. 0.)then
          fmin = 0.
          f2   = 0.
else
```

```
            fmin = gc/(gc+gm_mm)
            f2   = (fmin*(ds/dmax))
endif

f1 = 0.
f1 = (f0*(1.-(ds/dmax)))
f  = f1 + f2

!Ci/Cs (mg/m3):
!Ci: intercellular CO2 concentration
!Cs: CO2 concentration at surface (leaf or canopy)
ci = 0.
ci = (cs*f) + ((1.-f)*gama)

!ep: initial quantum use effeciency (mg/J PAR)
ep = 0.
ep = ep0*((cs-gama)/(cs+(2.*gama)))

!Am: photosynthetic rate at saturation light intensity (mg/m2s)
const1 = 0.
am     = 0.
const1 = (-gm_mm*0.001*(ci-gama))/ammax
am     = ammax*(1.-(exp(const1)))

!Rd: dark respiration (mg/m2s) following Goudriaan (1994)
rd = 0.
rd = (50.*(2.**((tl-20.)/10.)))/1000.

!Am,g: Am+Rd (mg/m2s)
amg = 0.
amg = am + rd

!Cmin: minimum intercellular CO2 concentration, at An=Amin (mg/m3)
cmin = 0.
if(gc .eq. 0.)then
            cmin = (gm_mm*gama)/gm_mm
else
            cmin = ((gc*cs)+(gm_mm*gama))/(gc+gm_mm)
endif

 !Amin: minimum Am, at Ds=Dmax (mg/m2s)
amin = 0.
amin = gm_mm*0.001*(cmin-gama)
end
```

```
!************************************************************************
!************************************************************************

!4  Returns the CO2 assimilation and gs at each vertical level
subroutine assim2(gs,gsc,an,transp,gama,rd,am,ci,cs,amg,amin,ep,par,ds,dmax,gc,
wind,gm_mm)
real gs,gsc,an,transp,gama,rd,am,ci,cs,amg,amin,ep,par,ds,dmax,gc,wind
real ag,gsc_estr,gs_estr,transp2,gbl,gm_mm
real rho,mv,ma,k,wl,rt

!Constants
rho = 1.22            !Air density (kg/m3)
mv  = 18.             !Molecular mass of water (g/mol)
ma  = 28.9            !Molecular mass of air (g/mol)
k   = 0.0056          !Empirical constant for boundary layer conductance (m/s0.5)
wl  = 0.1             !Leaf's dimension parallel to the direction of wind (m)

!An: net photosyntetic rate of leaf (mg/m2s or micro mol/m2s)
an = 0.
an = (am+rd)*(1.-exp((-ep*par)/(am+rd)))-rd

!Ag: gross photosyntetic rate (mg/m2s)
ag = 0.
ag = an + rd

!gsc*: first guess of stomatal conductance to CO2 (mm/s)
gsc_estr = 0.
gsc_estr = an - (amin*((ds/dmax)*(ag/amg))) + (rd*(1.-(ag/amg)))
gsc_estr = (gsc_estr/(cs-ci))*1000.

!gs*: first guess of stomatal conductance to water wapour (mm/s)
 gs_estr = 0.
gs_estr = (1.6*gsc_estr) + gc

!Transpiration rate* (mg/m2s)
transp = 0.
transp= rho*gs_estr*ds

!gsc: stomatal conductance to CO2 (mm/s)
gsc = 0.
gsc = gsc_estr + (0.001*(transp*(ma/(rho*mv))*((cs+ci)/(2.*(cs-ci)))))

!gbl: boundary layers conductance to water vapor (mm/s)
gbl = 0.
```

```
gbl = (k*((wind/wl)**0.5))*1000.

!gs: stomatal conductance to water vapor (mm/s)
          gs = 0.
gs = (1.6*gsc) + gc

!gt: total conductance to water vapor (mm/s)
gt = 0.
gt = (1./gbl)+(1./gbl)+(1./gs)+(1./gm_mm)
rt = 1./gt

!Transpiration rate (mg/m2s)
transp2 = 0.
transp2 = (rho*ds)/rt
transp  = transp2

end

!*******************************************************************************
!*******************************************************************************
```